STUDY ON THE HEAT AND MASS TRANSFER TAKING PLACE IN A DIRECT EXPANSION (DX) AIR COOLING AND DEHUMIDIFICATION COIL

XIA LIANG

Ph.D

The Hong Kong Polytechnic University

2010

The Hong Kong Polytechnic University
Department of Building Services Engineering

Study on the Heat and Mass Transfer Taking Place in a Direct Expansion (DX) Air Cooling and Dehumidification Coil

Xia Liang

A thesis submitted in partial fulfillment of the requirements

for the Degree of Doctor of Philosophy

December 2009

Certificate of Originality

I hereby declare that this thesis is my own work and that, to the best of my knowledge and belief, it reproduces no material previously published or written, nor material that has been accepted for the award of any other degree or diploma, except where due acknowledgement has been made in the text.

Xia Liang

Department of Building Services Engineering

The Hong Kong Polytechnic University

Hong Kong SAR, China

December, 2009

Abstract

Direct expansion (DX) Air Conditioning (A/C) units are commonly seen in small to medium sized buildings. In the evaporator of a DX A/C unit, or a DX air cooling coil, usually simultaneous heat and mass transfer, in the form of cooling and dehumidifying of the warm and humid air flowing through the cooling coil, takes place, when the surface temperature of the DX cooling coil is lower than the dew point temperature of the air stream.

The use of a DX A/C unit having a single-speed compressor and air supply fan, normally relies on on-off control to only maintain indoor dry-bulb temperature, resulting in an uncontrolled equilibrium indoor humidity, and leading to a reduced level of thermal comfort, poor indoor air quality (IAQ) and low energy efficiency. Hence, DX A/C units having variable-speed compressor and air supply fan are increasingly used for pursuing a thermally comfortable indoor environment at a higher energy efficiency. Therefore, it is important to study the performance of the simultaneous heat and mass transfer taking place in the DX air cooling coil of a DX A/C unit having a variable-speed compressor and air supply fan, which has been inadequately investigated.

This thesis begins with addressing the calculation of an important dimensionless parameter, i.e., steady state Equipment Sensible Heat Ratio (SHR) of a DX air

cooling coil, which is defined as the ratio of the output sensible cooling capacity to the total output cooling capacity from the DX cooling coil. The determination of Equipment SHR is essential because a satisfactory indoor thermal environmental control in a space requires not only a match between the total output cooling capacity from the DX A/C unit serving the space and the total space cooling load, but also a match between unit's Equipment SHR and an Application SHR which is defined as a ratio of the space sensible cooling load to the total space cooling load. A Calculation Method for the Equipment SHR of a DX cooling coil has been developed and reported. The calculation method was validated through a comparison between its results and the experimental results from different operating conditions, i.e., different combinations of compressor speed and air supply fan speed, and different inlet air conditions to the DX cooling coil. With the Method developed, the effect of refrigerant evaporating temperature at fixed inlet air conditions on Equipment SHR was theoretically analyzed.

Secondly, the thesis presents an experimental study on estimating on the dehumidification effect on the airside of the superheated region (SPR) in a DX cooling coil. Previously when investigating the heat and mass transfer taking place in DX cooling coils, a dry airside in a SPR was normally assumed without validation. This assumption conflicted with the experimental observation from an operating DX cooling coil. Therefore, an experimental study has been carried out to examine the validity of such an assumption under different operating conditions. A lumped

parameter calculation procedure was developed specifically for processing the experimental data. The experimental results suggested that the airside surface of the SPR in a DX air cooling coil was either fully or partially wet under all experimental conditions. Consequently assuming a dry airside in the SPR could lead to an underestimated total amount of water vapor condensed on the entire airside of the DX cooling coil.

Thirdly, the thesis reports on the development of a modified Logarithmic Mean Enthalpy Difference (LMED) method for evaluating the total heat transfer rate in a wet air cooling coil operating under both unit and non-unit Lewis Factors ($Le^{2/3}$) conditions. The development stemmed from the inaccurate assumption of Lewis Factor being unit in the existing LMED method, which has been extensively applied to modeling the combined heat and mass transfer taking place in both DX and chilled water cooling coils. The assumption resulted in calculation errors when non-unit Lewis Factors were encountered, which has been however observed by many researchers. A modified LMED (m-LMED) method has been therefore developed for calculating the total heat transfer rate under both unit and non-unit Lewis Factors. Although the m-LMED method was validated by comparing its prediction of the total heat transfer rate to that from numerically solving the fundamental governing equations of the heat and mass transfer in a wet chilled water cooling coil, the m-LMED method can also be applied to the DX cooling coils.

Finally, the analytical solutions for evaluating the heat and mass transfer in both a wet DX cooling coil and a wet chilled water cooling coil, respectively, have been developed and are reported. The analytical solutions were validated by comparing their predictions with those from numerically solving the fundamental governing equations of the heat and mass transfer taking place in wet air cooling coils. With the analytical solutions, the distributions of air temperature and moisture content along the air flow direction in either a wet DX or a wet chilled water cooling coil can be evaluated. The analytical solutions can be a low-cost replacement to numerically solving the fundamental heat and mass transfer governing equations.

Publications Arising from the Thesis

Journal Papers

- **Xia Liang**, M.Y. Chan and Deng Shiming. Development of a method for calculating steady-state equipment sensible heat ratio of direct expansion air conditioning units. *Applied Energy*, 85 (2008) 1198-1207 (Based on Chapter 5).

- **Xia Liang**, M.Y. Chan, Deng Shiming and Xu Xiangguo. Dehumidification effects in the superheated region (SPR) of a direct expansion (DX) air cooling coil. *Energy Conversion and Management*, 50(2009) 3063-3070 (Based on Chapter 6).

- **Xia Liang**, Deng Shiming and M.Y. Chan. Effect of indoor environment on the condensing rate and the air side sensible heat transfer resistance of a direct expansion (DX) cooling coil. Accepted by *Indoor and Built Environment*, 2010.

- **Xia Liang**, M.Y. Chan, Deng Shiming and Xu Xiangguo. A modified logarithmic mean enthalpy difference (LMED) method for evaluating the total heat transfer rate of a wet cooling coil under both unit and non-unit Lewis Factors. *International Journal of Thermal Sciences*, 48(2009) 2159-2164 (Based on Chapter 7).

- **Xia Liang**, M.Y. Chan, Deng Shiming and Xu Xiangguo. Analytical solutions for evaluating the thermal performances of wet air cooling coils under both unit and non-unit Lewis Factors (Based on Chapter 8 and submitted to *Energy Conversion and Management*).

Acknowledgements

I must express my grateful thanks to my Chief Supervisor, Dr. M.Y. Chan, Assistant Professor, and my Co-Supervisor, Dr. Shiming Deng, Associate Professor, both from the Department of Building Services Engineering (BSE), The Hong Kong Polytechnic University, for their readily available supervision, valuable suggestions, patient guidance, continuous help and encouragement throughout the course of the work.

My special thanks go to The Hong Kong Polytechnic University for financially supporting this project. I would like to also thank Mr. Xiangguo Xu, Dr. Qi Qi and Miss Minglu Qu for their assistance in my simulation and experimental work. I am also grateful to Dr. Zheng Li for the inspirations that I got from her work. In addition, I wish to express my gratitude to the technicians in the Heating Ventilation and Air Conditioning Laboratory of the BSE Department for their supports during my experimental work.

Finally, I would like to express my deepest appreciation to my family members: my wife, Yanping Liang, my parents and my brother. I could not have finished my work without their on-going loves, supports, patience and understandings.

Table of Contents

List of Figures

List of Tables

Nomenclature

Variable	Description	Unit
A	area	m^2
A_f	overall fin surface area of a DX cooling coil	m^2
A_m	minimum windward area of air flow	m^2
A_o	overall heat and mass transfer area in a DX cooling coil	m^2
A_p	overall outside area of tubes in a DX cooling coil	m^2
a	the linear coefficient relating the specific enthalpy of saturated moist air to air temperature	kJ/(kg ^oC)
B	louver fin perimeter	m
b	parameters in Eq. (8.11)	kJ/kg
C	a parameter defined by Eq. (5.19)	kg/(kg ^oC)
C_p	specific heat capacity	kJ/(kg ^oC)
C_{pa}'	specific heat capacity of moist air	kJ/(kg ^oC)
C_1	a ratio defined by Eq. (6.3)	ND
d_i	inside tube diameter	mm
d_o	outside tube diameter	mm
G_a	air mass flux based on minimum air flow area	kg/m^2s
H	overall heat transfer coefficient in the LMED method	m^{-2}
H_M	overall heat transfer coefficient in the m-LMED method	m^{-2}
h	specific enthalpy	kJ/kg
h_{fg}	specific latent heat of vaporization of water	kJ/kg
k	heat conductivity of the fin	W/(m ^oC)
L	length of the coil along air flow direction	m
Le	Lewis Number	ND
$Le^{2/3}$	Lewis Factor	ND
L_f	length of fin	m

M	a parameter defined related to Hong-Webb Equation	m^{-1}
M_{cond}	water vapor condensing rate in the entire DX cooling coil surface	kg/s
m	mass flow rate	kg/s
m_{cond}	water vapor condensing rate in the SPR	kg/s
N	number of tube rows	ND
P	the ratio of outside area to the length of an incremental control volume in Eq. (5.1)	m
Pr	Prandtl Number	ND
p_{asw}	ambient saturated water vapor pressure	kPa
p_l	longitudinal tube pitch	m
p_t	transverse tube pitch	m
q	total heat transfer rate	W
q_l	latent heat transfer rate	W
q_s	sensible heat transfer rate	W
RH	relative humidity of air	ND
Re	Reynolds Number	ND
R_o	equivalent outside radius	m
r_i	inside tube radius	m
r_o	outside tube radius	m
SHR	Sensible Heat Ratio	ND
Sp_a	ratio of supply air fan speed to its maximum speed	%
Sp_c	ratio of compressor speed to its maximum speed	%
S_f	fin spacing	m
S_p	fin pitch	m
T	temperature	^oC
T_{adp}	air dew point temperature	^oC
t	fin thickness	m
U_o	overall heat transfer coefficient of the cooling coil	W/ ($m^2{}^oC$)
$U_{o,w}$	overall heat transfer coefficient of wet cooling coil	m^{-2}
Un	uncertainty	%
W	length of the windward area in a DX cooling coil	m
W_f	width of the fin	m

w	moisture content	g/kg
x	spatial coordinate	m
Y	fin thickness	m

Greek symbols

α	convective heat transfer coefficient	W/(m^2 ^{o}C)
α_m	convective mass transfer coefficient	kg/(m^{2}s)
η	fin efficiency	ND
η_o	overall fin efficiency	ND
ε_I, σ_I, ζ_I	parameters in Eq. (8.22)	ND
ε_{II}, σ_{II}, ζ_{II}	parameters in Eq. (8.23)	ND
Φ	a dimensionless parameter defined related to Hong-Webb Equation	ND
Γ, Λ, Π, Ω, Ψ	parameters defined in Eq. (8.16)	ND
Θ	parameters in Eq. (8.29)	ND

Note: ND = No Dimensions

Subscripts

1	airside inlet of a cooling coil
2	airside outlet of a cooling coil
3	turning point in the partially wet condition
a	air or airside
c	cooling medium or cooling medium side
d	dry or dry-bulb
lm	logarithmic mean
r	refrigerant or refrigerant side
s	saturated condition
sf	airside surface area of cooling coil
t	total
w	wet or wet-bulb

List of Abbreviations

A/C	air conditioning
COP	coefficient of performance
DAS	data acquisition system
DX	direct expansion
EEV	electronic expansion valve
HVAC	heating, ventilation and air conditioning
LGU	load generating unit
PI	proportional-integral
PID	proportional-integral-derivative
RD	relative deviation
RTD	resistance temperature device
SPR	superheated region at refrigerant side
TPR	two-phase region at refrigerant side
VSD	variable speed drive

Chapter 1

Introduction

The development of air conditioning (A/C) technology is a natural consequence to both pursuing high quality living and working environment, and at the same time addressing the issue of sustainability. For small- to medium-scaled buildings, currently, the most commonly used A/C systems are of direct expansion (DX) type. DX A/C systems have a number of advantages when compared to larger central chilled water-based A/C installations. These include a higher energy efficiency, simpler system configuration and costing less to own and maintain. However, most DX A/C systems are equipped with single-speed compressors and supply fans, relying on on-off cycling compressors as a low-cost approach to maintaining only indoor air dry-bulb temperature, resulting in either space overcooling or an uncontrolled equilibrium indoor relative humidity (RH) level. With the advancement of A/C technology and the wider application of variable-speed drive (VSD) technology, it becomes possible for a DX A/C unit to have the speeds of its compressor and supply fan varied. Therefore, when there are changes in both sensible and latent cooling load in an air conditioned space served by a DX A/C unit, it becomes possible to simultaneously vary the speeds of its compressor and supply fan for simultaneous indoor temperature and RH control.

In order to better engage a DX A/C unit to simultaneously control the indoor

temperature and RH, it is necessary to study the characteristics of the simultaneous heat and mass transfer taking place in its DX cooling coil which is an important component in the DX A/C unit under different operating conditions.

This thesis starts with an extensive literature review on previously related studies on the heat and mass transfer in air cooling coils and its related modeling work. The fundamental issues of indoor RH and its effects on thermal comfort and indoor mould growth have been reviewed. A review of the previous studies on dehumidification using A/C systems and the established current strategies of controlling both indoor temperature and RH is also reported. This is followed by reviewing the previous work on modeling the simultaneous heat and mass transfer in DX cooling coils. A number of important issues requiring further in-depth research work to study the simultaneous heat and mass transfer in a DX cooling coil have been identified. These are the expected targets of investigation reported in this thesis.

The research proposal covering the aims and objectives, the project title and the methodologies adopted in this project is presented in Chapter 3.

Chapter 4 describes an experimental DX A/C station available to facilitate the research work reported in this thesis. Detailed descriptions of the experimental station and its major components are firstly given. This is followed by describing the computerized measuring devices and a data acquisition system (DAS). A computer

supervisory program used to operate and control the experimental station is also detailed. The availability of the experimental DX A/C station has been expected to be helpful in successfully carrying out the research work proposed in Chapter 3.

In Chapter 5 the development of a Calculation Method for the steady state Equipment Sensible Heat Ratio (SHR) of a DX A/C system is presented. The determination of Equipment SHR is essential for a satisfactory indoor thermal environmental control using a DX A/C system. The calculation method was experimentally validated. With the Method developed, the effect of refrigerant evaporating temperature on Equipment SHR at fixed inlet air conditions was theoretically analyzed.

Chapter 6 reports an experimental study on evaluating the dehumidification effect on the airside of the superheated region (SPR) in a DX cooling coil. Previously when investigating the heat and mass transfer performance taking place in DX cooling coils, a dry airside in the superheated region (SPR) was normally assumed without validation. This assumption conflicted with the experimental observation from an operating DX cooling coil. Therefore, an experimental study has been carried out to examine the validity of such an assumption under different operating conditions. A lumped parameter calculation procedure was developed specifically for processing the experimental data. The experimental results suggested that the airside surface of the SPR in a DX air cooling coil was either fully or partially wet under all

experimental conditions. Consequently, assuming a dry airside in the SPR could lead to an underestimated total amount of water vapor condensed on the entire airside of the DX cooling coil.

Chapter 7 reports on the development of a modified Logarithmic Mean Enthalpy Difference (LMED) method for evaluating the total heat transfer rate in a wet air cooling coil operating under both unit and non-unit Lewis Factors ($Le^{2/3}$) conditions. The development stemmed from the inaccurate assumption of Lewis Factor being unit in the existing LMED method, which has been extensively applied to modeling the combined heat and mass transfer taking place in DX and chilled water air cooling coils. The assumption resulted in calculation errors when non-unit Lewis Factors were encountered, which has been however observed by many researchers. The modified LMED (m-LMED) method has been therefore developed for calculating the total heat transfer rate under both unit and non-unit Lewis Factors. Although the m-LMED method was validated by comparing its prediction of the total heat transfer rate to that from numerically solving the fundamental governing equations of the heat and mass transfer in a wet chilled water cooling coil, the m-LMED method can also be applied to the DX cooling coils.

Chapter 8 presents the development of the analytical solutions for evaluating the heat and mass transfer in both a wet DX cooling coil and a wet chilled water cooling coil, respectively. The analytical solutions were validated by comparing their predictions

with those from numerically solving the fundamental governing equations of the heat and mass transfer taking place in wet air cooling coils. With the analytical solutions, the distributions of air temperature and moisture content along the air flow direction in either a wet DX or a wet chilled water cooling coil can be evaluated. The analytical solutions can be a low-cost replacement to numerically solving the fundamental heat and mass transfer governing equations.

The conclusions of the thesis and the proposed future work are presented in the final Chapter.

Chapter 2

Literature Review

2.1 Introduction

Heating, ventilation, and air conditioning (HVAC) technology has been developed for more than a century. The development of HVAC technology is a natural consequence to both pursuing high quality living and working environment and at the same time, addressing the issue of sustainability. The extensive use of mechanical-cooling based air conditioning (A/C) technology however started about 50-60 years ago. Currently, A/C installations have been widely seen in almost all types of buildings, like industrial, commercial and residential buildings for different purposes such as providing/maintaining a thermally comfortable living or working indoor environment to building occupants or an indoor thermal environment that is required by an industrial process. Very often, however, air conditioning is perceived as air cooling only, with air dehumidification being overlooked.

Such a simple understanding of A/C is neither sufficiently useful nor accurate. A/C is in fact a process of treating air in an internal environment to establish and maintain the required air state in terms of temperature, humidity, cleanliness and motion [Edward 1989]. This clearly suggests that these are the four basic parameters an A/C system will have to deal with.

For buildings located in hot and humid subtropics such as Hong Kong, serious indoor thermal environmental control problems, often in the form of a relatively higher indoor humidity level, may be experienced. In Hong Kong, summer is hot and humid from May through September, and most of the rainfall comes during this period. On the other hand, Hong Kong is also one of the most densely populated places in the world. Over 90% residential buildings are high-rise blocks, usually of 10 to 30 stories. Currently, with the increased household income and consequently the increased living standard, people would view A/C as an essential provision to maintaining a thermally appropriate environment in different types of buildings. In residential buildings, split-type, window-type and packaged-type direct expansion (DX) A/C units are commonly used. Consequently, the energy use by DX A/C units dominates the total residential energy consumption, at one third of the total electricity use in residential buildings in recent years [Lam 1996, Lam 2000].

A DX A/C unit is a piece of single packaged equipment that provides the basic functions of air distribution, outdoor air induction and filtration, and cooling / heating. This type of A/C installation has a number of advantages when compared to large central chilled water-based A/C installations, such as a simpler configuration, more energy efficient and generally costing less to own and maintain. Because of these advantages, DX A/C units are widely used in small-to-medium scaled buildings, in particular in residential buildings, in different parts of the world.

However, most DX A/C units are currently equipped with single-speed compressors and fans, relying on on-off cycling compressors to maintain only indoor air dry-bulb temperature, resulting in either space overcooling or an uncontrolled equilibrium indoor relative humidity (RH) level. Therefore, the use of an on-off controlled DX A/C unit often causes a reduced level of occupants' thermal comfort, in addition to poor IAQ and low energy efficiency [Fanger 2001, Brandemuehl and Katejanekarn 2004]. In order to improve the indoor thermal comfort level in buildings, in particular those located in hot and humid climates, served by DX A/C units, a number of novel control strategies have been developed to maintain an appropriate indoor comfort level and acceptable IAQ, while minimizing energy use. Accurately analyzing and modeling the heat and mass transfer taking place in a DX air cooling coil has been crucial in successfully developing the novel control strategies.

This Chapter firstly reviews the fundamental issues of indoor RH and its effect on thermal comfort, including both the sources of indoor moisture and the effects of RH level on thermal comfort and indoor mould growth. Secondly, a review of previous studies on dehumidification using A/C systems is reported. Thirdly, a review of the previous studies on established current strategies of controlling both indoor air temperature and RH using DX A/C units is presented. This is followed by reviewing the previous work on modeling the thermal performances of DX cooling coils. A number of important issues where further extensive research work is required are identified successfully in studying these issues will help better understand and more

accurately evaluate the fundamental heat and mass transfer taking place in DX air cooling coils, so as to provide a more solid foundation of developing novel control strategies for DX A/C systems.

2.2 Indoor RH level and its effect on human thermal comfort

2.2.1 Sources of indoor moisture

When the issue of indoor environmental control is addressed, it is important to look at the sources of indoor moisture, as the amount of moisture removal must be equal to the amount being introduced into an indoor space, both externally and internally.

2.2.1.1 External sources

Fundamentally, the external source for indoor moisture is the water vapor carried by outdoor air. It may be classified into three categories. The first is by water vapor diffusion through building envelope from outdoors. Moisture migrates from a place of high vapor concentration to a place of lower vapor concentration by diffusion through materials. As a result of diffusion, the moisture flow is a function of the difference in vapor partial pressure between the two sides of a supporting wall in a building, the permeability of construction materials and the exposed surface area

[Shakun 1992]. However, this category of moisture gains cannot be easily identified [Barringer and McGugan 1989]. The second is through the infiltration of outdoor air. The amount of moisture accumulated inside a conditioned space as a result of air infiltration is a function of infiltrated air mass flow rate and moisture content difference between outdoor air and indoor air. Although the infiltration through a building enclosure is intermittent and unintentional, it has been emphasized that its effects on indoor RH level cannot be overlooked [Kohloss 1981, Fairey and Keresteciogl u 1985, Straube 2002]. Henderson et al. [1992] concluded that infiltration would have a great impact on space latent cooling load by simulating a typical building in both Miami and Atlanta, USA. At a constant indoor air dry-bulb temperature of 25.5°C, the space latent cooling load would increase from at 11% of the total space cooling under an average infiltration rate of 0.54 air change per hour (ACH) to at 17% of the total under that of 1.08 ACH. In general, air infiltration impacts more than vapor diffusion on indoor RH levels, producing 10 to 200 times more water vapor than vapor diffusion [Shakun 1992, Harriman III et al. 2001]. The third and the most important is the outdoor air supplied through A/C systems. In ASHRAE Standard 62.2P, Ventilation and Acceptable IAQ in Low-rise Residential Buildings, there is a special consideration that the moisture from outdoor air is of particular concern in hot and humid climates [Sherman 1999]. For a conditioned space, it is apparently that the latent cooling load from ventilation air is greater than all other latent cooling loads combined [Brandemuehl and Katejanekarn 2004]. Most residential buildings require the ASHRAE-recommended minimum ventilation rate

to ensure IAQ and occupants' thermal comfort [McGahey 1998]. During occupied hours, both sensible and latent cooling loads from ventilation air are continuous. Furthermore, if the latent cooling load from ventilation air is allowed to blend into that of return air stream, a simple, constant-air volume DX A/C unit would have a very difficult time to remove it [Kohloss 1981**,** Berbari 1998, Harriman III and Judge 2002]. In particular during part load conditions in hot and humid subtropics, the latent cooling load from ventilation air would have greater effects on indoor RH than that at full load condition and therefore should receive more attentions. Assuming that the minimum outdoor air intake at all time is 20% of the supply airflow rate at design/full load, at half load operation, the ratio of outdoor air would change to 40% of the supply airflow rate. In other words, ventilation requirement dictates the increased percentage of outdoor air during part load operation. At the same time, outdoor air dry-bulb temperature is lower, close to indoor air dry-bulb temperature, but its dew point temperature is higher than that at design condition. Therefore, space sensible cooling load is reduced but space latent cooling load is increased [Shaw and Luxton 1988]. For example, according to a study by Lstiburek [2002], based on ASHRAE Standard 62.2P, for a single detached house (three bedrooms, 186 m^2), the desired controlled ventilation is quantified at 24 L/s, or between 0.15 and 0.2 ACH, based on typical house volume (ceiling height ranging between 2.4 m and 3 m). At part load conditions, the space latent cooling load is effectively doubled in this typical house when the required ventilation rate remains unchanged. The higher the moisture content of outdoor air, the higher the space latent cooling load a DX

A/C unit would have to deal with.

2.2.1.2 Internal sources

There are two internal sources for indoor moisture load. The first includes the moisture gains from occupants and other indoor activities, such as washing, cooking, etc. The second is however, related to the operation of a DX A/C unit. As in most buildings conditioned by DX A/C units, a supply fan in a DX A/C unit is usually operated continuously regardless of its compressor status. When the compressor is on, moisture is condensed over cooling coil surface and collected in a drain pan. However, if the supply fan is on when the compressor cycles off, moisture from the wet cooling coil and drain pan may be reintroduced into supply air stream due to constant air circulation, raising the RH level in a conditioned space [Khattar et al. 1987, Shirey 1993, Arens and Baughman 1996, Kosar et al.1998, Amrane et al. 2003, Shirey and Henderson 2004]. The amount of moisture re-evaporated depends on the physical characteristics of both the evaporator coil and drain pan such as fin spacing and pan slope, the thermostat cycling rate and the time constant of air conditioner latent performance at compressor start-up [Henderson and Rengarajan 1996].

Part of the moisture from the internal moisture sources becomes directly part of space latent cooling load, while others would be absorbed by internal surfaces of

building envelope and indoor furnishings, which may be regarded as “moisture capacitors”, such as wall paper, furniture and carpet etc., before a dynamic equilibrium of moisture transfer is achieved between indoor air and these capacitors.

For the moisture load which directly becomes part of space latent cooling load, such as those from occupants, indoor activities and reintroduced from a cooling coil, a parameter defined as indoor moisture generation rate (IMGR) can be used. IMGR is essential both to studying the effects of moisture generation on indoor RH level and to accurately predicting heat and moisture transfer for system design. Using a heat and moisture transfer model and the actual measured results from a test building, Lu [2003] compared the calculated indoor moisture content and RH by using the model with the measured values. When IMGR was assumed to be zero, both the calculated indoor moisture content and RH were lower than that measured. Therefore, IMGR must be taken into account [Henderson 1992, Trowbridge et al. 1994]. ASHRAE Handbook of HVAC Systems and Equipment 2000 correctly points out that the moisture load contributed by human occupancy depends on the number of occupants and the level of their physical activities, and recommends an average rate of moisture generation of 320 g/h for a family of four [ASHRAE 2000]. However, TenWolde pointed out that IMGR had no clear relationship with the number of occupants; other factors like domestic cleaning and plants may also contribute. Very often, IMGR value may have to be experimentally determined. Therefore, moisture production rates in residences would vary widely.

2.2.1.3 Moisture capacitors

There have been a number of previous studies on the moisture from internal and external sources absorbed by indoor "moisture capacitors". It has been estimated that as much as one third of the moisture generated in a room could be absorbed by its surfaces [Kusuda 1983]. It further indicated that the interaction between moisture storage and releasing can have impacts on indoor RH level. According to a research program carried out in Florida Solar Energy Center, if a building was cooled at nighttime with humid outdoor air, the building's internal surfaces would absorb moisture from outdoor air. If an A/C was used during the forthcoming day to cool the building, it experienced an additional space latent cooling load as the moisture absorbed was released from internal surfaces of envelope and indoor furnishings [Fairey et al. 1986]. This type of space latent cooling load also contributed to the starting load of an A/C unit [Bailey et al. 1996]. On the other hand, a larger number of methods have been developed to deal with the dynamic behavior of the moisture exchange between indoor air and the internal surfaces of building envelope. For example, Miller [1984] theoretically suggested using a simple resistor-capacitor electric circuit to describe the dynamic behavior. Plots of moisture content against time indicated that absorption rate appeared to follow an exponential decay. A finite element model and an implicit finite difference model to evaluate moisture absorption and desorption of building materials were developed by Fairey and

Keresteciogl u [1985]. In other studies, the lumped parameter analysis was used and an effective penetration depth theory was established [Keresteciogl ue et al. 1990]. More recently, Biot number was used to classify the building materials into three main categories, and then a governing equation had been established and solved by analytical-numerical method or transfer function method [El Diasty et al. 1993]. All of these methods have their own advantages, but they also have some limitations and are impractical to a certain extent.

Based on the discussions in this Section, it can be therefore observed that for an A/C unit, during part load operation in hot and humid subtropical regions, the sensible load imposed is reduced or may actually become negative. However, the mass transfer from both external and internal sources, which occurs in parallel to the heat transfer, will usually increase the space latent cooling load and therefore lead to the problem that indoor RH is out of control [Shaw and Luxton 1988, Brandemuehl and Katejanekarn 2004].

2.2.2 The effects of RH level on human thermal comfort

Previous studies on the levels of RH affecting IAQ and thermal comfort have shown that both a high and a low level RH can cause health problems to occupants. High levels of indoor air RH may cause health problems to occupants in spite of thermal

neutrality due to the growth on surfaces of contaminated aerosols produced by spray humidification systems [Arens and Baughman 1996]. In general, health-related agents in connection with indoor RH level include dust mites, fungi, bacteria, viruses, and nonbiological pollutants. It has been shown that an indoor RH level above 50% would help increase dust mites population. An indoor RH level above 70% would provide an excellent environment for the growth of fungi. Fungi and dust mites found inside residences have been identified as the main causes of asthma and hay fever [Arens and Baughman 1996]. All the agents affect human health, primarily through their inhalation of indoor air, although some of them have lesser effects through the skin. The discomfort caused by the uncomfortably high levels of insufficient cooling of the mucous membranes in upper respiratory tract by inhalation of humid and warm air, and skin humidity would increase the risk of individuals with allergies [Toftum and Fanger 1999]. In addition, a number of chemicals found indoors interact with water vapor to form respiratory and dermal irritants. Effects of high RH levels on chemical substances include increased off-gassing of formaldehyde from building and furnishing materials; combination with sulphur dioxide to form aerosols, salts and acids including sulphuric acid and sulphate salts; and increased irritative effects of odor, particles and vapors, for example acrolein [Sterling et al. 1985].

While a high RH level is problematic, a low RH level would also have comfort and

health impacts. Firstly, a low RH level can lead to the drying of skin and mucous surfaces, promoting the accumulation of electrostatic charges at fabric and other materials in buildings. On respiratory surfaces, drying can concentrate mucous to the extent that ciliary clearance and phagocytic activities will be reduced. Therefore, comfort complaints about dry nose, throat, eyes and skin often occur in low RH conditions, typically when the dew point is less than 0°C. A low RH level can also increase the susceptibility to respiratory disease as well as discomfort, for example asthmatics. Individuals with allergies, newborns and elderly are more susceptible to respiratory infections [Green 1982]. Secondly, a low RH level enhances the formation of ozone indoors. Very high ozone levels, in combination with poorly ventilated equipment, will also produce an irritating effect on the mucous membrane of eyes, nose, throat and respiratory tract. Thirdly, low RH levels are well known as a general catalyst of chemical interactions resulting in a large variety of irritants and toxic substances commonly referred to as “smog”. Indoor smog could well be responsible for a large proportion of similar symptoms of ozone. The smog is commonly associated with tight building syndrome occurring in office and commercial buildings [Sterling 1985].

2.2.3 Suitable range of indoor RH for thermal comfort

When indoor RH control is addressed, the value of moisture content is less important than that of RH, because practically the latter is more convenient to be measured. In summer, according to ASHRAE Handbook of Fundamentals 2001, the temperature range for comfort falls between 23°C and 26°C [ASHRAE 2001]. Similarly, a suitable indoor RH range is also required for assessing IAQ and thermal comfort.

Although the temperature dimension for measuring comfort has been well defined and supported by laboratory and field observations, the RH limits are less certain, particularly for the upper limit. At low RH levels, thermal sensation is a good indicator of overall thermal comfort level and acceptability. However, at high RH levels, it has been found that thermal sensation alone is not a reliable predictor of thermal comfort [Tanabe et al. 1987]. In addition, the upper limit of RH affects the design and operation of A/C units, as this determines the amount of dehumidification, influencing energy use, peak power demand, design and operation of both buildings and their engineering systems. In addition, the upper limit of RH determines the range of climatic conditions under which ventilative and direct evaporative cooling are available alternatives to conventional cooling [Fountain et al. 1999].

The upper limit of RH in the comfort zone is controversial and not clearly defined, as evidenced by the evolution of indoor RH standards, which has begun from the turn

of last century [Olesen and Brager 2004]. Prior to 1915, documentation from the American Society of Heating and Ventilating Engineers (ASHVE) focused almost exclusively on the ventilation rates for different classes of buildings, with indoor RH being rarely mentioned. In 1915, ASHVE introduced an upper RH limit of 50% as being desirable but not mandatory. In 1920, ASHVE adopted a "Synthetic Air Chart" with an air wet-bulb temperature limit of 17.8°C. For the next 75 years since the use of the Chart, the upper RH limit had changed between 60% and 100%. In 1932, ASHVE Ventilation Standard extended the Chart's upper RH limit to 70% across all temperatures. In 1938, ASHVE specified 75% as an upper limit and this value stayed over the next 20 years. In 1966, with the introduction of the ANSI/ASHRAE Standard 55, this upper limit of 75% was lowered to 60%. In 1974, the upper RH limit was set at a moisture content of 12 g/kg dry air (65% RH at 24°C dry-bulb temperature or at 16.8°C dew point temperature), which was still valid in 1981 Edition of ANSI/ASHRAE Standard 55 [Fountain et al. 1999]. In 1985, Theodore Sterling Ltd. and Simon Fraser University in British Columbia, Canada, completed a research project and established a widely accepted chart showing the optimum RH range between 30% and 60% [Sterling et al. 1985]. In 1989 and 1992 Editions, ANSI/ASHRAE Standard 55 specified the upper RH limit at 60%, based primarily on the considerations of mold growth. For ANSI/ASHRAE Standard 55, in 1992R and 2004 Editions, the recommended upper humidity limit was reversed to 12 g/kg dry air moisture content, which did not concern the condensation on building surfaces and contamination and damage to building components, and there were no

established lower humidity limits for thermal comfort [ANSI/ASHRAE 2004]. In addition, in ASHRAE Handbook of Fundamentals 2001, the ASHRAE summer comfort zone was confirmed as an area on a psychrometric chart between 23°C and 26°C dry-bulb effective temperature (ET), and between 2°C dew point temperature and 20°C wet-bulb temperature [ASHRAE 2001]. Furthermore, in ASHRAE Handbook of HVAC Systems and Equipment 2000, the range of acceptable RH was narrowed to between 30% and 60% at normal room temperature in order to minimize both the growth of bacteria and biological organisms and the speed at which chemical interactions occur [ASHRAE 2000]. Finally both ANSI/ASHRAE Standard 62-2001 Ventilation for Acceptable Indoor Quality and the United States Environmental Protection Agency (EPA) recommend that indoor RH be maintained between 30% and 60% to minimize the growth of allergenic or pathogenic organisms [ANSI/ASHRAE 2001]. Therefore, for all buildings, the upper limit should be set at 60% RH and the suitable range for indoor RH between 30% and 60% RH, while that for indoor air dry-bulb temperature should be between 23°C and 26°C.

2.3 Dehumidification using A/C systems

The use of HVAC systems for indoor thermal environmental control gains increasing attention, so that an optimal level of indoor RH may be reached and maintained to ensure a comfortable and healthy indoor environment. For buildings located in hot

and humid subtropical region, indoor RH level is often higher than the recommended level, thus dehumidification using A/C systems becomes necessary. There are mainly two types of dehumidification used in A/C systems: mechanical dehumidification and chemical dehumidification.

2.3.1 Mechanical dehumidification

Mechanical dehumidification, utilizes mechanical means to cool air and so to dehumidify it. If the air comes into contact with a cooling coil whose mean surface temperature is lower than air dew point temperature, condensation of a part of the water vapor in the air and thus dehumidification is obtained. The moisture content of air leaving a cooling coil depends on the apparatus dew point of the coil, which is principally a function of either the refrigerant temperature inside the coil when a DX cooling coil is used, or the chilled water temperature when a chilled water coil is used. To increase the dehumidification capacity of a cooling coil, it would be better to use a large number of fins, with a moderate air velocity and a low fin density [Mazzei et al. 2005]. The dehumidification behavior of a standard cross-flow type plate fin heat exchanger, used as a dehumidifier and cooler, was investigated by Saman and Alizadeh [2002] both experimentally and numerically. In many HVAC systems, mechanical dehumidification has strong advantages at a higher dehumidifying demand where cooling is needed in addition to dehumidification

because a cooling coil cools and dehumidifies the air simultaneously. It is energy efficient compared to other methods of removing moisture from air. However, the disadvantage of mechanical dehumidification is that because the sensible cooling capacity and latent cooling capacity of a cooling coil are coupled, it is not easy to simultaneously control temperature and RH of the air leaving the cooling coil. Therefore, energy is often wasted in the traditional HVAC systems by over cooling and reheating the air to maintain an appropriate level of RH in spaces.

2.3.2 Chemical dehumidification

Chemical dehumidification removes the moisture from the air by transferring it to a water absorbing material such as desiccants through adsorption or absorption. Desiccants are materials with a high affinity for water vapor and may be in the form of either solid or liquid. If the physical or chemical nature of the desiccant, generally being solid for example silica gel, remains unchanged in a dehumidification process, then adsorption takes place. On the other hand, absorption takes places when a change occurs, generally with liquid desiccants. Liquid desiccants are used as a dehumidification agent in many industrial applications and have been studied for use in space air conditioning applications [Peng and Howell, 1981]. A mathematical model for analyzing heat and mass transfer in an absorber was developed by Saman and Alizadeh [2002]. Dehumidification equipment using solid desiccant may be

classified into two types, active type and passive type. The equipment using heated reactivation air is called an active dehumidifier. The heat used for reactivation often comes from distributed power generation or natural gas, all of which are inexpensive during humid seasons. A passive dehumidifier however, uses a building's dry exhaust air instead of heated air for reactivation [Harriman III et al. 2001, Harriman III et al. 1999]. A solid-desiccant based dehumidifier is more compact, but presents a higher pressure drop for both the air to be dehumidified and the air for regeneration, therefore, a higher fan power is required. The final temperature of the processed air is always high, leading to a decrease of the adsorption capacity of desiccant. In addition, heat generated by a solid desiccant dehumidifier affects thermal comfort [Andersson and Lindholm 2001, Capehart 2003, Subramanyam et al. 2004, Alpuche et al. 2005].

On the other hand, comparing to a solid desiccant-based system, a liquid desiccant-based system needs a lower fan power. The use of a liquid desiccant-based system can help more easily control the air temperature during absorption, resulting in a lower temperature of the processed air. Another advantage of using liquid desiccant is better air cleaning. It is believed that the liquid desiccant's washing action in hospital environment would both reduce airborne bacteria and remove particulate matter [Dai et al. 2001, Dieckmann et al. 2004, Rowland et al. 2005, Elsarrag et al. 2005]. Latent heat and sensible heat of water vapor extracted from the air are dumped into cooling water of the absorber, in order to keep low dew point of

the processed air. This operation is cooled by a chiller, thus requiring further additional operating costs. Therefore the operating costs using desiccants for dehumidification are higher when compared to other indoor RH control strategies [Lstiburek 2002].

2.4 Indoor environmental control with an emphasis on RH control using DX A/C units

For buildings located in hot and humid climates, the provisions of A/C installations have become indispensable. DX A/C systems are widely seen in small- to medium-scale buildings for indoor thermal environmental control. Much research work has been undertaken, focusing on temperature control using DX A/C units. For the design and application of DX A/C units, indoor RH control however, still remains problematic.

2.4.1 Problems experienced in indoor RH control

When the issue of indoor RH control is addressed, it is worthy mentioning both sensible load which is temperature related and latent load which is moisture related, as well as the SHR which is defined as a ratio of sensible load capacity to the total

load capacity. An Equipment SHR for an A/C unit occurs at a cooling coil, but an Application SHR occurs in a conditioned space. An Equipment SHR is largely a function of a cooling coil's dew point, the larger the temperature difference between the coil surface temperature and the entering air wet-bulb temperature, the greater the ability the coil has to remove excess moisture. How A/C units are designed, operated and controlled would govern the coil surface temperature. On the other hand, an Application SHR depends largely on the latent cooling load generated within a building, infiltrated through envelope or introduced as ventilation requirement. Part load operation can affect an Equipment SHR, as well as an Application SHR [Amrane et al. 2003].

The main problem for indoor environmental control with a DX A/C unit stems from the unit's inherent characteristics. A DX A/C unit removes moisture as a by-product of a cooling process. The current trend in designing an A/C unit is to have a smaller moisture removal capacity, in an attempt to boost its energy-efficiency ratings (EER) and Coefficient of Performance (COP) [Kittler 1996]. The method used to improve efficiency is to increase the heat exchanger surface area. Such a strategy allows an A/C unit to run at a higher refrigerant temperature in its evaporator and a lower refrigerant temperature in its condenser, resulting in a lower latent capacity of the unit.

As a result, the Equipment SHR of standard residential DX A/C units has been

designed at between 0.7 and 0.8 at the Standard ARI rating conditions (the dry-bulb and wet-bulb temperatures for the air entering the cooling coil are 26.7°C and 19.4°C, respectively, and the dry-bulb outdoor air temperature is 35°C) [Henderson et al. 1992, Shirey 1993, Kittler 1996, Lstiburek 2002, Amrane et al. 2003, Westphalen 2004]. However, for many buildings experiencing higher ratios of space latent cooling load at between 40% and 50% of the total, the corresponding Application SHRs are too low. It is therefore not possible for standard DX A/C units to deal with such a large space latent cooling load, even when the total output cooling capacity from a DX A/C unit is equal to the total space cooling load. Therefore, potentially an A/C unit will provide a desired temperature control but not a desired humidity control [McGahey 1998, Murphy 2002, Westphalen 2004, Brandemuehl and Katejanekarn 2004, Westphalen et al. 2004]. This inadequacy was demonstrated in a study by Kohloss [1981] and was further confirmed by Katipamula et al. [1988]. In hot and humid subtropics, such as in Houston, Texas, USA, an A/C unit with an Equipment SHR greater than 0.8 failed to maintain indoor conditions within ASHRAE comfort zone for as much as 30% of its operating time.

The second problem for indoor environmental control using DX A/C units is capacity match during part load operation. A DX A/C unit is usually sized for full load with safety margins and, therefore, is oversized for part load operating hours [Khattar et al. 1987]. When a DX A/C unit is suitable for full load operation, it would be a final insult to the building and its occupants during part load conditions

with relatively low sensible heat factors accompanied by a further requirement on indoor RH control. Although at a steady-state operational condition, the numerical values of both Equipment SHR and Application SHR are equal to each other, the total output cooling capacity may be larger than the reduced total space cooling load; there can be either surplus or deficit of both sensible and latent components in the total output cooling capacity. Therefore, the air conditioned space may be overcooled or indoor RH would rise to above the design level [Shirey 1993, Berbari 1998, Lstiburek 2002, Murphy 2002, Harriman III and Judge 2002, Amrane et al. 2003, Hourahan 2004, Shirey and Henderson 2004]. Under the part load conditions, A/C units oversized by 20% might achieve space latent cooling load removal of approximately 15% of the total, whereas, correctly sized A/C units would achieve moisture removal of up to approximately 30%. Even with correctly sized standard systems, the part load problem associated with latent load remains, albeit not to the same extent [Lstiburek 2002]. Furthermore, when a DX A/C unit is operated at part load conditions, indoor RH control problem would become worse with on-off cycling its compressor. The compressor will remove the sensible load with very little run-time to easily satisfy the thermostat setpoint and cycle off long before moisture removal can be affected [Jalalzadeh-Azar et al. 1998, Hourahan 2004].

The third problem is related to energy consumption. Usually, overcooling occurs as air has to be cooled to a suitable low dew point temperature to remove the space latent cooling load, but reheating is required to avoid overcooling a space. The

challenge is that the limited natural resources cannot keep pace with this wasteful method for dehumidification [Coad 2000]. Recognizing the need for a revised energy standard, ASHRAE has eliminated the use of additional energy for reheating for constant-air-volume (CAV) systems with their design cooling capacities exceeding 40000 Btu/h (11724 W) [Hickey 2001]. On the other hand, after being more informed and aware of the importance of energy conservation and high energy cost, occupants have raised their thermostat setpoints in summer to avoid overcooling. As a result, some buildings suffer from poor IAQ problems such as high indoor RH level and mold growth [Kurtz 2003]. These situations could well be exacerbated when a low ventilation rate is used for energy conservation and when there is inadequate exhaust of indoor moisture sources [Arens and Baughman 1996].

2.4.2 Applying variable-speed compressor and supply fan in a DX A/C unit

For a DX A/C unit, the sensible and latent components of its total output cooling capacity may be altered by varying its supply fan speed and compressor speed simultaneously. One available strategy is to control the space temperature by varying compressor speed and the space RH level by varying supply fan speed, separately. Variation of the two speeds enables variation of the sensible and latent components of the total output cooling capacity of a DX A/C unit [Krakow et al. 1995].

An experimental verification for the feasibility of such a control strategy was carried out by Krakow et al. [1995]. The conditioned space was a 76.5 m^3 room on the ground floor of a large building in Canada. The experimental results illustrated that the space temperature and RH were maintained within ±0.3°C and ±2.5% RH, respectively, of their setpoints. The sensible and latent components of the A/C unit's output cooling capacity appeared to respond to the variations of the applied and transmitted space cooling loads. The applied space cooling load on the A/C unit consisted of the heat output from electrical-resistance space heaters and a humidifier. The transmitted space cooling load consisted of indeterminate amounts of heat conducted through external and internal envelope, etc. A numerical simulation model incorporating Proportional-Integral-Differential (PID) control was also developed. The experimental and simulation results confirmed the feasibility of this control strategy. However in this study, only simple comparisons and analysis were given, without revealing detailed temperature and RH data and the related energy consumption. Moreover, it was observed from the experimental results that the transient behaviors were poor, as it took approximately 2 hours after increasing the power input to the humidifier for indoor RH to return to its original level before the disturbance.

In addition, in the simulation study carried out by Andrade et al. [2002], a detailed physically based A/C simulation model was augmented by adding load equations describing space sensible and latent cooling loads experienced by a typical

residential building. The simulation results showed that the use of a variable-speed compressor and a variable-speed supply fan can help prevent short on-off cycling and improve indoor RH control while possibly increasing system efficiency by having different combinations of compressor and fan speeds at the expense of running a DX A/C unit longer. This study was essentially for on-off cycling, not continuous control over the condensing unit in a DX A/C unit. Li and Deng [2007] experimentally investigated the total cooling capacity and SHR under different combinations of compressor speed and fan speed under fixed indoor air temperature and RH. The experimental results revealed the inherent operational characteristics of a DX A/C system having a variable-speed compressor and an air supply fan. Based on these experimental results, a control-algorithm was developed by Li and Deng [2007a, 2007b] using Application SHR as a controlled variable to simultaneously control space air temperature and RH.

It can be seen that all the problems mentioned in Section 2.4.1 stem from the mismatch between Equipment SHR and Application SHR and that between the total cooling capacity and the total cooling load. Although Li and Deng's experimental results for the inherent operational characteristics of a DX A/C system having a variable-speed compressor and an air supply fan can be applied to determine the Equipment SHRs and the total cooling capacities of the DX A/C system under different combinations of compressor speed and fan speed. They were obtained at a fixed combination of indoor air temperature and RH.

2.5 Modeling DX cooling coils

The research work based on mathematical modeling has gained more and more recognition because it could not only save the cost of research and development work, but also help understand the operational characteristics of a physical system under study over its entire operating range. It can help investigate the operational performance of a system, to verify the feasibility of a new control strategy and to detect and diagnose the faults of a system, etc. Modeling heat exchangers has always been in the spotlight of simulation-based research work for HVAC and Refrigeration systems. For a DX A/C system, the thermal performance of the evaporator (or DX air cooling coil) is the most important part when modeling the complete system.

There are two sides in a DX cooling coil: airside and refrigerant side. At its refrigerant side, a DX cooling coil (evaporator) can be assumed to have two regions according to the status of refrigerant, a two-phase region (TPR) and a superheated region (SPR). Refrigerant enters the TPR as a mixture of vapor and liquid at evaporating pressure with a specific vapor fraction. When flowing through the cooling coil, liquid refrigerant absorbs the heat from the air and vaporizes. The two-phase ends and the SPR commences at the point where all liquid refrigerant vaporizes and the vapor fraction becomes unity.

On the other hand, at the airside, either a dry cooling process, i.e., no dehumidification effects, or a wet cooling process, i.e., with simultaneous cooling and dehumidifying, may take place.

2.5.1 Correlations of the thermodynamics of refrigerants

In accordance with the Montreal Protocol, R22 will be gradually phased out by 2020. Currently, more environmental friendly alternative refrigerants, such as R134a, R410a and R407c, have been widely used in HVAC&R systems. This is particularly true in developed countries and regions.

In practice, the working fluid in the refrigeration circuit of a DX refrigeration plant is a mixture of refrigerant and lubricating oil or contaminants. The compositions perhaps vary from case to case, affecting the thermodynamic properties of a pure refrigerant. In order to well understand the effects of thermo-physical properties of refrigerant on the operating performance of a refrigeration plant, Martz et al. [1996] and Hesse and Kruse [1988] attempted to predict the thermodynamics of oil refrigerant mixtures through mathematical modeling. However, because the exact molecular composition of lubricating oil was diversified and often difficult to be ascertained, the precision and applications of their models for oil refrigerant mixtures to the simulation-based research were limited. On the other hand, the modification of a refrigerant thermodynamic model considering the presence of oil would make the

dynamic simulation for a DX A/C system much more complicated, but would be of little help to study its control performance.

In 1981 Chan and Halselden [1981a, 1981b, 1981c] published a set of computer subroutines for refrigerant thermodynamic properties. These have been widely used because they were based on the recommendations of a Working Party set up by International Institute of Refrigeration (IIR) and hence were authoritative. In order to incorporate a model representing the thermodynamic properties of a particular refrigerant into a dynamic simulation model of a refrigeration system, in 1986, Cleland [1986] published a set of curve-fitting polynomial equations of refrigerants that were computationally much quicker than those by Chan and Haselden. The Cleland equations agreed well with those by Chan and Haselden with deviations of about 0.25%, which was tolerable for simulation-based research. Because the above mentioned equations for refrigerants were of implicit nature, iteration was often inevitable. Based on the Sectional Smooth Technique, Ding et al. [1992] and Zhang et al. [2000] developed a cubic linear function, which was implicitly data-fitted but could be solved explicitly, for refrigerant thermodynamic properties that can avoid iteration. In 1994, Cleland [1994] extended his curve-fitting correlations, which were firstly proposed in 1986 and have been widely accepted since, to include the correlations for refrigerant R134a. His correlations were based on the data set for R134a published by the IIR and the range of saturation temperature was -40 ^{o}C to 70 ^{o}C. Furthermore, calculations of the refrigerant heat transfer rate were also seen [Gungor and Winterton 1987, Shah 1982, Kandlikar 1990, Boissieux et al. 2000].

2.5.2 Correlations of the airside heat transfer coefficient

When modeling a heat exchanger, its heat transfer and fluid flow characteristics are embodied in the mathematical correlations of heat transfer coefficients and the total pressure drop. For a refrigerant-to-air heat exchanger using various finned tube for heat transfer enhancement, the airside heat transfer resistance may account for over 80% of the total heat transfer resistance. Hence, the correlations of the air-side heat transfer coefficient would significantly affect the modeling accuracy of the overall heat transfer. A set of relatively simple correlations for the average heat transfer coefficient for a plate-finned tube was developed by Turaga et al. [1988]. An experimental comparison by Corberan and Melon [1998] showed that the correlations for a multiple-row heat exchanger having flat fin provided by Gray and Webb [1986] agreed well with the experimental data. It was recommended that an airside heat transfer coefficient for wavy and louvered fins, which were widely used in air conditioning & refrigeration installations, could be evaluated using the coefficient for a flat fin and multiplying it by an enhancement factor appropriate to a given fin design. Webb [1990] developed an enhancement factor correlation for wavy fins that could take into account the flow conditions and geometric variables of a heat exchanger. Currently, the most commonly enhanced surface used in DX A/C systems is of louvered fin type that can result in a higher average heat transfer coefficient. Wang et al. [1999, 2000a and 2000b] proposed general heat transfer correlations for louvered fin geometry having round tube configurations under both

dry and wet conditions, respectively. A total of 49 samples of louvered fin-and-tube heat exchangers with different geometric parameters, including louver pitch, louver height, longitudinal tube pitch, transverse tube pitch, tube diameter and fin pitch, were included in the correlations developed.

2.5.3 Modeling the heat and mass transfer taking place on the airside of DX air cooling coils

On the airside of both DX air cooling coils and chilled water cooling coils, simultaneous heat and mass transfer takes place when the temperature of the airside surface is below the dew point temperature of air. Consequently, the airside surfaces of the cooling coils are hence wet. There are generally three approaches to modeling the thermal performances of wet cooling coils: 1). lumped parameter models; 2). distributed numerical models; 3). analytical solutions to the fundamental governing equations.

Most of the models developed are either lumped parameter based or distributed parameter based. Lumped parameter models are convenient in application because the spatial distributions of air temperature, RH and the temperature of either chilled water or refrigerant are not calculated. It is critical when a lumped parameter model is developed to determine the driving force of the heat and mass transfer between hot

and cold sides. The driving force for simultaneously transferring both the heat and mass from warm and moist airside to chilled water or refrigerant side in a wet cooling coil is not the same as that for only transferring heat in a dry cooling coil. In the case of heat transfer only, the driving force is the temperature difference between hot side and cold side. For dry cooling coils, logarithmic mean temperature difference (LMTD) as shown in Eq. (1.1), and Effectiveness-Number of heat transfer units (ε-NTU) methods are generally used.

In the case of simultaneous heat and mass transfer, however, the enthalpy difference between the air and the cooling medium (chilled water or refrigerant) has been used as the driving force [Threlkeld, 1970]. The total heat transfer rate can be evaluated by the product of an overall heat transfer coefficient, surface area and the logarithmic mean enthalpy difference (LMED) as shown in Eq. (1.2)

$$q_d = U_{o,d} A_o \Delta T_{lm} \tag{1.1}$$

$$q_w = U_{o,w} A_o \Delta h_{lm} \tag{1.2}$$

where q_d and q_w are the total heat transfer rates in a cooling coil under a dry condition and a wet condition, respectively; $U_{o,d}$ and $U_{o,w}$, the overall heat transfer coefficients under a dry condition and a wet condition; ΔT_{lm} and Δh_{lm}, the logarithmic mean temperature and enthalpy differences, respectively; A_o, the overall

heat transfer area.

Analogous to the LMTD method, the use of LMED method provides a quick and convenient means to predicting the thermal performances of DX or chilled water air cooling coils. Hence since its proposition, this method has been widely used [Elmahdy and Mitalas 1977, McQuiston 1978, McQuiston and Parker 1994, Jacobi and Goldschmidt 1990, ASHRAE Fundamentals 2005, Theerakulpisut and Priprem 1998, Jin et al. 2006].

The equivalent dry-bulb temperature (EDT) method is another lumped parameter modeling approach proposed by Wang and Hihara [2003]. With the definition of EDT method, the description of driving force is replaced by equivalent dry-bulb temperature difference rather than enthalpy difference, yielding

$$q_w = \alpha_{a,w} A_a (T_{a,d}{}^e - T_s) \tag{1.3}$$

where $\alpha_{a,w}$ is the airside heat transfer coefficient under wet condition; A_a, the airside heat transfer area; T_s, the airside surface temperature; $T_{a,d}{}^e$, the equivalent dry bulb temperature of moist air, which can be obtained from the constant enthalpy line in the psychrometric chart. The EDT method was shown to be capable of predicting the thermal performance of cooling coils and has therefore been used in previous studies [Xia and Jacobi 2005, Huzayyin et al. 2007].

Although lumped parameter models are convenient in calculation, certain assumptions are inevitably necessary. These assumptions would include: 1) a linear relationship between enthalpy of saturated moist air and its temperature in calculating the overall heat transfer coefficient; 2) unit Lewis number in establishing the linear relationship between the total heat transfer rate and the enthalpy difference in a micro-scale element; 3) constant thermal properties for air and cooling mediums; 4) one dimensional counter- or parallel- flow cooling coils to represent three dimensional cross flow cooling coils. These assumptions would apparently lead to some calculation errors when using the lumped parameter method.

Distributed parameter numerical models are developed based on the fact that the variations of all the thermal variables, such as the temperatures and moisture contents of air and the temperatures of chilled water or refrigerant, are continuous along their own flow directions. Therefore, it is reasonable to divide an entire cooling coil into many connected micro-scale elements in which the spatial distributions of the thermal variables are neglected, while the differences of the thermal variables in different elements can be evaluated to reflect the distributions of the thermal variables in the cooling coil. Fundamental differential governing equations of heat and mass transfer are discretized and calculated iteratively. Therefore, distributed numerical models are able to provide accurate results at the expense of requiring more computational time and space.

Distributed parameter numerical models for air cooling coils can be seen in a large number of published literatures [Myers et al. 1970, Ramachandran 1984, Kabelac 1989, Hill and Jeter 1991, Mirth and Rmadhyani 1993, Vardhan and Dhar 1997, Yu et al. 2005, Jin et al. 2006, Jia et al. 1995, Jia et al. 1999, Liang et al. 2001, Byun et al. 2007]. Normally, the results of distributed parameter numerical models may be used as a basis to validate the results of other types of models because of their accuracy.

Using analytical models is the third approach to investigating the thermal performance of wet cooling coils. When developing an analytical model, the fundamental differential governing equations are analytically solved. The solutions can then be used to determine the variations of all the thermal variables along air and cooling medium flow directions. Because of the complexity of air cooling coils in actual applications, not many analytical models have been proposed for evaluating the thermal performance of an entire DX air cooling coil which is normally a fin-and-tube heat exchanger, except an analytical model developed for the fin in a fin-and-tube air cooling coil [Xia and Jacobi 2004]. Furthermore, analytical models have also been developed to investigate the thermal performance for other types of heat exchangers [Klein and Eigenberger 2001, Kabashnikov et al. 2002, Bielski and Malinowski 2005, Ren and Yang 2006, Bandyopadhyay et al. 2008].

2.5.4 Equipment Sensible heat ratio (SHR) for DX air cooling coils

For a DX cooling coil, its Equipment SHR is an important parameter as discussed in Section 2.4.1, [Lstiburek 2002, Amrane et al. 2003, Hourahan 2004]. The value of Equipment SHR of a DX cooling coil is strongly related to its operation thermal performance, and may be evaluated through modeling the DX cooling coil.

An experimental study of the inherent operational characteristics of a DX A/C unit with a viable-speed compressor and a variable air supply fan at fixed inlet air temperature and RH to the cooling coil suggests that it is evaporating temperature, T_r, which varies with both compressor speed and the mass flow rate of supply air influencing the value of Equipment SHR [Li and Deng 2007]. In addition, a study of Equipment SHR of a chilled water cooling coil was conducted by Wang et al. [Wang et al. 2007]. A model was developed for a chilled water cooling coil where sensible and latent heat transfer was decoupled. The coil was divided into 10 parts and Equipment SHR in each part was assumed to be constant. The results illustrated that a higher inlet air RH would lead to a lower Equipment SHR. Although Equipment SHR of a DX cooling coil is an important parameter for controlling the indoor thermal environment, its theoretical or numerical analysis has not been seen in open literature.

2.5.5 Fully wet, fully dry and partially wet conditions

When a DX cooling coil is operated under different operating conditions, there can be three different surface conditions at its airside: fully wet, fully dry and partially wet. These three different conditions will have to be dealt with when modeling a DX cooling coil.

When the air dew point temperature is equal to or greater than the fins' tip temperature in a finned cooling coil, all fins and tube surfaces are wetted and the coil is operated at a fully wet condition. When the air dew point temperature lies between the fins' tip temperature and fins' base temperature (tube surface temperature), only the tube surfaces are wetted and the entire coil surface becomes partially wet. When the air dew point temperature is lower than the fins' base temperature, no condensation occurs and the coil is operated under a fully dry condition. In order to fully understand the heat and mass transfer performance of a cooling coil in actual operation, its surface condition should be determined firstly. The first step of the process to determine the surface condition of an individual fin is to assume temperatures at both fin base and tip. The temperatures are calculated from air-fin convective heat transfer rate and the conductive heat transfer rate inside the fin. Finally, the assumed and calculated fin base and fin tip temperatures are compared. The above process will be repeated if the calculated and assumed temperatures are

not equal. With these temperatures, the surface condition of a cooling coil can then be determined.

For the three surface conditions, the LMED method can be applied to the fully wet condition, and the LMTD method can be applied to the fully dry condition, while the EDT method can be applied to the partially wet condition [Wang and Hihara 2003, Huzayyin et al. 2007].

Partially wet is the most complicated surface condition among all the three because the ratio of the dry part surface area to the wet part surface area should be taken into account when evaluating the thermal performance in a partially wet cooling coil. Therefore, distributed parameter numerical models are more applicable to a partially wet cooling coil and it has been widely adopted in published literatures [Oskarsson et al. 1990, Ragazzi 1995 Judge et al. 1997, Liang et al. 2000, Pirompugd et al. 2006, Pirompugd et al. 2007].

Few analytical models have been found in modeling the thermal performance of a partially wet cooling coil for different surface conditions in published literatures. However, analytical models are adopted for evaluating the thermal performances of a single fin and a fin assembly [Wu and Bong 1994, Salah El-Din 1998, Kazeminejad 1995, Kundu 2007].

As mentioned earlier, a DX air cooling coil in actual operation can be assumed to have two regions, i.e., TPR and SPR at its refrigerant side. In previous distributed parameter models [Chi and Didion 1982, MacArthur 1984, Wang and Touber 1991, Jia et al. 1995, Jia et al. 1999] and lumped parameter models [Fisher and Rice 1983, Mullen et al. 1997, Theerakulpisut and Priprem 1998, Deng 2000, Qi and Deng 2008], a dry airside surface of SPR was assumed without a detailed analysis.

2.5.6 Non-unit Lewis Factor

Lewis number is a dimensionless number defined as the ratio of the thermal diffusivity to the mass diffusivity of the same substance. It is used to characterize fluid flows where there is simultaneous heat and mass transfer by convection. Using Lewis number, *Le*, or Lewis Factor, i.e., $Le^{2/3}$, the mass transfer coefficient, α_m, is correlated to heat transfer coefficient, α_a, as follows.

$$\alpha_m = \alpha_a (C_{pa} Le^{2/3})^{-1} \tag{1.4}$$

where C_{pa} is the specific heat capacity of air.

In a lumped parameter model, the enthalpy difference between air and a cooling medium is treated as the driving force of simultaneous heat and mass transfer. Such a

treatment was firstly proposed by Threlkeld, based on the assumption of unit Lewis Factor [Threlkeld 1970], and has been widely adopted [Elmahdy and Mitalas 1977, Fisher and Rice 1983, Jacobi and Goldschmildt 1990, Mullen et al. 1997, Theerakulpisut and Priprem 1998, Deng 2000, Wang and Hihara 2003, Yu et al. 2005]. It was recommended by ASHRAE [22]. However, a number of studies have also suggested that the Lewis Factor may well deviate from being one. Hong and Webb [Hong and Webb 1996] suggested that Lewis Factor was between 0.7 and 1.1. Seshimo et al. [1988] also suggested a value of 1.1. Eckels and Rabas [1987] reported similar values of 1.1 to 1.2, based on their test results for plain-fin-and-tube cooling coils. Pirompugd et al. [2007] also reported that Lewis Factor ranged from 0.6 to 1.1. In addition, Wang [2008] considered that Lewis Factor would slightly decrease as the Reynolds Number increased.

The use of unit-Lewis Factor assumption can lead to errors when a lumped parameter model is used in evaluating the thermal performances of air cooling coils. Xia and Jacobi [2005] pointed out that an error of 8% could be introduced in the total heat transfer rate, at a sensible heat ratio of 50%, as the value of Lewis Factor changed from 1 to 1.16. Hence, the previous lumped-parameter models using unit-Lewis Factor assumption cannot accurately evaluate the simultaneous heat and mass transfer in DX cooling coils. However, for distributed parameter models and analytical solutions, it is not necessary to assume a unit Lewis Factor, when simultaneous heat and mass transfer was encountered. Ren and Yang [2006]

developed an analytical solution model for the simultaneous heat and mass transfer process in a parallel/counter indirect evaporative cooler under real operating conditions. In this investigation, non-unit Lewis Factors were used in the calculation. However, developing analytical solutions for the heat and mass transfer taking place in a DX cooling coil involving both unit and non-unit Lewis Factors has not been reported.

2.6 Conclusions

The development of air conditioning technology is a natural consequence to both pursuing high quality living and working environment, and at the same time, addressing the issue of sustainability. Compared to large central chilled water-based A/C installations, DX A/C systems have a number of advantages, such as simpler configuration, higher energy efficiency and generally costing less to own and maintain. Because of these advantages, DX A/C systems have been widely used in small- to medium- scaled buildings.

As presented in Section 2.4.1, for buildings using DX A/C units for indoor thermal environmental control, the key problem for indoor thermal environmental control is the mismatch between the output sensible and latent cooling capacities from the DX A/C units and the space sensible and latent cooling loads. In order to efficiently

control both the indoor air temperature and RH, variable-speed compressors and air supply fans have been used in DX A/C systems. Previous related studies indicated that both indoor air temperature and RH may be controlled within suitable ranges by varying simultaneously the speeds of both compressor and supply fan.

Various control strategies have been developed for controlling DX A/C systems to maintain comfortable indoor thermal environment. Some of these control strategies are established based on the understandings of the operating characteristics of DX A/C systems having variable-speed compressors and supply fans. On the other hand, simulation-based research work has been regarded as an efficient and effective means to investigate the operating characteristics and control performance of a DX A/C system. When modeling an entire DX A/C system, modeling the thermal performance of its DX cooling coil has always been the most important part of the work.

In a DX cooling coil, normally simultaneous heat and mass transfer takes place when the dew point temperature of air is higher than the temperature of coil surface. This simultaneous heat and mass transfer process has complicated the modeling of the thermal performance of a DX cooling coil.

To numerically investigate the quantitative relationship between the heat and mass transfer rate in a DX cooling coil, Equipment SHR may be used. The mismatch

between the Equipment SHR of a DX A/C unit and the Application SHR of a space served by the DX A/C unit would result in an uncontrolled indoor thermal environment. The determination of the Equipment SHR under different operational conditions is essential to understand the operating thermal performance of a DX cooling coil and to further develop effective control strategies. However, as reported in Section 2.5.4, a detailed calculation method to numerically evaluate the Equipment SHR of a DX cooling coil under different operating conditions is not seen in the open literatures.

Mathematical models have been developed to describe the operating characteristics of DX cooling coils. Most of these models can be divided into two categories: distributed parameter models and lumped parameter models, respectively. Distributed parameter models require greater computational efforts and may potentially encounter numerical instabilities. However, Section 2.5.5 shows that in lumped parameter models, a dry airside in a SPR of a DX cooling coil has been commonly assumed. To accurately evaluate the dehumidification effect of an entire DX cooling coil, there is a need to re-examine the dry airside assumption.

In both lumped and distributed parameter models, Lewis number has always been assumed to be one, as discussed in Section 2.5.6. However, previous experimental results have suggested that Lewis number, or Lewis Factor, may deviate from one. Therefore, the unit Lewis Factor assumption can result in calculation error. A

calculation method for evaluating the thermal performance of a DX cooling coil under both non-unit and unit Lewis Factors should be developed.

The literature review presented in this Chapter has identified a number of important areas where further in-depth research work is required. These are the expected targets of the investigation reported in this thesis.

Chapter 3

Proposition

3.1 Background

It is evident from the literature review presented in Chapter 2 that DX A/C systems are widely used in small- to medium-scaled buildings due to their advantages of simple configurations, higher energy efficiency and a lower cost to own and maintain. The use of DX A/C systems having variable-speed compressor and supply fan is the most efficient method to control both the indoor air temperature and relative humidity within suitable ranges. In order to develop advanced novel control strategies for a DX A/C system, detailed understandings of the thermal performance of the DX cooling coil in a DX A/C system has always been essential.

There have been previous studies on modeling the thermal performances of DX cooling coils under different operating conditions, and on the inherent operating characteristics under different combinations of compressor and supply fan speeds. However, no previous studies focusing on determining a quantitative relationship between the sensible heat transfer rate and the total heat transfer in a DX cooling coil under different operating conditions may be identified. This suggests a need developing a calculation method for evaluating the said quantitative relationship.

Three approaches can be used in establishing mathematical models for evaluating the thermal performances of DX cooling coils. The lumped parameter approach is commonly used. However, in all lumped parameter models, the airside surface of the SPR of a DX cooling coil has always been assumed to be dry without any further detailed analysis. It is therefore necessary to further study the dehumidification effects on the airside of the SPR in a DX cooling coil. Furthermore, the literature review presented in Chapter 2 also reveals that in previous models for evaluating the thermal performance of a DX cooling coil, Lewis Number or Lewis Factor has been usually assumed to be one. However, a number of experimental studies suggested that Lewis Factor could deviate from one. Hence, a method to evaluate the simultaneous heat and mass transfer in a DX cooling coil under both unit and non-unit Lewis Factors should be developed.

3.2 Project title

The thesis focuses on the following major issues related to modeling the simultaneous heat and mass transfer taking place in a DX cooling coil under different operating conditions: (1) developing a calculation method for evaluating the ratio of the output sensible cooling capacity to the total output cooling capacity, or Equipment SHR, of a DX cooling coil under different operating conditions; (2) evaluating the dehumidification effect on the airside of the SPR of a DX cooling coil;

(3) proposing a new lumped parameter model for evaluating the airside thermal performance of both a wet DX and a wet chilled water cooling coil under both unit and non-unit Lewis Factors; (4) developing fundamental analytical solutions to the distributions of air temperature and moisture content along air flow direction in both a wet DX and a wet chilled water cooling coil. The proposed research project is therefore entitled “Study on the Heat and Mass Transfer Taking Place in a Direct Expansion (DX) Air Cooling and Dehumidification Coil”.

3.3 Aims and objectives

The objectives of the research work reported in this thesis are as follows:

1) To develop a calculation method for calculating the Equipment SHR of a DX cooling coil under different operating conditions and to validate it experimentally;
2) To evaluate the dehumidification effects on the airside of the SPR in a DX cooling coil and its share of the total dehumidification effects for the entire cooling coil;
3) To establish a new model for evaluating the simultaneous heat and mass transfer performance in a wet cooling coil under both unit and non-unit Lewis Factors and to validate the model through comparing its predictions with the results

obtained from numerically solving the fundamental equations governing the heat and mass transfer;

4) To obtain the analytical solutions to the fundamental equations governing the heat and mass transfer in a wet DX cooling coil under both unit and non-unit Lewis Factors, to speedly and accurately evaluate the variations of the distributions of the air temperature and humidity along the air flow direction in a DX cooling coil under different Lewis Factors.

3.4 Research methodologies

The development of both the calculation method of Equipment SHR and the fundamental equations governing heat and mass transfer taking place in a DX cooling coil will be based on the mass and energy conservation principles. Both the equipment SHR of, and the analytical solution to the distribution of air temperature and moisture content along the flow direction in a DX cooling coil, can be explicitly expressed.

The numerical solutions to the fundamental heat and mass transfer governing equations are to be obtained by firstly discretizing the governing equations in air flow direction, then carrying out an iteration for solving the discretized governing equations.

All the experimental work will be carried out in an experimental DX A/C station available in the HVAC laboratory in the Department of Building Services Engineering, The Hong Kong Polytechnic University. High-accuracy measuring and control devices including a DAS and PI programmable controller are available in the experimental DX A/C station. When carrying out the experiments, both the inlet air temperature and RH will be discretely varied within the operating ranges commonly seen in actual buildings, and both compressor and supply fan speeds will be discretely varied between their maximums and minimums.

Chapter 4

The Experimental DX A/C Station

4.1 Introduction

An experimental DX A/C station is available in the HVAC Laboratory of Department of Building Services Engineering, The Hong Kong Polytechnic University. The primary purpose of having the experimental station is to facilitate carrying out the research work related to DX A/C technology.

The experimental station resembles a typical DX A/C system. Advanced technologies such as variable-speed compressor and supply fan, and electronic expansion valve (EEV), as well as a computerized data measuring, logging and control system, have been incorporated into the experimental station.

This Chapter presents firstly detailed descriptions of the experimental station and its major components. This is followed by describing the computerized instrumentation and a DAS. Finally, a computer supervisory program used to operate and control the experimental station is detailed.

4.2 Detailed descriptions of the experimental system and its major components

The experimental DX A/C station is mainly composed of two parts, i.e., a DX refrigeration plant (refrigerant side) and an air-distribution sub-system (air side). The schematic diagrams of both the complete experimental station and the DX refrigeration plant are shown in Fig. 4.1 and Fig. 4.2, respectively.

4.2.1 The DX refrigeration plant

As shown in Fig. 4.2, the major components in the DX refrigeration plant include a variable-speed rotor compressor, an EEV, a high-efficiency tube-louver-finned DX evaporator and an air-cooled tube-plate-finned condenser. The evaporator is placed inside the supply air duct to work as a DX air cooling and dehumidifying coil whose details are shown in Fig. 4.3. Its louver fins are made of aluminum and tubes made of copper. The geometric parameters of the DX cooling coil are shown in Table 4.1. The design air face velocity for the DX cooling coil is 2.5 m/s. The nominal output cooling capacity from the DX refrigeration plant is 9.9 kW (~2.8 RT). The actual output cooling capacity from the DX refrigeration plant can however be modulated from 15% to 110% of the nominal capacity. Other details of the compressor can be found in Table 4.2. The compressor is driven by a VSD. The EEV includes a throttling needle valve, a step motor and a pulse generator. It is used to maintain a desired degree of refrigerant superheat at the evaporator exit. The working fluid of the plant is refrigerant R22, with a total charge of 5.3 kg.

In addition, two three-way connectors and two flexible joints, whose locations are

indicated in Fig. 4.2, are reserved in the refrigerant pipeline for the purpose of possibly modifying the station for other related studies. A condenser air duct, which is not normally required in real applications, is used to duct the condenser cooling air carrying the rejected heat from the condenser away to outdoors. The condenser fan, housed inside the condenser air duct, is variable-speed operated. An electric heater controlled by a Solid State Relay (SSR) is used to adjust

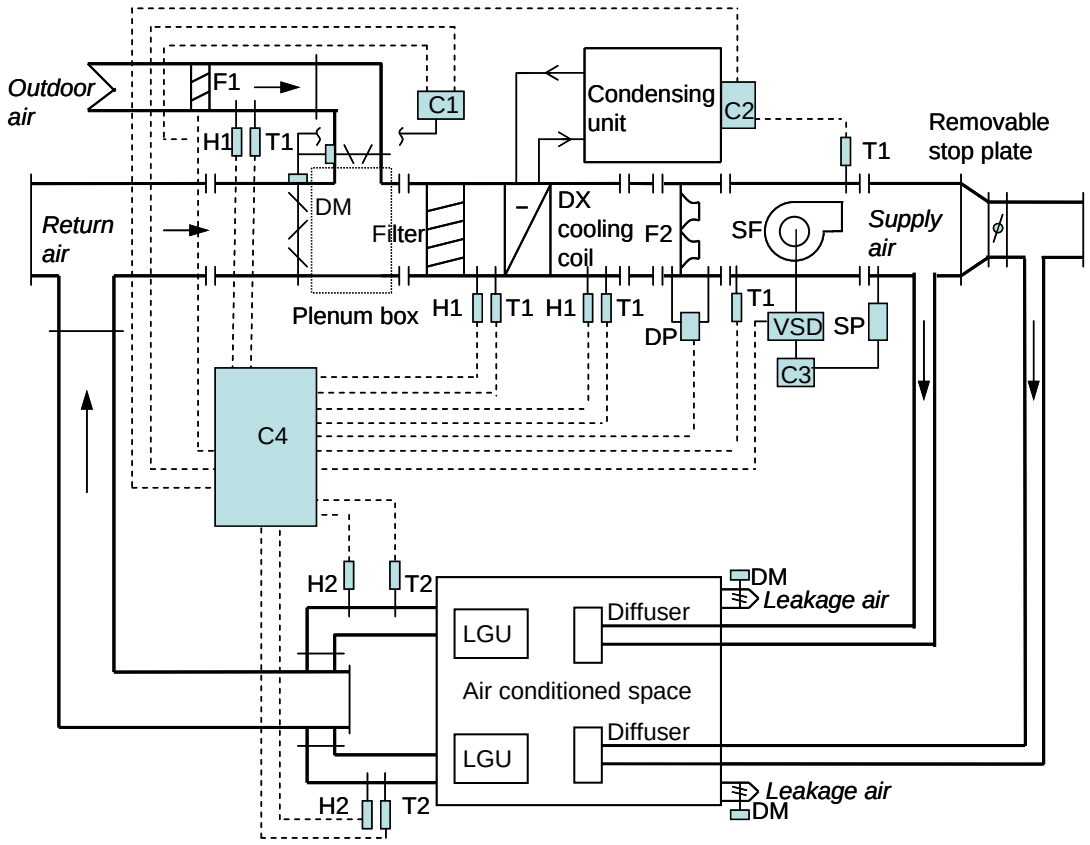

C1-controller of outdoor/return air C2-controller of condensing unit C3-controller of supply fan
C4-data acquisition and control unit DM-damper DP-differential pressure transducer
F1-hot film anemometer F2-supply airflow rate measuring H1-air wet-bulb temperature sensor
H2-air humidity meter LGU-load generating unit SF-supply fan with motor outside
SP-static pressure measuring device T1,T2-air dry-bulb temperature VSD-variable speed drives

Fig. 4.1 The schematic diagram of the complete experimental DX A/C station

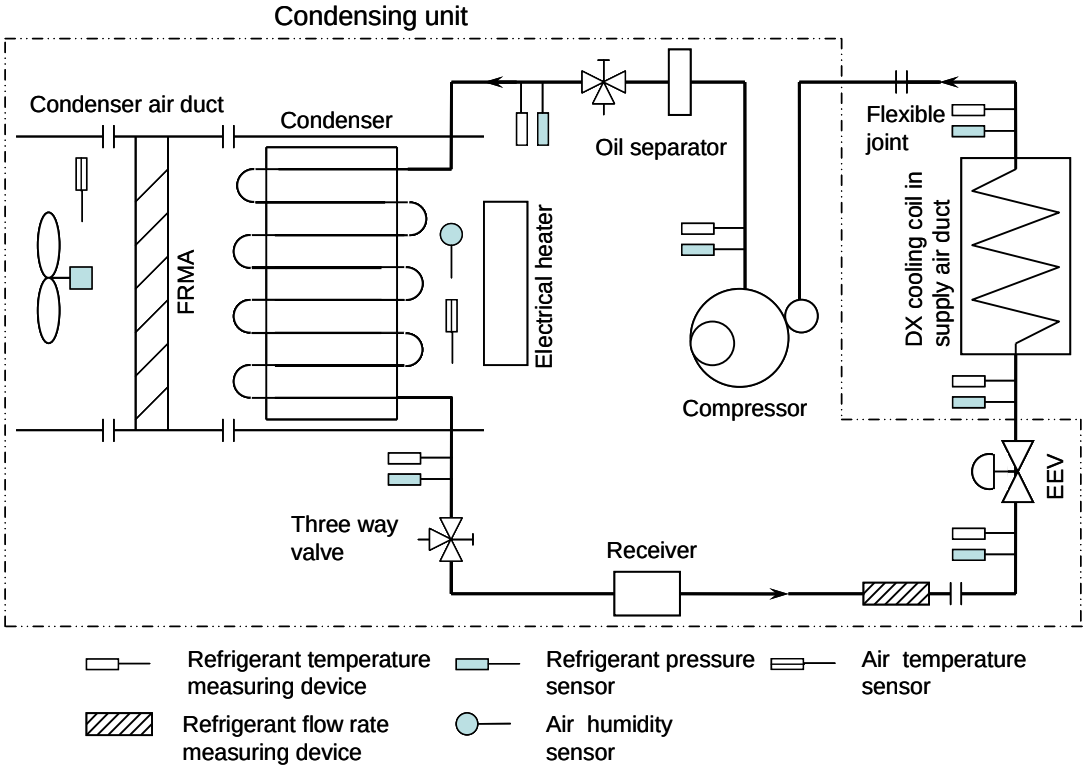

Fig. 4.2 The schematic diagram of the DX refrigeration plant

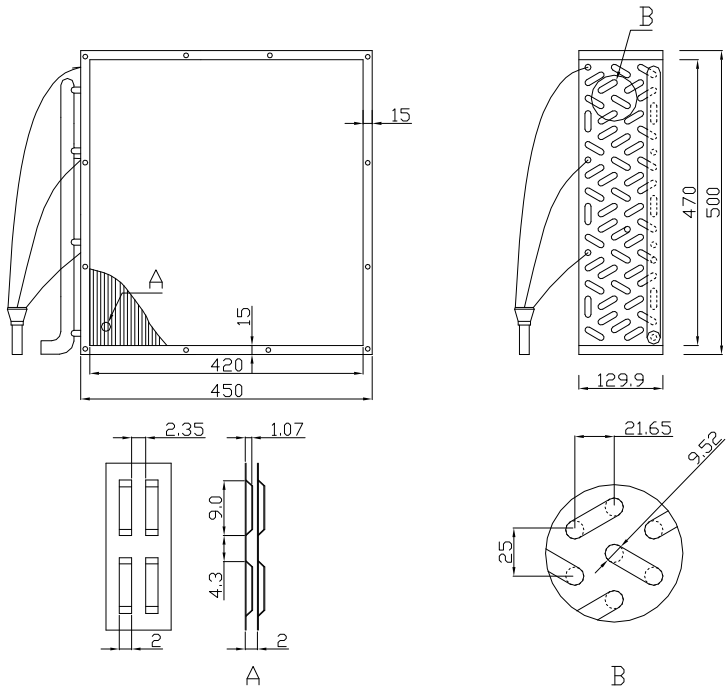

Fig. 4.3 The details of the DX air cooling and dehumidifying coil used in DX experimental station

the temperature of the cooling air entering the condenser for various experimental purposes. A refrigerant mass flow meter is installed upstream of the EEV. Other necessary accessories and control devices, such as an oil separator, a refrigerant receiver, a sight glass and safety devices, are provided in the refrigeration plant to ensure its normal and safe operation.

4.2.2 Air-distribution sub-system

The air-distribution sub-system in the experimental DX A/C station is schematically shown in Fig. 4.1. It includes an air-distribution ductwork with return and outdoor air dampers, a variable-speed centrifugal supply fan with its motor placed outside the duct, and a conditioned space. The supply fan is driven by a VSD. The details of the supply fan are given in Table 4.3.

The size of the air conditioned space is 7.6 m (L) ×3.8 m (W) ×2.8 m (H). Inside the space, there are sensible heat and moisture load generating units (LGU). The units are intended to simulate the cooling load in the conditioned space. Its heat and moisture generation rate as regulated by SSR may be varied manually or automatically with a pre-set pattern through operator's programming. In addition, leakage outlets with residual-pressure relief dampers are installed in the space so that a positive internal pressure of not more than 20 Pa can be maintained at all time. In the air-distribution sub-system of the experimental DX A/C station, return air from the space mixes with outdoor air in a plenum box upstream of an air filter. The

mixed air is filtrated and then cooled and dehumidified by the DX cooling coil. Afterwards, the cooled and dehumidified air passes through the supply fan, to be supplied to the space to deal with the cooling load from LGUs.

Table 4.1 Geometrical parameters of the DX cooling and dehumidifying coil

Parameter	Value	Unit
Outside tube diameter:	9.52	mm
Inside tube diameter:	8.86	mm
Length of the windward area:	420	mm
Height of the windward area:	470	mm
Length of coil along air flow direction:	129.9	mm
Overall heat and mass transfer area of the coil:	24.64	m^2
Overall outside area of tube:	1.36	m^2
Fin pitch:	2.0	mm
Fin thickness:	0.15	mm
Number of the windward transverse tube:	18	−
Number of the tube row:	6	−
Number of refrigerant loop:	4	−

Table 4.2 Details of the variable-speed compressor

Model	HITACHI THS20MC6-Y
Allowable Frequency range	15~110 Hz
Rated Capacity	9900 W at 90 Hz
Displacement	3.04 ml/rev

Table 4.3 Details of the variable-speed supply fan

Model	KRUGER BSB 31
Nominal flow rate	1700 m^3/h (0.47 m^3/s)
Total pressure head	1100 Pa

4.3 Computerized instrumentation and data acquisition system (DAS)

The computerized instrumentation for the experimental DX A/C station is also shown in both Fig. 4.1 and Fig. 4.2. The station is fully instrumented for measuring all of its operating parameters, which may be classified into three types, i.e., temperatures, pressures and flow rates. Since all measurements are computerized, all sensors and measuring devices are able to output direct current (DC) signals of 4-20 *mA* or 1-5 *V*, which are transferred to a DAS for logging and recording.

4.3.1 Sensors/measuring devices for temperatures, pressures and flow rates

Five sets of air temperature and humidity measuring sensors are located in the air-distribution sub-system of the experimental station. Air RH is indirectly measured via measuring air dry-bulb and wet-bulb temperatures. On the other hand, as shown in Fig. 4.2, there are five temperature sensors for measuring refrigerant temperatures in the DX refrigeration plant. To ensure fast response of the sensors for facilitating the study of transient behaviors of the DX refrigeration plant, these temperature sensors are inserted into the refrigerant circuit, and are thus in direct contact with the refrigerant. The temperature sensors for air and refrigerant are of

platinum Resistance Temperature Device (RTDs) type, using three-wire Wheatstone bridge connection and with a pre-calibrated accuracy of ±0.1°C. The specifications of the RTDs are: CHINO Pt100/0 °C -3W, Class A, SUS Φ 3.2-150L.

Refrigerant pressures in various locations in the DX refrigeration plant are measured using pressure transmitters with an accuracy of ±0.13% of full scale reading (Model: SETRA C206). The atmospheric pressure is measured with a barometer having an accuracy of ±0.05kPa (Model: VAISALA PTB-101B).

There are two sets of air flow rate measuring apparatus (FRMA) in the air-distribution system. One set of FRMA is used to measure the total supply airflow rate, i.e., the airflow rate passing through the DX cooling coil. The other is for measuring the airflow rate passing through the condenser. The two sets of FRMA are constructed in accordance with ANSI/ASHRAE Standards 41.2, consisting of nozzles of different sizes, diffusion baffles and a manometer with a measuring accuracy of ±0.1% of full scale reading (Model: ROSEMOUNT 3051). The number of nozzles in operation can be altered automatically.

On the other hand, outdoor airflow rate is measured using a hot-film anemometer with a reported accuracy of ±0.1 m/s (Model: E+E 70-VT62B5). The anemometer is installed 500 mm, which is longer than the recommended length of entrance of 200 mm by its manufacturer, downstream of the outdoor air inlet, to ensure the measuring accuracy of outdoor airflow rate. The power consumption of the variable-speed compressor is measured using a pulse-width-modulation (PWM) digital power meter with a reported uncertainty of ±2% of reading (Model:

EVERFINE PF9833). The refrigerant mass flow rate passing through the EEV is measured by a Coriolis mass flow meter with a reported accuracy of ±0.25% of full scale reading (Model: KROHNE MFM1081K+F). The supply air static pressure is measured using a manometer with a reported accuracy of ±0.1% of full scale reading (Model: ROSEMOUNT 3051).

In order to ensure the measuring accuracy for the temperatures of the air flowing inside air duct, standardized air sampling devices recommended by the ISO Standard 5151 are used in the experimental station.

4.3.2 The DAS

A data acquisition unit (Model: AGLIENT 34970A/34902A) is used in this experimental station. It provides up to 48 channels for monitoring various types of system parameters. The DC signal from various measuring devices/sensors can be scaled into their real physical values of the measured parameters using a logging & control (L&C) supervisory program which is developed using LabVIEW programming platform. The minimum data sampling interval is one second. It should be noted that the flow rates of both supply air and condenser cooling air are calculated using the air static pressure drops across their respective nozzles. The outdoor airflow rate is evaluated by multiplying the measured air velocity with the sectional area of the outdoor air duct. The output cooling capacity from the DX A/C unit is calculated based on the enthalpy-difference of air across the DX cooling coil.

4.4 LabVIEW logging & control (L&C) supervisory program

A computer supervisory program which is capable of performing simultaneously data-logging and parameter-controlling is available to communicate with not only the data acquisition unit, but also conventional standalone digital programmable PI controllers which are to be detailed in Section 4.5. A commercially available programming package, LabVIEW, provides a powerful programming and graphical platform for data acquisition and analysis, as well as for control application.

A L&C supervisory program has been developed using LabVIEW, with all measured parameters real-time monitored, curve-data displayed, recorded and processed. The program can also perform the retrieval, query and trend-log graphing of historical data for measured parameters. The program runs on a personal computer (PC).

On the other hand, the LabVIEW-based L&C supervisory program enables the PC to act as a central supervisory control unit for different low-level control loops, which will be discussed in Section 4.5, in the experimental station. The PC can therefore not only modify the control settings of those standalone microprocessor-based PI controllers, but also deactivate any of these controllers. The LabVIEW-based L&C supervisory program also provides an independent self-programming module (SPM) by which new control algorithms may be easily implemented through programming. A SPM performs in a similar manner to a central processing unit of a physical digital controller. The variables available from all measured parameters can be input to, and processed according to a specified control algorithm in a SPM to produce required

control outputs. Once a SPM is initiated to replace a given standalone controller, the controller must be deactivated, but works as a digital-analog converter to receive the control output from the SPM. An analogue control signal is then produced by the controller to initiate the related actuator for necessary control action.

4.5 Control loops in the experimental station

Totally, there are ten local control loops in this experimental station. These loops either are activated using the LabVIEW-based supervisory program or use PI controllers which are of digital programmable type with RS-485 communication port (Model: YOKOGAWA UT350-1). The controller's proportional band, integral times, and setpoints are all allowed to be reset.

Among the ten control loops, four are for varying heat and moisture generation rate of the LGUs located inside the space. Electrical power input to the LGU is regulated using SSR according to the instructions from their respective control loops, to simulate the space cooling load. In addition, there is one control loop for maintaining the condenser inlet air temperature at its setting through regulating electrical power input by SSR.

The remaining five PI control loops are as follows: supply air temperature by regulating the compressor speed; supply air static pressure by regulating the supply fan speed; condensing pressure by regulating the condenser fan speed; refrigerant superheat by regulating EEV opening; outdoor airflow rate by jointly regulating both

outdoor and return air dampers' openings. These five control loops can be activated by using the physical digital PI controller available in the experimental station.

4.6 Conclusions

An experimental DX A/C station is available for carrying out the proposed project. The station consists of two parts: a DX refrigeration plant having a variable-speed compressor and EEV; and an air-distribution sub-system having a variable speed supply fan.

The experimental DX A/C station has been fully instrumented using high quality sensors/measuring devices. Totally forty-three operating parameters in the station can be measured and monitored simultaneously and ten PI feedback control loops are provided. Two sets of airflow rate measuring apparatus are constructed in accordance with ANSI/ASHRAE 41.2. Sensors for measuring refrigerant properties are in direct contact with refrigerant, and a Corioli mass flow meter is used for measuring the refrigerant flow rate passing through the EEV.

A L&C supervisory program has been developed specifically for this experimental station using LabVIEW programming platform. All parameters can be real-time measured, monitored, curve-data displayed, recorded and processed by the L&C program.

The availability of such an experimental DX A/C station is expected to be extremely

useful in investigating the thermal performance of a DX cooling coil under different operating conditions. Simultaneous heat and mass transfer taking place on the airside of the DX cooling coil under different operating conditions can thus be thoroughly studied.

Photos showing the experimental DX A/C station are in Appendix.

Chapter 5

Development of A Calculation Method for Steady State Equipment SHR of DX Air Conditioning Units

5.1 Introduction

As mentioned in Chapter 2, in buildings, controlling indoor humidity level at an appropriate level is important since this directly affects occupants' thermal comfort, indoor air quality and the operating efficiency of building air conditioning installations. Based on the established thermal comfort standards and considering the environmental hygiene, indoor RH level should be controlled within a relatively narrow range [ASHRAE 2000, ANSI/ASHRAE 2001].

In small- to medium- scaled buildings, DX A/C units have been widely used, because they are simple, more energy efficient and cost less to own and maintain when compared to chilled water based large central air conditioning installations. On the other hand, for buildings located in hot and humid subtropics, like Hong Kong, controlling indoor air RH has always been a challenge when a DX A/C unit is used. This is because to ensure a satisfactory indoor thermal environment control using a DX A/C unit, the total output cooling capacity and its latent/sensible components from a DX A/C unit, respectively, must match the total space cooling load and its latent/sensible components. The mismatch between them would significantly

influence the effectiveness of indoor thermal environment control [Lstiburek 2002, Hourahan 2004]. Hence, for effective indoor thermal environmental control in a space served by a DX A/C unit, the total output cooling capacity of the DX A/C unit should be equal to the total space cooling load, its Equipment SHR must also match the Application SHR of the space.

Previous studies [Amrane et al. 2003, Li and Deng 2007, Wang et al. 2007] related to Equipment SHR are reported in Chapter 2. However, in these studies no theoretical or numerical analysis on Equipment SHR of a DX cooling coil has been carried out. This Chapter reports on the development of a complete set of Calculation Method for the steady-state Equipment SHR for a DX cooling coil. The development is based on the fundamentals of simultaneous heat and mass transfer taking place in a DX air cooling coil. The Calculation Method has been experimentally validated.

5.2 Development of the Calculation Method

The DX cooling coil shown in Fig. 4.3 was used in developing the Calculation Method. Figure 5.1 shows the simplified schematics of the DX cooling coil. The air entered the coil on the right hand side, as shown, and flowed through louver fin surfaces. The refrigerant flowed in a cross-counter flow arrangement. The geometrical parameters of the DX cooling coil are shown in Table 4.1.

5.2.1 Assumptions

The following assumptions were made in developing the Calculation Method:

- The cross-flow cooling coil was treated as a counter-flow heat exchanger, an assumption extensively adopted in previous studies [Stevens et al. 1957, ASHRAE 1983, Elmahdy and Mitalas 1977, Mirth and Ramadhyani 1993]. Fig. 5.2 shows the counter flow arrangement for the DX cooling coil, where "1" is used to denote the air inlet and refrigerant outlet; "2" to denote refrigerant inlet and air outlet; respectively;

- The heat transfer resistance of coil metallic tubes was small thus negligible [ASHRAE 2000];

- The thickness of condensation water film was small [Myers 1967] thus its thermal resistance was assumed negligible;

- The refrigerant was assumed to be two-phase state for the entire DX cooling coil. Normally the refrigerant side of a DX cooling coil could be divided into a two-phase and a superheated region. However, according to Chen and Deng's

study [2006], the heat transfer taking place in the two-phase region accounted for more than 90% of the total heat transfer and an experimental percentage of 93.4% was obtained in a previous model validation exercise [Deng 2000]. On the other hand, when the averaged temperature of air passing through was at 20^{o}C (at 25 ^{o}C return or indoor temperature, and 15^{o}C supply air temperature), and the evaporating temperature at 5^{o}C with a normal degree of superheat of 6^{o}C, the temperature difference between air and refrigerant are 15^{o}C in the two-phase region and 12^{o}C, respectively, or 25% difference in heat transfer temperature difference. Therefore, the overall deviation will be ~2% in heat transfer if it was assumed that the whole DX coil was at two-phase region on the refrigerant side.

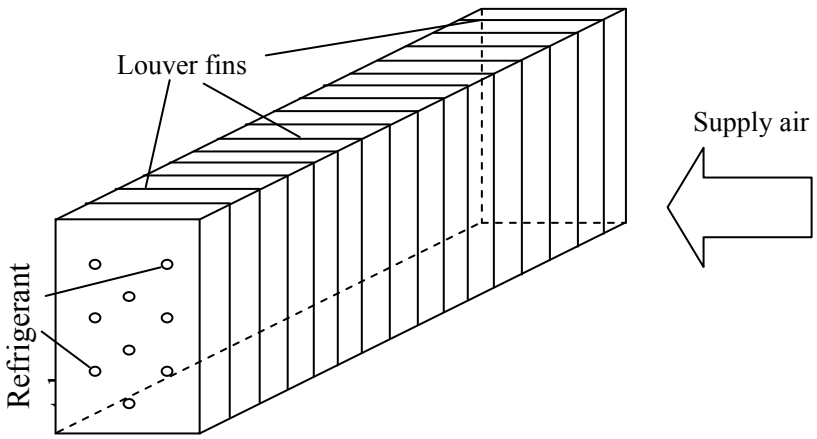

Fig. 5.1 Simplified schematics of the DX cooling coil

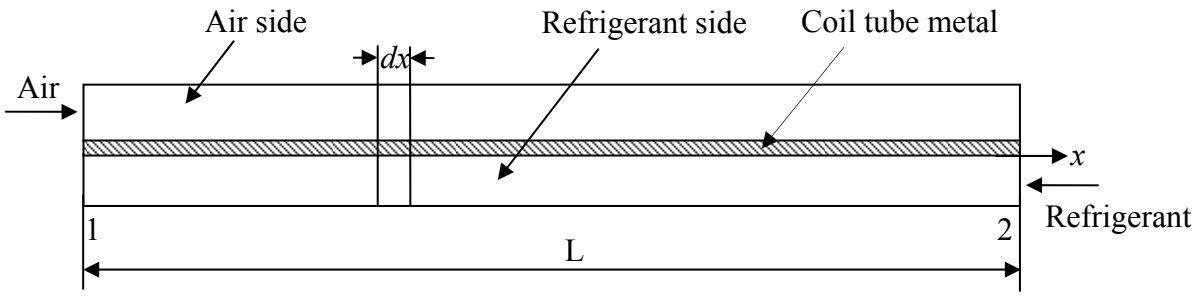

Fig. 5.2 Schematics of counter flow arrangement and an incremental control volume

5.2.2 Development of the new Calculation Method

An incremental overall outside heat and mass transfer area, dA_o, was considered to be linearly related to the length of the incremental control volume, dx, as shown in Fig. 5.2, with a linear coefficient of P, or:

$$dA_o = Pdx \tag{5.1}$$

The sensible heat transfer rate between air and refrigerant, dq_s, in the incremental control volume was:

$$dq_s = U_o(T_a - T_r)Pdx \tag{5.2}$$

where U_o was the overall heat transfer coefficient of the DX cooling coil, and may be calculated with Eq. (5.3),

$$\frac{1}{U_o A_o} = \frac{1}{\alpha_r A_r} + \frac{1}{\alpha_a \eta_o A_o} \tag{5.3}$$

On the other hand, sensible heat transfer rate from 0 to x in the air side could also be calculated by the temperature difference between air temperatures at 0 and x, yielding:

$$q_s = m_a C_{pa} (T_{ad,1} - T_a) \tag{5.4}$$

For calculating q_s, substituting Eq. (5.4) into Eq. (5.2) to eliminate T_a, yielded:

$$dq_s = -U_o (\frac{q_s}{m_a C_{pa}} + T_r - T_{ad,1}) P dx \tag{5.5}$$

Integrating Equation (5.5) from 0 to x and noting $q_s = 0$ when x was zero, to obtain q_s:

$$q_s = m_a C_{pa} (T_{ad,1} - T_r) + m_a C_{pa} (T_r - T_{ad,1}) \exp(-\frac{U_o P x}{m_a C_{pa}}) \tag{5.6}$$

Similarly, for latent heat transfer:

$$dq_l = h_{fg}\alpha_m(w_a - w_r)\eta_o P dx \tag{5.7}$$

$$q_l = m_a h_{fg}(w_{a,1} - w_a) \tag{5.8}$$

where w_r was the equivalent saturated moisture content at the refrigerant evaporating temperature, T_r. Substituting Eq. (5.7) into Eq. (5.8) to eliminate w_a,

$$q_l = m_a h_{fg}(w_{a,1} - w_r) + m_a h_{fg}(w_r - w_{a,1})\exp(-\frac{\alpha_m \eta_o P x}{m_a}) \tag{5.9}$$

As defined, the Equipment SHR was the ratio of total sensible heat transfer rate to the total heat transfer rate which was the heat transfer ratio from 0 to L, i.e.,

$$SHR = \frac{\int_0^L dq_s}{\int_0^L dq_s + \int_0^L dq_l} \tag{5.10}$$

Substituting Eqs. (5.6) and (5.9) into Eq. (5.10), Equipment SHR could be calculated as:

$$SHR = \frac{1}{1 + \dfrac{m_a h_{fg}(w_{a,1} - w_r) + \dfrac{{m_a}^2 h_{fg}(w_r - w_{a,1})}{\alpha_m \eta_o A_o}[1 - \exp(-\dfrac{\alpha_m \eta_o A_o}{m_a})]}{m_a C_{pa}(T_{ad,1} - t_r) + \dfrac{{m_a}^2 {C_{pa}}^2 (T_r - T_{ad,1})}{U_o A_o}[1 - \exp(-\dfrac{U_o A_o}{m_a C_{pa}})]}} \tag{5.11}$$

Based on the Lewis Relation (5.12),

$$\alpha_a / \alpha_m = C_{pa} \cdot Le^{\frac{2}{3}} \tag{5.12}$$

In Eq. (5.11), T_r was evaporating temperature which was assigned as an input variable to the Calculation Method. In addition, Lewis Number, *Le*, was 0.857 based on the normal operating environment of a DX cooling coil [Threlkeld 1970].

There have been a number of approaches proposed [Gungor and Winterton 1987, Shah 1982, Kandlikar 1990] to calculate the refrigerant heat transfer coefficient, α_r. However, these approaches were complicated. After carrying out extensive review and some experimental work, Boissieux et al. [2000] suggested that the averaged value of heat transfer coefficient for R-22 in a wide operational range was at about 4000 W/ ($m^{2o}C$). For simplification, this value was applied in the current study.

The air side heat transfer coefficient, α_a, was obtained from Turaga et al. [1988]:

$$\alpha_a = 0.04 G_a C_{pa} \left(\frac{A_o}{A_p}\right)^{0.23} \left(\frac{S_p}{Y}\right)^{1.15} \mathrm{Re}_a^{-0.75} \mathrm{Pr}^{-\frac{2}{3}} \tag{5.13}$$

where Prandtl Number, Pr, was 0.71. Applying Lewis Relation, the mass transfer coefficient, α_m, was evaluated as:

$$\alpha_m = 0.04 G_a \left(\frac{A_o}{A_p}\right)^{0.23} \left(\frac{S_p}{Y}\right)^{1.15} \mathrm{Re}_a^{-0.75} \mathrm{Pr}^{-\frac{2}{3}} Le^{-\frac{2}{3}} \tag{5.14}$$

In Eqs. (5.13) and (5.14), the air mass flux, G_a, was evaluated based on the minimum flow area of air side, A_m, as:

$$G_a = \frac{m_a}{A_m} \tag{5.15}$$

The overall fin efficiency, η_o, may be evaluated by Hong-Webb Equation [Hong and Webb 1996],

$$\eta_o = \frac{\tanh(Mr_o\phi)\cos(0.1Mr_o\phi)}{Mr_o\phi} \tag{5.16}$$

where Φ and M were evaluated by the following two equations:

$$\phi = \left(\frac{R_o}{r_o} - 1\right)\left[1 + 0.35\ln\left(\frac{R_o}{r_o}\right)\right] \tag{5.17}$$

$$M = \left[\frac{\alpha B}{kA_c}\left(1 + C\frac{h_{fg}}{C_{pa}}\right)\right]^{\frac{1}{2}} \tag{5.18}$$

In Eq. (5.18), C was defined as:

$$C = \frac{w_a - w_r}{T_a - T_r} \tag{5.19}$$

Substituting Eqs. (5.6) and (5.9) into Eqs. (5.4) and (5.8) to eliminate q_s and q_l, respectively, the distribution equations of T_a and w_a could be evaluated by:

$$T_a = (T_{ad,1} - T_r)\exp(-\frac{U_o Px}{m_a C_{pa}}) + T_r \tag{5.20}$$

$$w_a = (w_{a,1} - w_r)\exp(-\frac{\alpha_m \eta_o Px}{m_a}) + w_r \tag{5.21}$$

From Eqs. (5.20) and (5.21), C was evaluated as follows:

$$C = \frac{w_{a,1} - w_r}{T_{ad,1} - T_r}\exp(\frac{U_o Px}{m_a C_{pa}} - \frac{\alpha_m \eta_o Px}{m_a}) \tag{5.22}$$

It should be pointed out that C as determined by Eq. (5.22) and to be used in Eq. (5.18), was different from the McQuiston Assumption [McQuiston 1975], which assumed C as a constant only relating to the temperature and moisture content of inlet air to a cooling coil. Using Eq. (5.22), a trial and error calculating procedure was required to obtain the values of both C and η_o in each incremental control volume.

The calculating procedure was as follows:

1. Assume an initial value of C.
2. Use Eq. (5.16) to calculate η_o.
3. Obtain new calculated values of C using Eq. (5.22) and η_o using Eq. (5.16). If the error between new and assumed values of C satisfied the convergence condition, then the new calculated value of C and the corresponding η_o were accepted.

Equations (5.1) − (5.22) formed a complete set of the Calculation Method for evaluating the steady state Equipment SHR of a DX cooling coil. As mentioned earlier, the refrigerant evaporating temperature of the DX coil has been assigned as an input variable and therefore must be known. It may be obtainable experimentally or through modeling analysis, and input to the Method to calculate the steady-state Equipment SHR for the cooling coil, under fixed inlet air temperature and relative humidity to the cooling coil, which are normally the settings of indoor air. The numerical results using the Calculation Method have been obtained and compared to the experimental results obtained from the experimental DX air conditioning station described in Chapter 4 under the same operating conditions for validation purpose.

5.3 Experimental conditions and data reduction

5.3.1 Experimental conditions

Experimental conditions for validating the Calculation Method are shown in Table 5.1. To investigate the effect of T_r on Equipment SHR, three Types of Experiments were carried out as:

1. Fixing both air temperature, $T_{ad,1}$, and relative humidity, RH_1 at the cooling coil inlet; fixing the supply air fan speed at 2448 rpm while changing compressor speed from its minimum to maximum with 6 equal increments as shown in Table 5.2.
2. Fixing both air temperature, $T_{ad,1}$, and relative humidity, RH_1, at the cooling coil inlet; fixing the compressor speed at 3442 rpm while changing supply fan speed from its minimum to maximum with 6 equal increments as shown in Table 5.2.
3. Fixing both supply air fan speed and compressor speed at 2736 rpm and 5016 rpm, respectively, changing the output of LGUs following the 7 selected sensible and latent load combinations, as shown in Table 5.3.

The mass flow rate and inlet temperature of condensing cooling air remained unchanged during all experiments.

Table 5.1 Operating conditions applied to both the calculation and experiments

Operating parameters		Value	Unit
Inlet air dry-bulb temperature:	$T_{ad,1}$	24	^{o}C
Inlet air relative humidity:	RH_1	50%	
Condenser cooling air flow rate:		3100	m^3/h
Condenser cooling air inlet temperature:		35	^{o}C
Refrigerant degree of superheat:		6	^{o}C

Table 5.2 Selected experimental compressor speeds and supply fan speeds

Rotational speed (rpm) of compressor for Type 1 Experiment	Rotational speed (rpm) of supply air fan for Type 2 Experiment
2904	1584
3432	1872
3960	2160
4488	2448
5016	2736
5544	3024
6072	3312

Table 5.3 Selected combinations of sensible and latent heat loads from the LGUs for Type 3 Experiment

Combination Number	Sensible heat load (kW)	Latent heat load (kW)
1	3.94	1.72
2	4.87	1.69
3	5.95	1.57
4	6.65	1.61
5	5.70	2.62
6	5.78	2.29
7	5.52	3.29

5.3.2 Experimental data reduction

The sensible and the total heat removed are evaluated respectively by:

$$q_s = m_a C_{pa}(T_{ad,1} - T_{ad,2}) \tag{5.23}$$

$$q_t = m_a(h_{a,1} - h_{a,2}) \tag{5.24}$$

The measured Equipment SHR was:

$$SHR = \frac{q_s}{q_t} = \frac{C_{pa}(T_{ad,1} - T_{ad,2})}{h_{a,1} - h_{a,2}} \tag{5.25}$$

where air specific enthalpy, h_a, was evaluated by:

$$h_a = 1.005T_a + 0.001w_a(2500 + 1.84T_a) \tag{5.26}$$

In Eq. (5.26), w_a was the moisture content of air, and it was evaluated by:

$$w_a = \frac{(2500 - 1.347T_{aw})w_{as} - 1010(T_a - T_{aw})}{2500 + 1.84T_a - 4.187T_{aw}} \tag{5.27}$$

w_{as}, was evaluated by:

$$w_{as} = \frac{622\,p_{asw}}{101.325 - p_{asw}} \tag{5.28}$$

where p_{asw} was the ambient saturated water vapor pressure which was a function of T_{aw} and was calculated by the following equation when T_{aw} was between 0 and 200 ^{o}C.

$$\begin{aligned} p_{asw} = {} & \frac{1}{1000}\exp[-5.80\times10^{3}(T_{aw}+273)^{-1} + 1.391 \\ & -0.0486(T_{aw}+273) + 0.418\times10^{-4}(T_{aw}+273)^{2} \\ & -0.145\times10^{-7}(T_{aw}+273)^{3} + 6.546\ln(T_{aw}+273)] \end{aligned} \tag{5.29}$$

The experimental results obtained were processed using Eqs. (5.23 - 5.29).

5.4 Validation of the Calculation Method and Discussion

The comparison between the calculated and measured Equipment SHR was evaluated based on Relative Error, defined as:

$$\text{Relative Error} = \frac{\text{Calculated Equipment } SHR - \text{Measured Equipment } SHR}{\text{Measured Equipment } SHR} \quad (5.30)$$

Figures 5.3, 5.4 and 5.5 show the relative errors and measured refrigerant evaporating temperature in the three Types of Experiments. It can be seen that all of the relative errors were within ±6%. These suggested that Calculation Method for Equipment SHR developed has been experimentally validated.

Using the calculation model, the effect of T_r, $T_{ad,1}$ and $w_{a,1}$ on Equipment SHR can be numerically investigated. Normally, T_{ai} and RH_1 are controlled at their fixed set points, while the evaporating temperature, T_r, may vary with different operating conditions leading to the change of Equipment SHR. Fig. 5.6 shows the relationship between calculated Equipment SHR and refrigerant evaporating temperature, T_r, using the data from Type 1 and 2 Experiments. With the Method developed, it is

possible to explain the impacts of T_r on Equipment SHR by considering the order of $\alpha_m \eta_o A_o$ which is about 2~5 times of that of m_a. Thus Eq. (5.11) could be simplified to:

$$SHR = \frac{1}{1 + \frac{(h_{fg}/C_{pa})w_{a,1} - (h_{fg}/C_{pa})w_r}{T_{ad,1} - T_r}} \tag{5.31}$$

When T_r is increased, w_r is also increased. However, because the order of $(h_{fg}/C_{pa})w_r$ is larger than that of T_r, Equipment SHR would be increased according to Eq. (5.31). The trends shown in Fig. 5.6 verify such an analysis.

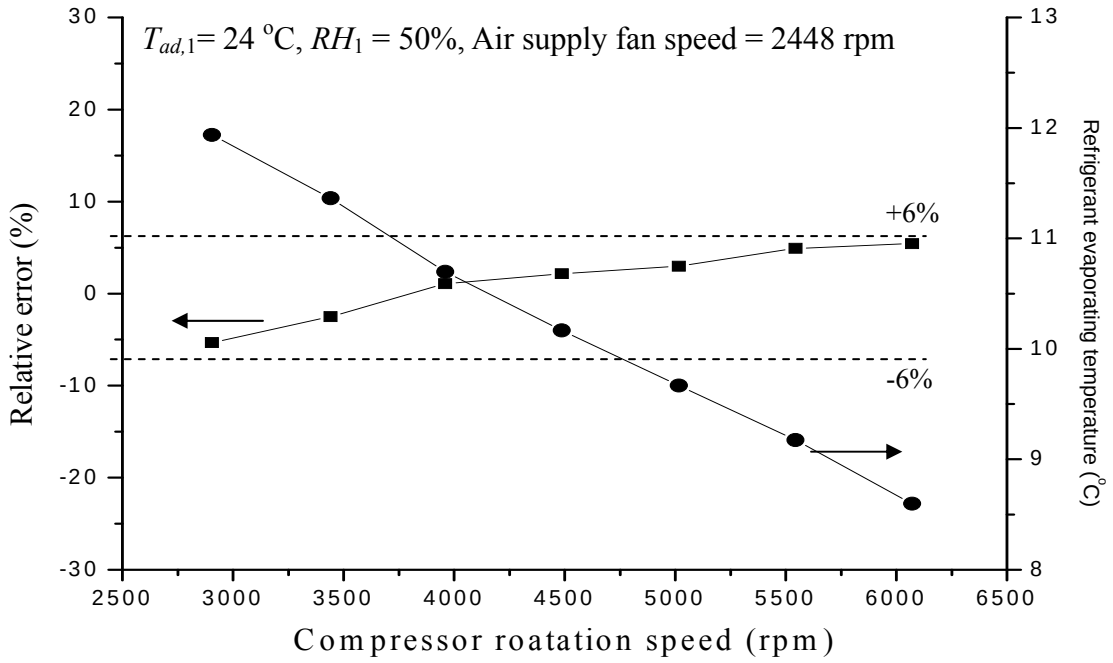

Fig. 5.3 Relative errors and measured refrigerant evaporating temperature in Type 1 Experiment

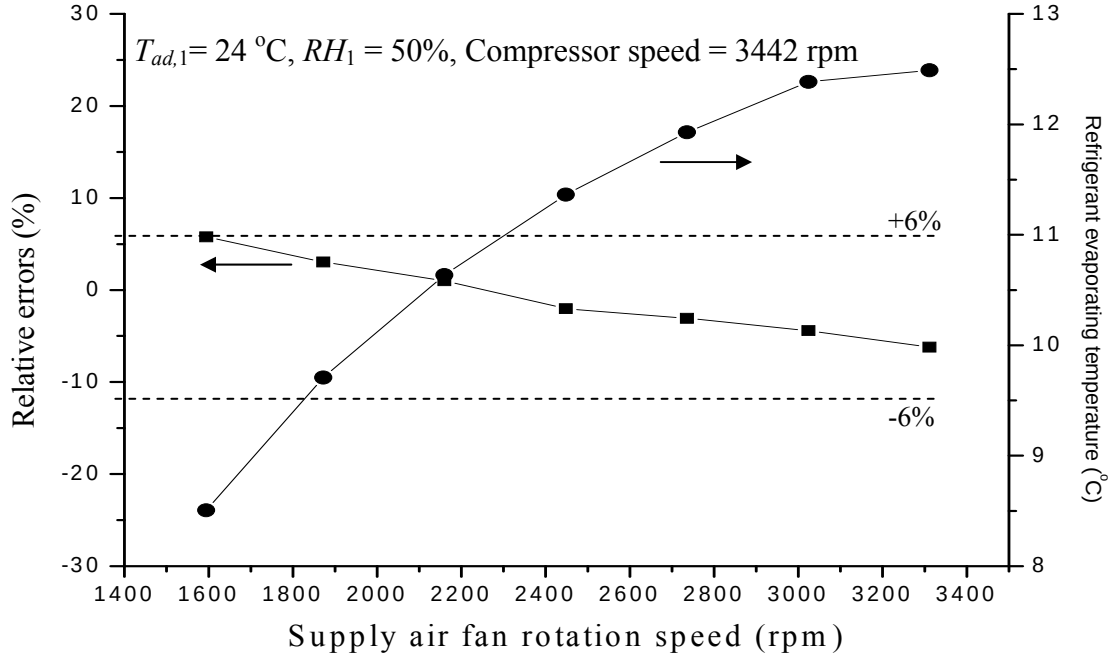

Fig. 5.4 Relative errors and measured refrigerant evaporating temperature in Type 2

Experiment

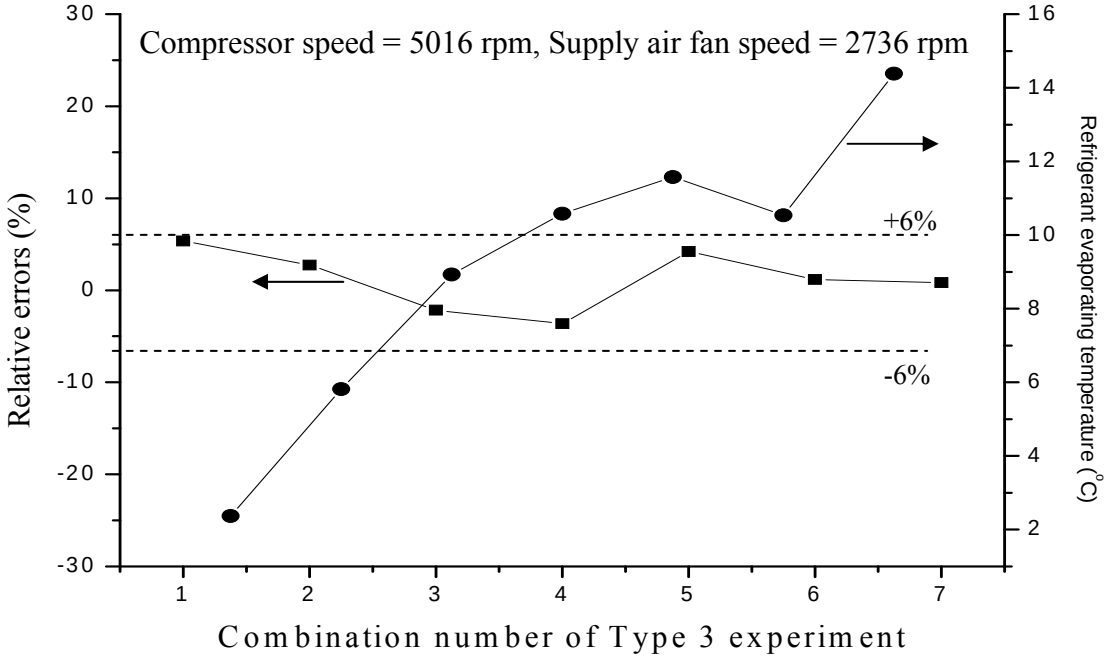

Fig. 5.5 Relative errors and measured refrigerant evaporating temperature in Type 3

Experiment

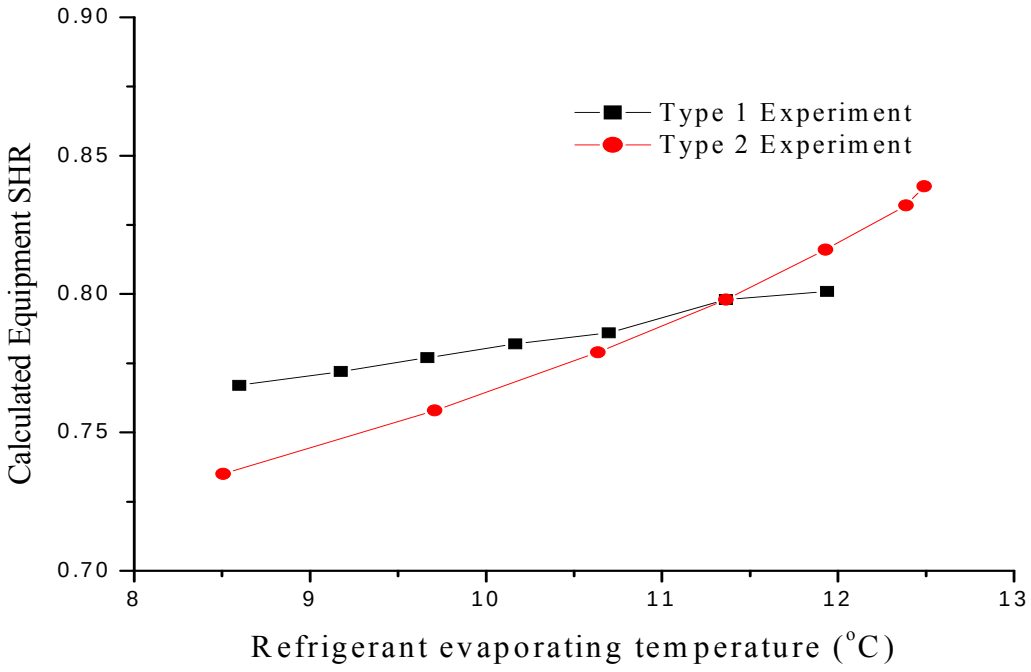

Fig. 5.6 Relationship between calculated Equipment SHR and refrigerant evaporating temperature in Type 1 and 2 Experiments

The uncertainties associated with the experimental measurements of the inlet air temperatures (dry- and wet-bulb temperatures), refrigerant temperatures and mass flow rate of air of the DX cooling coil when experimentally validating the Calculation Method were evaluated.

According to the descriptions of the instruments used in the experimental DX A/C station presented in Chapter 4, the uncertainties due to estimated maximum measurement errors for these parameters were:

Air dry-bulb temperature: ±0.1°C

Air wet-bulb temperature: ±0.1^{o}C

Evaporating refrigerant temperature: ±0.1^{o}C

Mass flow rate of air: ±0.1% full scale of 0.71 kg/s

Then the uncertainty in the calculated results of the Equipment SHR, Un_{SHR}, can be obtained from [Holman 1994]:

$$Un_{SHR} = \sqrt{(\frac{\partial(SHR)}{\partial T_{ad,1}} Un_{T_{ad,1}})^2 + (\frac{\partial(SHR)}{\partial T_{aw,1}} Un_{T_{aw,1}})^2 + (\frac{\partial(SHR)}{\partial T_r} Un_{T_r})^2 + (\frac{\partial(SHR)}{\partial m_a} Un_{m_a})^2} \quad (5.32)$$

where Un_{Tai}, Un_{Tawi}, Un_{Tr} and Un_{ma} are uncertainties of T_{ai}, T_{awi}, T_r and m_a, respectively. The values of the partial derivatives of Equipment SHR in Eq. (5.32) can be evaluated using Eq. (5.11). Hence the result of uncertainty of SHR arising from the experimental errors was 0.97%.

The highest relative error of Calculation Method of the Equipment SHR was approximately ±6%. This may be attributed to the assumptions made during the derivation of the calculated method, like neglecting the existence of a superheated region (at ~2% error). Nonetheless, with the relative errors identified, it was believed that accuracy of the method was acceptable.

5.5 Conclusions

A complete set of Calculation Method for calculating the steady-state Equipment SHR has been developed and reported in this Chapter. The Method which is based on known refrigerant evaporating temperature in a DX cooling coil has been experimentally validated.

With the Method developed, the Equipment SHR may well be predicted and analyzed with change of refrigerant evaporating temperature. This would be helpful for further studying simultaneous the heat and mass transfer in a DX cooling coil and developing effective control strategies to obtain comfortable indoor thermal environment.

Chapter 6

Dehumidification Effects on The Airside of the SPR of A DX Air Cooling Coil

6.1 Introduction

As mentioned earlier in Chapter 2, DX A/C units such as split-type air conditioners and window-type air conditioners are commonly used in small- to medium- scaled buildings. For example, in the US, based on Department of Energy, packaged rooftop DX A/C systems accounted for about 60% of the total installed cooling capacity [Bordick and Gilbride 2002].

The key component in a DX A/C unit is DX air cooling coil, where simultaneous air cooling and dehumidification takes place at the airside, if its surface temperature is below the dew point temperature of incoming air. A DX air cooling coil in operation can be assumed to have two regions, i.e., TPR and SPR at its refrigerant side. As reported in Chapter 2, in previous distributed parameter models [Chi and Didion 1982, MacArthur 1984, Wang and Touber 1991, Jia et al. 1995, Jia et al. 1999] and lumped parameter models [Fisher and Rice 1983, Mullen et al. 1997, Theerakulpisut and Priprem 1998, Deng 2000, Qi and Deng 2008], a dry airside surface in SPR has always been assumed without further detailed analysis.

The fact that dehumidification effect on the airside of SPR in a DX cooling coil has been commonly ignored may well be due to the factor that the airside surface area in a SPR only accounts for a small fraction of the entire airside coil surface area, which was also utilized in Chapter 5 when developing the Calculation Method for equipment SHR. However, as shown in Fig. 6.1, water droplets are clearly visible on the external surface of the refrigerant suction pipe of a DX cooling coil in an experimental observation using the experimental DX A/C station, when the coil inlet air temperature and relative humidity (RH) were 24^{o}C and 60%, respectively. A refrigerant suction pipe has been commonly regarded as part of a SPR. Therefore, the experimental observation suggests that there is a need to re-evaluate the assumption of dry airside in a SPR of a DX cooling coil.

Fig. 6.1 Water droplets formed on the surface of a refrigerant suction pipe

This Chapter reports a study on the dehumidification effects on the airside of a SPR in a DX cooling coil through a series of experiments under different operating

conditions carried out using the experimental DX A/C station described in Chapter 4. Firstly, the experimental conditions are briefly described. This is followed by reporting a calculation procedure specifically developed to process experimental data. With the calculation procedure, the surface condition and water vapor condensing rate on the airside of SPR of the DX cooling coil under different operating conditions have been evaluated and are presented.

6.2 Experimental conditions

In order to evaluate the dehumidifying performance on the airside of the SPR in the DX air cooling coil under various operating conditions, two types of experimental work were designed and carried out.

Type 1: The experimental operating conditions are shown in Table 6.1. In this type of experiments, inlet air temperature and RH to the DX cooling coil were varied, with compressor speed and supply fan speed fixed at 5016 rpm and 2448 rpm, respectively.

Type 2: The experimental operating conditions are shown in Table 6.2. In this type of experiments, both compressor and supply air fan speeds were varied, with the inlet air dry-bulb temperature and RH to the cooling coil fixed at 24^{o}C and 50%, respectively.

Table 6.1 Operating conditions in Type 1 Experiments

Variable inlet air parameters	Inlet air dry-bulb temperature:	From 22°C to 26°C, with an increment of 2°C
	Inlet air relative humidity	From 30% to 90%, with an increment of 10%
Fixed operating parameters	Compressor speed	5016 rpm
	Air supply fan speed	2448 rpm

Table 6.2 Operating conditions in Type 2 Experiments

Fixed inlet air parameters	Inlet air dry-bulb temperature:	24°C
	Inlet air relative humidity:	50%
Variable operating parameters	Compressor speed:	From 30% to 90% of its maximum speed (7166 rpm), with an increment of 10%
	Air supply fan speed:	From 30% to 90% of its maximum speed (4080 rpm), with an increment of 10%

Other system operating parameters which were kept unchanged during both types of experiments are shown in Table 6.3.

Table 6.3 Other constant experimental parameters

Parameters	Value (Unit)
Condenser cooling air flow rate:	3100 (m^3/h)
Condenser cooling air inlet temperature:	35 (^oC)
Refrigerant degree of superheated:	6 (^oC)

6.3 A calculation procedure for evaluating dehumidification effect on the airside of a SPR

A calculation procedure for processing the experimental data so as to evaluate the dehumidifying effects on the airside of a SPR in a DX cooling coil has been specifically developed and is reported in this section.

The following assumptions have been used in developing the calculation procedure.

1. A counter-flow heat exchanger for the DX cooling coil was assumed, and the schematics of counter-flow arrangement for the SPR is shown in Fig. 6.2.
2. The thermal resistance of the refrigerant tube metal was negligible, so the outside

surface temperature of refrigerant tube was the same as the refrigerant temperature at the same location.

3. For wetted airside of the SPR, the thermal resistance of water film was negligible.

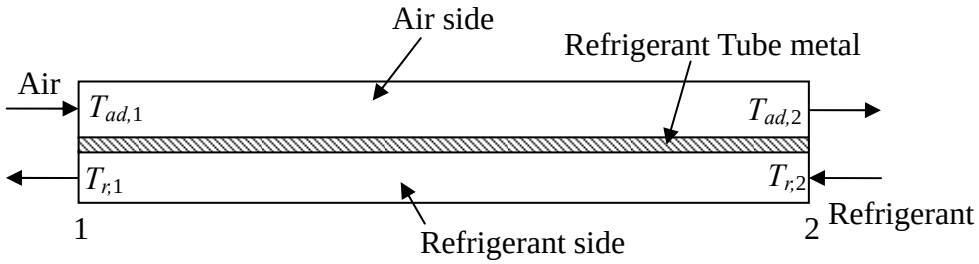

Fig. 6.2 Schematics of the counter flow arrangement in the SPR of a DX cooling coil

There can be three different surface conditions on the airside of the SPR, i.e., fully dry, fully wet and partially wet. Three different lumped parameter calculation approaches were separately developed, as follows.

Approach 1: For fully dry condition

For dry airside, the heat transfer rate, q, in the SPR could be evaluated by using the LMTD method, as follows:

$$q = U_{o,d} A_o \frac{(T_{ad,1} - T_{r,1}) - (T_{ad,2} - T_{r,2})}{\ln(\frac{T_{ad,1} - T_{r,1}}{T_{ad,2} - T_{r,2}})} \tag{6.1}$$

where $U_{o,d}$ and A_o were the overall heat transfer coefficient and heat transfer area on the airside of the SPR, respectively. The overall heat transfer coefficient could be determined by:

$$\frac{1}{U_{o,d}A_o} = \frac{1}{\alpha_r A_r} + \frac{1}{\eta_{o,d}\alpha_{a,d}A_o} \tag{6.2}$$

where A_r was the inside refrigerant tube surface area; α_r, $\alpha_{a,d}$ the heat transfer coefficients on the refrigerant and air sides, respectively; $\eta_{o,d}$ the overall fin efficiency in fully dry condition.

In Eq. (6.2), A_o and A_r were not known. However, for a particular cooling coil, A_o and A_r could be linked by:

$$A_o = C_1 A_r \tag{6.3}$$

where C_1 could be determined based on the geometrical characteristics of a coil. Then U_o could be evaluated if the α_r, $\alpha_{a,d}$ and $\eta_{o,d}$ were available. On the other hand, α_r could be evaluated by using the 'Dittus-Boelter Equation' [1930]. For calculating the heat transfer coefficient on the airside in dry condition, $\alpha_{a,d}$, Turaga's correlation [1988] was adopted.

The overall fin efficiency at a dry condition, $\eta_{o,d}$, was determined by:

$$\eta_{o,d} = 1 - \frac{A_f}{A_o}(1 - \eta_d) \tag{6.4}$$

where η_d and A_f were fin efficiency and the entire fin surface area of the DX cooling coil, and η_d was evaluated by the Hong and Webb Approach [Hong and Webb 1996] in dry condition.

On the other hand, the energy balance on both the air and refrigerant sides, respectively, yielded:

$$q = m_a C_{pa}(T_{ad,1} - T_{ad,2}) \tag{6.5}$$

$$q = m_r C_{pr}(T_{r,1} - T_{r,2}) \tag{6.6}$$

Using Eqs. (6.1), (6.5) and (6.6), and other known system parameters, q, $T_{ad,2}$ and A_o could be calculated. Based on $T_{ad,2}$ and $T_{r,2}$, the airside surface temperature at the outlet of SPR, $T_{sf,2}$, could be calculated by:

$$T_{sf,2} = \frac{(\alpha_r T_{r,2} + \eta_{o,d}\alpha_{a,d} C_1 T_{ad,2})}{(\alpha_r + \eta_{o,d}\alpha_{a,d} C_1)} \tag{6.7}$$

Approach 2: For fully wet condition

For wet airside, the sensible heat transfer rate, q_s, in the SPR could be evaluated by using the LMTD method, as follows:

$$q_s = U_{o,w} A_o \frac{(T_{ad,1} - T_{r,1}) - (T_{ad,2} - T_{r,2})}{\ln(\frac{T_{ad,1} - T_{r,1}}{T_{ad,2} - T_{r,2}})} \tag{6.8}$$

where $U_{o,w}$ was the overall heat transfer coefficient. Similar to Eq. (6.2), the overall heat transfer coefficient could be determined by [Xia and Jacobi 2005]:

$$\frac{1}{U_{o,w}} = \frac{q}{q_s} \cdot \frac{C_1}{\alpha_r} + \frac{1}{\eta_{o,w} \alpha_{a,w}} \tag{6.9}$$

where C_1 was the parameter defined in Eq. (6.3); $\alpha_{a,w}$ the heat transfer coefficient on the airside; $\eta_{o,w}$ the overall fin efficiency for wet operation condition. For calculating $\alpha_{a,w}$ and $\eta_{o,w}$, Turaga's Correlation [Turaga 1998] and Hong and Webb Approach [Hong and Webb 1996] for wet condition were adopted.

The sensible heat transfer rate on the airside was calculated by:

$$q_s = m_a C_{pa} (T_{ad,1} - T_{ad,2}) \tag{6.10}$$

On the other hand, the latent heat transfer rate, q_l, could be calculated using the

method adopted by Deng [2000],

$$q_l = \alpha_m A_o \eta_{o,w} h_{fg} [\frac{(w_{a,1} + w_{a,2})}{2} - \frac{(w_{sf,1} + w_{sf,2})}{2}] \tag{6.11}$$

where h_{fg}, α_m were the specific latent heat of vaporization of water and mass transfer coefficient, respectively; $w_{a,1}$ and $w_{a,2}$ the moisture contents of air at inlet and outlet of SPR, respectively; $w_{sf.1}$ and $w_{sf,2}$ the moisture contents of saturated air under the coil surface temperatures at inlet and outlet of SPR, $T_{sf,1}$ and $T_{sf,2}$, respectively. Surface temperatures of SPR inlet and outlet, $T_{sf,1}$ and $T_{sf,2}$, were determined by the following equations:

$$T_{sf,1} = \frac{(q_s \alpha_r T_{r,1} + q\eta_{o,w} \alpha_{a,w} C_1 T_{ad,1})}{(q_s \alpha_r + q\eta_{o,w} \alpha_{a,w} C_1)} \tag{6.12}$$

$$T_{sf,2} = \frac{(q_s \alpha_r T_{r,2} + q\eta_{o,w} \alpha_{a,w} C_1 T_{ad,2})}{(q_s \alpha_r + q\eta_{o,w} \alpha_{a,w} C_1)} \tag{6.13}$$

Based on the availability of both $T_{sf,1}$ and $T_{sf,2}$, the moisture contents of saturated air at the surface temperatures of SPR inlet and outlet, $w_{sf.1}$ and $w_{sf,2}$, could be calculated using the thermal properties of saturated moist air [ASHRAE 2000],

$$w_{sf,1} = f(T_{sf,1}) \tag{6.14}$$

$$w_{sf,2} = f(T_{sf,2}) \tag{6.15}$$

The Lewis relation was used to correlate heat transfer to mass transfer. For most cooling coils used for air-conditioning, *Le* was approximately equal to unity [Deng 2000]. Therefore, the mass transfer coefficient was calculated by:

$$\alpha_m = \frac{\alpha_{a,w}}{C_{pa}'} \tag{6.16}$$

where C_{pq}' was the specific heat capacity of moist air and a mean value of 1.02 kJ/kg K was taken.

The latent heat transfer rate, q_l, could be calculated by:

$$q_l = m_a h_{fg}(w_{a,1} - w_{a,2}) \tag{6.17}$$

The total heat transfer rate was the summarization of both sensible and latent heat transfer rates:

$$q = q_s + q_l \tag{6.18}$$

On the other hand, the total heat transfer, q, could also be evaluated by:

$$q = m_r C_{pr}(T_{r,2} - T_{r,1}) \tag{6.19}$$

Using Eqs. (6.8), (6.10)-(6.15) and (6.17)-(6.19), $T_{ad,2}$, $w_{a,2}$, $T_{sf,1}$, $T_{sf,2}$, $w_{sf,1}$, $w_{sf,2}$, A_o, q_s, q_l and q could be calculated. Then the amount of water vapor condensed on the wet surface part of the airside in a SPR, m_{cond}, was:

$$m_{cond} = \frac{q_l}{h_{fg}} \tag{6.20}$$

Approach 3: For partially wet condition

In a partially wet operation, the wet part would appear after the dry part along the air flow direction because the refrigerant temperature decreased along this direction. Therefore, there existed a turning point separating the two surface conditions, as shown in Fig. 6.3. The subscript "3" was used to denote the turning point.

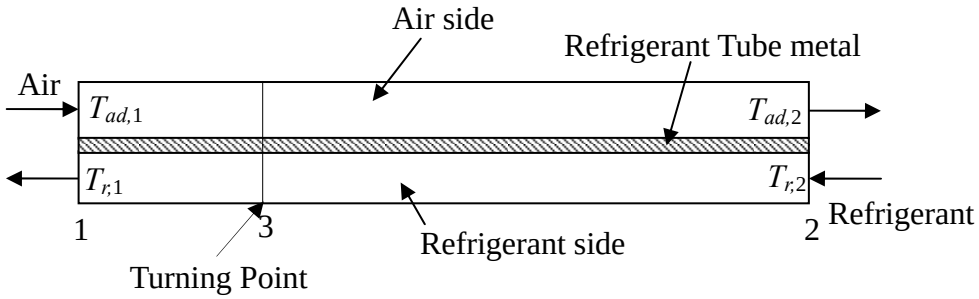

Fig. 6.3 The schematics of both air and refrigerant sides in a SPR in partially wet operation

Given that the moisture content of air in the dry part did not change, at turning point, $w_{a,3}$, should be equaled to $w_{sf,3}$. Hence, $T_{sf,3}$ was evaluated using the thermal properties of moist air [ASHRAE 2000],

$$T_{sf,3} = f^{-1}(w_{a,3}) = f^{-1}(w_{a,1}) \tag{6.21}$$

And $w_{a,3}$ was evaluated by:

$$w_{a,3} = w_{a,1} \tag{6.22}$$

The relationship between coil surface temperature of SPR at turning point, $T_{sf,3}$, and temperatures of air and refrigerant at turning point, $T_{ad,3}$ and $T_{r,3}$, gave:

$$T_{sf,3} = \frac{(\alpha_r T_{r,3} + \eta_{o,d}\alpha_{a,d} C_1 T_{ad,3})}{(\alpha_r + \eta_{o,d}\alpha_{a,d} C_1)} \tag{6.23}$$

Combining Eqs. (6.21)-(6.23) and Eqs. (6.1)-(6.6) which were for evaluating the thermal performance at the dry part in SPR, and also by replacing subscript "2" with "3", $T_{ad,3}$, $w_{a,3}$ and $T_{r,3}$ could be determined and then input to the Calculation Approach for wet part in SPR reported in Approach 2. The thermal performance in wet part in SPR could be calculated by using Eqs. (6.21)-(6.23) and Eqs. (6.8), (6.10)-(6.15) and Eqs. (6.17)-(6.19), and also by replacing subscript "1" with "3".

The Approaches 1-3 formed a complete calculation procedure for evaluating the thermal performance and dehumidification effect in SPR. Fig. 6.4 below shows the flowchart of applying the procedure.

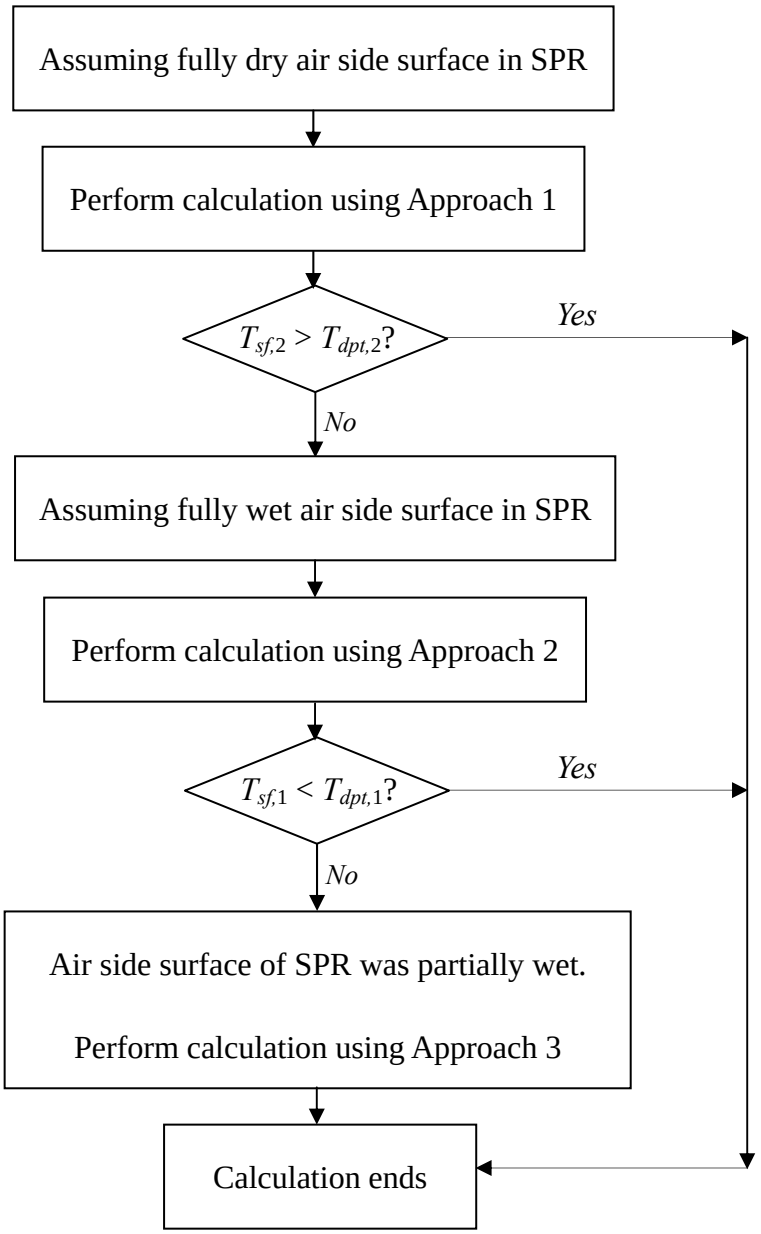

Fig. 6.4 Flowchart for applying the calculation procedure

With this calculation procedure, experimental data can be processed and the surface conditions and dehumidification effects on the airside of a SPR at different conditions evaluated.

6.4 Results and discussions

The experimental results obtained from Type 1 and 2 Experiments, which are needed to be input to the calculation procedure, are shown in Tables 6.4 and 6.5, respectively.

6.4.1 Results of Type 1 Experiments

The determination of surface conditions based on the experimental data showed that the airside of a SPR was fully wet when RH_1 was between 40% and 90%, and partially wet when RH_1 was 30%. The water vapor condensing rates on the airside of the SPR, m_{cond}, are shown in Fig. 6.5. It can be seen that m_{cond} was largely influenced by air relative humidity at the SPR inlet, RH_1. An increase in RH_1 would cause an increase in m_{cond}. It can also be seen that a higher $T_{ad,1}$ would lead to a larger condensing rate at the same RH_1.

Table 6.4 Results of Type 1 Experiments

$T_{ad,1}$=22°C, m_a=0.41kg/s							
RH_1	90	80	70	60	50	40	30
$T_{r,1}$	13.540	12.365	10.981	9.834	8.147	7.218	6.154
m_r	0.05	0.0479	0.046	0.0443	0.0426	0.0407	0.0372
$T_{ad,1}$=24°C, m_a=0.41kg/s							
RH_1	90	80	70	60	50	40	30
$T_{r,1}$	15.759	14.341	13.522	12.127	10.312	8.831	6.592
m_r	0.0527	0.0514	0.0485	0.0461	0.0448	0.0429	0.0409
$T_{ad,1}$=26°C, m_a=0.41kg/s							
RH_1	90	80	70	60	50	40	30
$T_{r,1}$	17.661	16.172	14.575	13.151	11.483	9.961	8.421
m_r	0.0555	0.0534	0.0512	0.0489	0.0466	0.0447	0.0424

Table 6.5 Results of Type 2 Experiments

Sp_c=90%							
Sp_a (%)	90	80	70	60	50	40	30
$T_{r,1}$	10.517	10.129	9.565	8.726	7.933	6.790	5.323
m_r	0.0523	0.0515	0.0505	0.0494	0.0481	0.0466	0.0447
m_a	0.548	0.506	0.458	0.409	0.358	0.306	0.255
Sp_c=80%							
Sp_a (%)	90	80	70	60	50	40	30
$T_{r,1}$	11.256	10.697	10.000	9.268	8.362	7.172	5.751
m_r	0.0617	0.0606	0.0599	0.0588	0.0580	0.0563	0.0549
m_a	0.548	0.506	0.458	0.409	0.358	0.306	0.255
Sp_c=70%							
Sp_a (%)	90	80	70	60	50	40	30
$T_{r,1}$	12.202	11.571	10.991	10.290	9.395	8.233	6.749
m_r	0.0479	0.0473	0.0466	0.0457	0.0445	0.0433	0.0415
m_a	0.548	0.506	0.458	0.409	0.358	0.306	0.255
Sp_c=60%							
$T_{r,1}$	12.927	12.414	11.872	11.218	10.263	9.203	7.773
m_r	0.0457	0.0452	0.0445	0.0434	0.0427	0.0413	0.0397
m_a	0.548	0.506	0.458	0.409	0.358	0.306	0.255

Table 6.5 (continued)

Sp_c=50%							
Sp_a (%)	90	80	70	60	50	40	30
$T_{r,1}$	14.064	13.393	12.859	12.200	11.312	10.340	8.964
m_r	0.0419	0.0415	0.0409	0.0403	0.0394	0.0382	0.0368
m_a	0.548	0.506	0.458	0.409	0.358	0.306	0.255
Sp_c=40%							
Sp_a (%)	90	80	70	60	50	40	30
$T_{r,1}$	14.964	14.426	13.989	13.421	12.628	11.678	10.442
m_r	0.0379	0.0376	0.0370	0.0363	0.0355	0.0345	0.0332
m_a	0.548	0.506	0.458	0.409	0.358	0.306	0.255
Sp_c=30%							
Sp_a (%)	90	80	70	60	50	40	30
$T_{r,1}$	15.831	15.466	15.000	14.384	13.785	12.932	11.773
m_r	0.0340	0.0337	0.0330	0.0325	0.0318	0.0311	0.0302
m_a	0.548	0.506	0.458	0.409	0.358	0.306	0.255

6.4.2 Results of Type 2 Experiments

The results of Type 2 Experiments suggested that, with the inlet air temperature and

RH being fixed at 24^{o}C and 50%, different combinations of compressor and supply fan speeds led to most likely a fully wet airside of a SPR, and partially wet conditions only existed when the DX air conditioning system was operated at low compressor speeds and high supply fan speeds. The calculated results of m_{cond} for Type 2 Experiments are shown in Fig. 6.6. As seen from the figure, the water vapor condensing rates were between 0.005 and 0.055 g/s.

Therefore, no fully dry airside surface existed in the SPR of the experimental DX cooling coil. Hence, the assumption of nil condensation on the airside surface of the SPR in a DX cooling coil was questionable. The calculation results here re-confirmed the experimental observation mentioned (Fig. 6.1) in this Chapter earlier.

Furthermore, it was possible to evaluate the total amount of water vapor condensed, M_{cond}, on the entire airside surface area of the DX cooling coil under different experimental conditions. Then the ratio of m_{cond}/M_{cond} may be used to assess the percentage error in evaluating the total amount of water condensed on the entire surface area of a DX cooling coil, which may have been resulted in by assuming dry airside of a SPR in lumped parameter models. M_{cond} was evaluated by,

$$M_{cond} = m_a(w_{a,1} - w_{a,out}) \tag{6.24}$$

where $w_{a,out}$ was the moisture content of air leaving the DX cooling coil, which was experimentally obtainable.

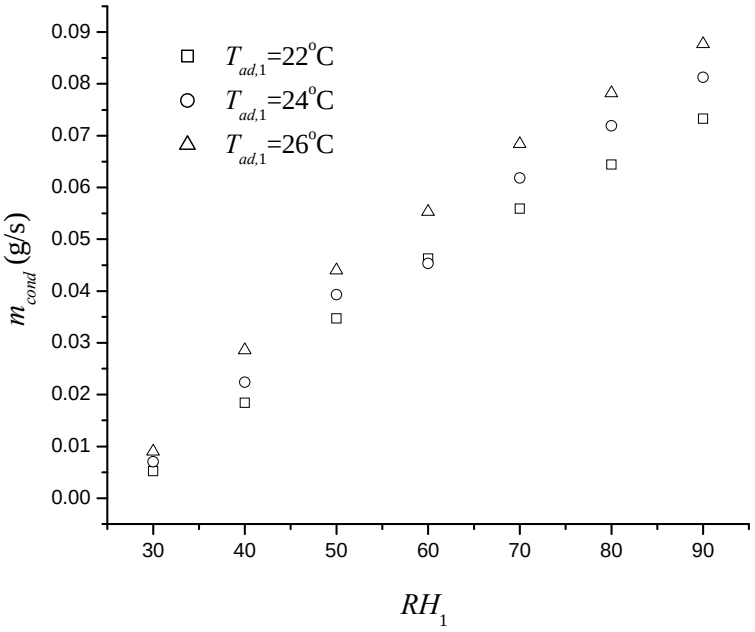

Fig. 6.5 Water vapor condensing rate on the airside of the SPR in Type 1 Experiments

The numerical values of experimental m_{cond}/M_{cond} obtained from Type 1 Experiments are shown in Fig. 6.7. They ranged from 3% to 7% in most cases, having an increasing trend when RH_1 was reduced. However, m_{cond}/M_{cond} would go over 7% when inlet air RH dropped to values lower than 40%. The values of m_{cond}/M_{cond} obtained from Type 2 Experiments are shown in Fig. 6.8. It can be seen that the

values of m_{cond}/M_{cond} were between 3% and 7% in all test points.

The fairly high values of m_{cond}/M_{cond} when inlet air RH dropped to below 40% might be due to two reasons. Firstly, M_{cond} was low under this operating *RH*; secondly, since the air firstly contacted and condensed on the airside surface of SPR in a counter flow heat exchanger, the condensable amount of water vapor in TPR became smaller.

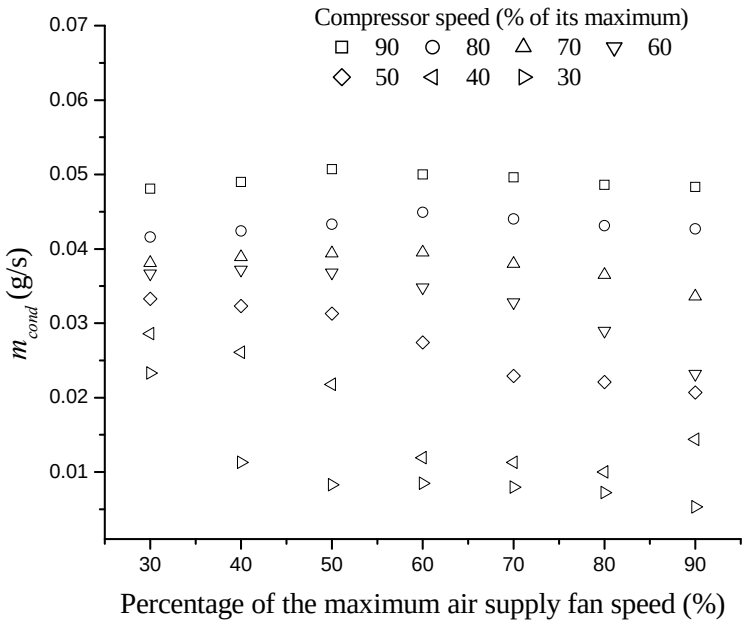

Fig. 6.6 Water vapor condensing rate on the airside of the SPR in Type 2 Experiments

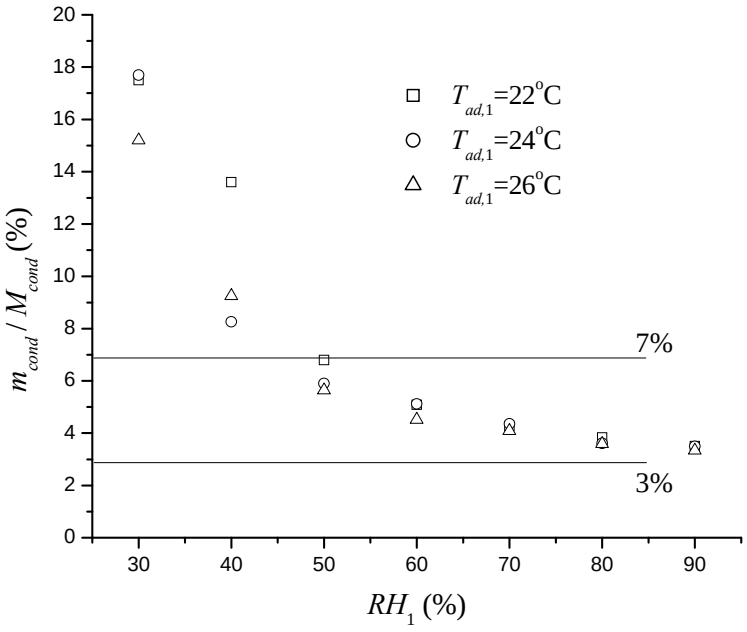

Fig. 6.7 The values of m_{cond}/M_{cond} in Type 1 Experiments

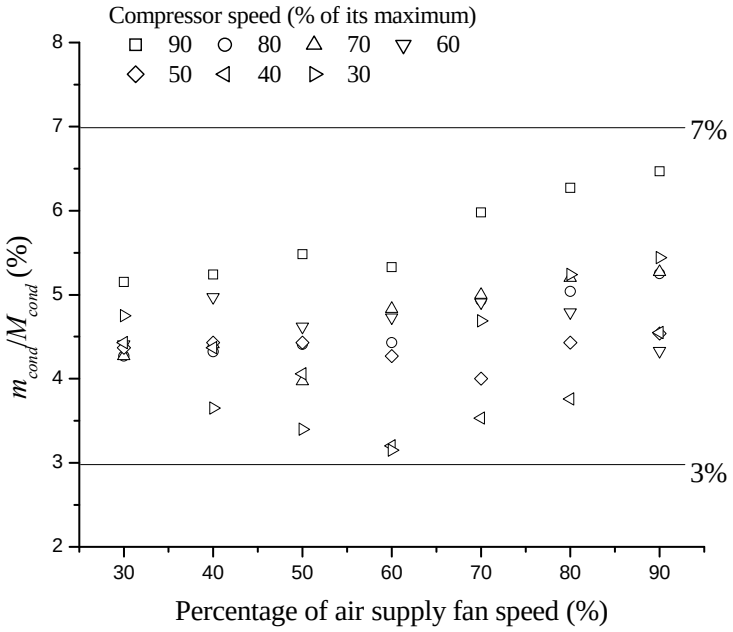

Fig. 6.8 The values of m_{cond}/M_{cond} in Type 2 Experiments

The above analysis suggested that assuming a dry airside of SPR in a DX cooling coil can lead to an underestimated amount of water vapor condensed in the entire airside surface area of the DX cooling coil. The percentage of underestimation most likely lies between 3% and 7%, but up to 18% of under a lower inlet RH of air.

Among other reasons, one major possible reason for assuming dry airside of SPR in DX air cooling coils in previous lumped-parameter models was computational time required for solving these models. Such an assumption could well help reduce computational time when high-speed computers were not readily available. However, this barrier is already removed nowadays. Therefore, it is suggested that with the powerful computational facilities available currently, and the availability of complete modeling procedure and algorithm for a wet coil surface (such as Eqs. (6.8) to (6.19) in this Chapter), the assumption of dry airside of TPR in a DX air cooling coil is no longer adopted in future new lumped parameter models.

It was worth noting that *Le* may not be actual unity according to some of the previous studies as reported in the Literature Review in Chapter 2, ranging between 0.6 and 1.2 [Hong and Webb 1996, Seshimo et al. 1988, Eckels and Rabas 1987, Pirompugd et al. 2007]. However, the calculation procedure developed in this Chapter may also be used when *Le* is not equal to 1, by inputting an actual *Le* value to Eq. (6.16), to obtain the mass transfer coefficient, α_m. Furthermore, all other results can be calculated using the calculation procedure. It is observed that for both

unity and non-unity *Le*, the calculated α_m is always greater than 0. Therefore, m_{cond} and m_{cond}/M_{cond} are greater than zero, suggesting that the assumption of dry airside of SPR extensively used in lumped parameter models is questionable.

6.4.3 Uncertainty analysis

The uncertainties of the derived/calculated parameters in the present investigation were estimated following the Single-sample Uncertainty Analysis method as proposed by Moffat [1988]. The results of the uncertainty analysis for both the measured and the derived/calculated parameters are shown in Table 6.6. It can be seen from the Table that all the uncertainties were less than 7%, suggesting that the experimental results were of adequate reliability.

6.5 Conclusions

Two types of experiments have been carried out for examining the assumption of dry airside in the SPR in a DX cooling coil. The experimental data were processed using a lumped parameter calculation procedure specially developed to determine the surface conditions of the airside and water vapor condensing rate in a SPR under different experimental conditions.

The experimental results showed that no dry airside surface in SPR existed in the experimental DX cooling coil during all experiments. Therefore, the assumption of dry airside in a SPR is questionable.

Assuming dry airside of SPR in a DX cooling coil can lead to an underestimated

Table 6.6 Uncertainties of the experimental and derived/calculated parameters

Parameters	Uncertainties	Parameters	Uncertainties
Uncertainties of measured parameters			
m_a	±0.00071 kg/s	$T_{ad,1}$	±0.1 ^{o}C
m_r	±0.00075 kg/s	$T_{aw,1}$	±0.1 ^{o}C
P_a	±0.05kPa	$T_{r,2}$	±0.1 ^{o}C
Uncertainties of derived/calculated parameters (%)			
$\alpha_{a,d}$	±1.14	$T_{sf,1}$, $T_{sf,2}$ and $T_{sf,3}$	±2.31, ±2.97 and ±3.10
$\alpha_{a,w}$	±1.50	q, q_s and q_l	±3.42, ±1.35 and ±4.77
$\eta_{o,d}$	±0.93	A_o	±3.18
$\eta_{o,w}$	±1.27	m_{cond}	±4.77
RH_1	±1.32	M_{cond}	±2.46
$T_{ad,2}$	±1.85	m_{cond} / M_{cond}	±6.92

total amount of water vapor condensed on the entire airside of a DX cooling coil, ranging most likely between 3% and 7%. Considering one major possible reason of assuming dry airside in a SPR being computational time, and with the advancement of computational facilities, it is suggested that in newly developed lumped parameter models, wet airside in a SPR be adopted to improve modeling accuracy.

Chapter 7

A Modified LMED Method for Evaluating The Total Heat Transfer Rate of A Wet Cooling Coil under Both Unit and Non-unit Lewis Factors

7.1 Introduction

As mentioned in Chapter 2, air cooling and dehumidifying coils have been widely used in air-conditioning systems. For an air cooling coil, if its surface temperature is below the dew point temperature of incoming air, simultaneous heat and mass transfer takes place on its air side, or the cooling coil is operated under a wet condition.

The total heat transfer rate in a micro-scale element of an air cooling and dehumidifying coil under wet condition can be evaluated based on the enthalpy difference:

$$dq = \frac{\alpha_a dA_a}{C_{pa}}(h_a - h_{sur}) \tag{7.1}$$

where dq and dA_a are the total heat transfer rate and air side surface area in the micro-scale element; α_a, C_{pa} the air side sensible heat transfer coefficient and specific heat capacity of air; h_a and h_{sur} the specific enthalpy of bulk air and the

saturated air specific enthalpy at coil surface temperature, respectively. When establishing Eq. (7.1), the Lewis Analogy and the assumption of unit Lewis Factor were used,

$$\frac{\alpha_a}{\alpha_m C_{pa}} = Le^{2/3} = 1 \tag{7.2}$$

where α_m is the mass transfer coefficient.

Equation (7.1) was originally proposed by Threlkeld [1970] for simplifying the calculation of the total heat transfer rate in a wet cooling coil. The LMED method was developed from Eq. (7.1).

$$q = HA_a \Delta h_{lm} \tag{7.3}$$

where Δh_{lm} is the logarithmic-mean enthalpy difference; H is the overall heat transfer coefficient based on the enthalpy difference.

Because of its simplicity and convenience in determining the total heat transfer rate of a wet cooling coil, the LMED method has been extensively applied since its establishment. Previous investigations show that Lewis number can well deviate from being one. Consequently, calculation error can be resulted when evaluating the total heat transfer rate of a wet cooling coil with the LEMD method [Xia and Jacobi

2005].

A modified LMED (m-LMED) method for calculating the total heat transfer rate of a wet cooling coil under both non-unit and unit Lewis Factors has been therefore developed and is reported in this Chapter. This m-LMED method has been validated by comparing its predictions of the total heat transfer rate to that obtained from numerically solving the fundamental governing equations of the heat and mass transfer in a wet cooling coil. Furthermore, the calculation results of the total heat transfer rates from using both the LMED and the m-LMED methods under the same operating conditions have been compared to indicate the errors resulted in where unit Lewis Factor is used, instead of the actual Lewis Factor values which may not be equal to 1.

7.2 Development of the m-LMED method

The difference between the specific enthalpies of bulk air and the saturated moist air at coil surface temperature could be calculated as:

$$h_a - h_{sur} = C_{pa}(T_a - T_{sur}) + h_{fg}(w_a - w_{sur}) \tag{7.4}$$

where h_a and h_{sur} are the specific enthalpy of bulk air and the specific enthalpy of

saturated moist air at coil surface temperature, respectively; T_a and T_{sur}, the temperatures of bulk air and coil surface, respectively; w_a and w_{sur}, the specific humidity ratio of bulk air and the saturated air humidity ratio at T_{sur}, respectively; C_{pa} and h_{fg}, the specific heat of air and the latent heat of vaporization of water, respectively.

Equation (7.4) could be transformed to:

$$h_a - h_{sur} = \frac{C_{pa}}{\alpha_a}[\alpha_a(T_a - T_{sur}) + \frac{\alpha_a}{C_{pa}} h_{fg}(w_a - w_{sur})] \tag{7.5}$$

The Lewis Relation was:

$$\frac{\alpha_a}{C_{pa}\alpha_m} = Le^{2/3} \tag{7.6}$$

In Eqs. (7.5) and (7.6), α_a and α_m are the air side heat and mass transfer coefficients, respectively; Le, the Lewis Number and $Le^{2/3}$, the Lewis Factor.

Applying the Lewis Analogy to Eq. (7.5) yielded:

$$h_a - h_{sur} = \frac{C_{pa}}{\alpha_a}[\alpha_a(T_a - T_{sur}) + Le^{2/3}\alpha_m h_{fg}(w_a - w_{sur})] \tag{7.7}$$

or:

$$h_a - h_{sur} = \frac{C_{pa}}{\alpha_a}[\alpha_a(T_a - T_{sur}) + \alpha_m h_{fg}(w_a - w_{sur}) + (Le^{2/3} - 1)\alpha_m h_{fg}(w_a - w_{sur})] \quad (7.8)$$

The total heat transfer rate was calculated by:

$$dq = [\alpha_a(T_a - T_{sur}) + \alpha_m h_{fg}(w_a - w_{sur})]dA_a \quad (7.9)$$

where q and A_a are the total heat transfer rate and total air side coil surface area, respectively; dq the heat transfer rate on the air side surface area in a micro-scale element of a cooling coil, dA_a.

Combining Eqs. (7.8) and (7.9) for calculating dq:

$$dq = \frac{\alpha_a}{C_{pa}}(h_a - h_{sur})dA_a - (Le^{2/3} - 1)\alpha_m h_{fg}(w_a - w_{sur})dA_a \quad (7.10)$$

Following the assumption that the ratio between the sensible heat transfer rate and the latent heat transfer rate remains constant in the entire coil, which was adopted previously [Xia and Jacobi 2005], the following equation held:

$$\frac{dq_s}{dq_l} = \frac{q_s}{q_l} \tag{7.11}$$

where q_s and q_l are the sensible and latent heat transfer rates in the entire coil; dq_s and dq_l, the sensible and latent heat transfer rates in the micro-scale element of the cooling coil.

Based on Eq. (7.11), the ratio between $(T_a - T_{sur})$ and $(w_a - w_{sur})$ could be determined by:

$$\frac{(T_a - T_{sur})}{(w_a - w_{sur})} = \frac{\alpha_m h_{fg}}{\alpha_a} \cdot \frac{dq_s}{dq_l} = \frac{\alpha_m h_{fg}}{\alpha_a} \cdot \frac{q_s}{q_l} \tag{7.12}$$

where α_m is the mass transfer coefficient for the moisture content of bulk air.

From Eqs. (7.4) and (7.12), the ratio between $(h_a - h_{sur})$ and $(w_a - w_{sur})$ could be calculated by:

$$\frac{(h_a - h_{sur})}{(w_a - w_{sur})} = \frac{h_{fg}}{Le^{2/3}} \frac{q_s}{q - q_s} + h_{fg} \tag{7.13}$$

Then $(w_a - w_{sur})$ could be evaluated by:

$$(w_a - w_{sur}) = \frac{(h_a - h_{sur})}{\frac{h_{fg}}{Le^{2/3}}\frac{q_s}{q - q_s} + h_{fg}} \tag{7.14}$$

Combining Eqs. (7.14), (7.10) and the Lewis Analogy, i.e., Eq. (7.6) gave

$$dq = \frac{\alpha_a dA_a}{C_{pa}}[1 - \frac{(Le^{2/3} - 1)}{\frac{q_s}{q - q_s} + Le^{2/3}}] \cdot (h_a - h_{sur}) \tag{7.15}$$

Comparing Eq. (7.15) with Eq. (7.1), it can be seen that the linear relationship between dq and (h_a − h_{sur}) remains unaltered, with the linear coefficient being different, due to the fact that Lewis Factor, $Le^{2/3}$, may deviate from being 1. However, if $Le^{2/3}$=1, Eq. (7.15) is exactly the same as Eq. (7.1).

Therefore, the m-LMED method could be established when replacing Eq. (7.1) with Eq. (7.15). Following the same approach used in deriving LMED method [Threlkeld 1970], the m-LMED method could be shown as:

$$q = H_M A_a \Delta h_{lm} \tag{7.16}$$

where H_M is the modified overall heat transfer coefficient based on enthalpy and Δh_{lm}, the logarithmic mean enthalpy difference.

Normally the heat transfer resistances due to tube metal and condensate film on the external surface of the cooling coil were small compared to those on both air side and cooling medium side, thus negligible. With this assumption, H_M could be evaluated by:

$$H_M = \frac{1}{A_a} \cdot [\frac{a}{A_c \alpha_c} + \frac{C_{pa}}{\eta_o A_a \alpha_a} (1 - \frac{Le^{2/3} - 1}{\frac{q_s}{q - q_s} + Le^{2/3}})^{-1}]^{-1} \tag{7.17}$$

where a is a linear coefficient relating the enthalpy of saturated moist air to air temperature.

For the LMED method, the overall heat transfer coefficient based upon enthalpy, H, was calculated by:

$$H = \frac{1}{A_a} \cdot (\frac{a}{A_c \alpha_c} + \frac{C_{pa}}{\eta_o A_a \alpha_a})^{-1} \tag{7.18}$$

Comparing Eq. (7.17) with Eq. (7.18), it can be seen that when Lewis Factor is 1, H_M should be equal to H, and the m-LMED method is the same as the LMED method. Hence, the LMED method can be regarded as a special case of the m-LMED method when $Le^{2/3}$=1.

In Eq. (7.17), the overall fin efficiency, η_o, was calculated by:

$$\eta_o = 1 - \frac{A_f}{A_a}(1-\eta) \tag{7.19}$$

where fin efficiency, η, is calculated by Hong-Webb Equation [Hong and Webb 1996]:

$$\eta = \frac{\tanh(Mr_o\phi)\cos(0.1Mr_o\phi)}{Mr_o\phi} \tag{7.20}$$

where Φ and M are evaluated by the following two equations:

$$\phi = (\frac{R_o}{r_o} - 1)[1 + 0.35\ln(\frac{R_o}{r_o})] \tag{7.21}$$

$$M = [\frac{2h_a}{kt}(1 + \frac{dq_l}{dq_s}\frac{h_{fg}}{C_{pa}})]^{\frac{1}{2}} \tag{7.22}$$

In Eq. (7.21), r_o is the outside radius of the tube and the equivalent radius, R_o, of a plate fin was calculated by:

$$R_o = 1.28W_f(L_f / W_f - 0.2)^{1/2} \tag{7.23}$$

where W_f and L_f are the width and length of the fin, respectively.

7.3 Validation of the m-LMED method

The m-LMED method reported in Section 7.2 has been validated by comparing its prediction of the total heat transfer rate to that from numerically solving the fundamental governing equations of the heat and mass transfer in a wet cooling coil. The numerical solution (NS) has been widely regarded as the most accurate solution to the fundamental governing equations and hence is used as the basis for comparison.

7.3.1 Numerical solution to the fundamental governing equations

The m-LMED method can be applicable to both counter-flow and parallel-flow air cooling and dehumidifying coils. In this Chapter, a counter-flow air cooling coil whose schematic diagram is shown in Fig. 7.1 has been studied.

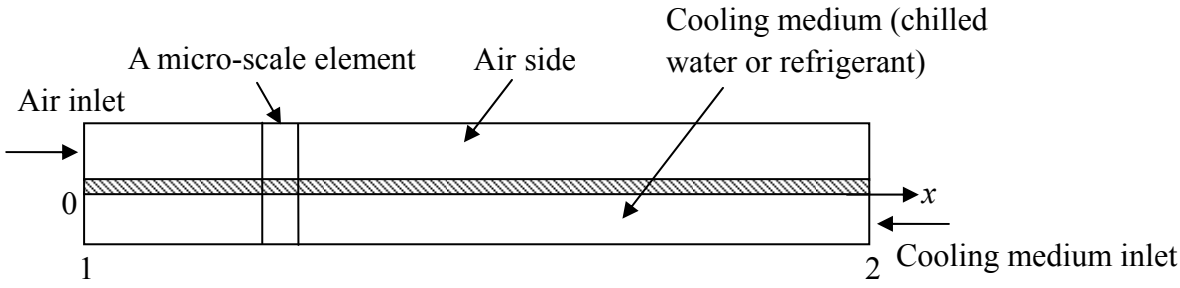

Fig.7.1 Schematics of a counter flow air cooling and dehumidifying coil under study

For the micro-scale element shown in Fig. 7.1, the fundamental equations governing the simultaneous heat and mass transfer, and energy conservation were

$$dq_s = \alpha_a (T_a - T_{sur}) \eta_o dA_a \tag{7.24}$$

$$dq_l = \frac{\alpha_a}{C_{pa} Le^{2/3}} h_{fg} (w_a - w_{sur}) \eta_{o,m} dA_a \tag{7.25}$$

$$dq_s = -m_a C_{pa} dT_a \tag{7.26}$$

$$dq_l = -m_a h_{fg} dw_a \tag{7.27}$$

$$dq = -\alpha_c (T_{sur} - T_c) dA_c \tag{7.28}$$

$$dq = dq_s + dq_l = -m_c C_{pc} dT_c \tag{7.29}$$

where η_o and $\eta_{o,m}$ are the overall heat and mass transfer fin efficiencies, respectively.

The fundamental governing Eqs. (7.24-7.29) could be transformed to differencing equations and solved using first-order discrete method to obtain the numerical solutions of $T_{a,1}$, $T_{a,2}$, $w_{a,1}$, $w_{a,2}$, $T_{c,1}$, $T_{c,2}$, q, q_s and q_l, for a specific cooling coil under a given operating condition.

7.3.2 The procedure for applying the m-LMED method

Applying the m-LMED method to the air cooling and dehumidifying coil shown in Fig.7.1 yielded:

$$q = H_M A_a \frac{(h_{a,1} - h_{c,1}) - (h_{a,2} - h_{c,2})}{\ln(\frac{h_{a,1} - h_{c,1}}{h_{a,2} - h_{c,2}})} \tag{7.30}$$

where $h_{c,1}$ and $h_{c,2}$ are the specific enthalpies of saturated moist air at the temperatures of $T_{c,1}$ and $T_{c,2}$; the overall heat transfer coefficient, H_M, can be determined by Eq. (7.17).

For calculating the total heat transfer rate using the m-LMED method, the results of $h_{a,1}$, $h_{a,2}$, $h_{c,1}$ and $h_{c,2}$ obtained from the NS to the fundamental governing equations were used as inputs to Eq. (7.30). The total heat transfer rate calculated by using the m-LMED method was compared to that from the NS to validate the m-LMED method.

In Eq. (7.24), for calculating the overall heat transfer coefficient, H_M, the value of $q_s/(q-q_s)$ should be assumed firstly. Consequently, the calculation procedure for using the m-LMED method is detailed.

i). Assuming an initial value of $q_s/(q-q_s)$.

ii). Calculating the total heat transfer rate, q, by using the m-LMED method with input $h_{a,1}$, $h_{a,2}$, $h_{c,1}$ and $h_{c,2}$, which are calculated from the NS of $T_{a,1}$, $T_{a,2}$, $w_{a,1}$, $w_{a,2}$, $T_{c,1}$ and $T_{c,2}$; and then calculating the sensible heat transfer rate, q_s, by using the logarithmic-mean temperature difference (LMTD) method, noting that in Eq. (7.22), the value of M is evaluated by using the assumed value of $q_s/(q-q_s)$.

iii). Calculating a new value of $q_s/(q-q_s)$ based on the calculated results of q and q_s using Eq. (7.30) and the LMTD method. Comparing the originally assumed and calculated values of $q_s/(q-q_s)$, the calculation procedure for the m-LMED method ended when a convergence arrives, otherwise, assuming a new value of $q_s/(q-q_s)$ and repeating ii) and iii).

7.3.3 Validation of the m-LMED method

To validate the m-LMED method, the total heat transfer rate calculated by using the m-LMED method was compared to that obtained from numerically solving the fundamental governing Eqs. (7.24 - 7.29), under the operating conditions shown in Table 7.1, for a chilled water air cooling coil whose geometrical parameters are shown in Table 7.2. The thermal properties of air and chilled water are shown in Table 7.3. Based on the results of previous studies on the actual Lewis Factors for a

wet cooling coil [Hong and Webb 1996, Seshimo et al. 1988, Eckels and Rabas 1987, Pirompugd et al. 2007, Wang 2008], the Lewis Factors were set at 0.6, 0.8, 1.0, 1.2 and 1.4, in the validation process, so that errors may be resulted under non-unit Lewis Factors.

Figure 7.2 shows the results of the total heat transfer rates calculated respectively by the m-LMED method and from numerically solving the fundamental equations. It can be seen that the variation trends of the total heat transfer rates calculated by the m-LMED method and from the NS are identical as the Lewis Factor changes from 0.6 to 1.4. With an increase of the Lewis Factor, the total heat transfer rate decreases.

Table 7.1 Operating conditions for validating the m-LMED method

Mass flow rate of chilled water, kg/s	0.35
Inlet temperature of chilled water to the cooling coil, ^{o}C	8
Mass flow rate of air, kg/s	0.6
Inlet air temperature, ^{o}C	24
Inlet air humidity ratio, kg/kg	0.016

In Fig.7.2, the total heat transfer rates calculated by the LMED method where unit Lewis Factors were applied regardless of the actual values of the Lewis Factor, are also included to illustrate the errors resulted in where unit Lewis Factor was used across the board, instead of actual Lewis Factor values which may not be equal to 1.

For example, in Fig.7.2, Point *a* represents the calculated total heat transfer rate by

Table 7.2 Geometrical parameters of the air cooling coil for validating the m-LMED method

Overall air side heat transfer area, m^2	24
Overall cooling medium side heat transfer area, m^2	1.25
Overall fin surface area, m^2	22.5
Fin length, m	0.013
Fin width, m	0.011
Fin thickness, mm	0.115
Outside diameter of the cooling medium tube, mm	9.52
Length of the cooling coil along the air flow direction, m	0.5

Table 7.3 Thermal properties of air and chilled water

Specific heat of chilled water, kJ/(kg K)	4193
Specific heat of air, kJ/(kg K)	1007
Convective Heat transfer coefficient of chilled water, W/(K m^2)	8000
Convective Heat transfer coefficient of saturated two phase R22, W/(K m^2)	5000
Convective Heat transfer coefficient of air in wet condition, W/(K m^2)	70
Convective Heat transfer coefficient of air in dry condition, W/(K m^2)	50
Total number of the micro-scale elements	100
Atmosphere pressure, kPa	101.325

using the LMED method, where the numerical values of all other operating parameters, except Lewis Factor, obtained from the NS at $Le^{2/3}$=0.6 were input to the LMED method. For Lewis Factor, instead of using its actual value of 0.6, unit Lewis Factor, i.e., $Le^{2/3}$=1, was used. Similar approaches were applied to all other points of *b, c* and *d*, where the actual Lewis Factors were 0.8, 1.2 and 1.4, respectively.

The sensible heat transfer rates calculated by the LMTD method and the m-LMED method and from the NS are shown in Fig.7.3. It can also be seen from Fig.7.3 that the variation trends for the sensible heat transfer rates calculated from both calculation approaches agree well.

The Relative Deviations of the total heat transfer rate calculated by the m-LMED method from that obtained from numerically solving the fundamental governing equations is defined as follows:

$$\text{Relative Deviation}=\left|\frac{q_{\text{m-LMED}}-q_{\text{numerical solution}}}{q_{\text{numerical solution}}}\right| \tag{7.31}$$

where $q_{\text{m-LMED}}$ and $q_{\text{numerical solution}}$ are the total heat transfer rates calculated by the m-LMED method and from the NS, respectively.

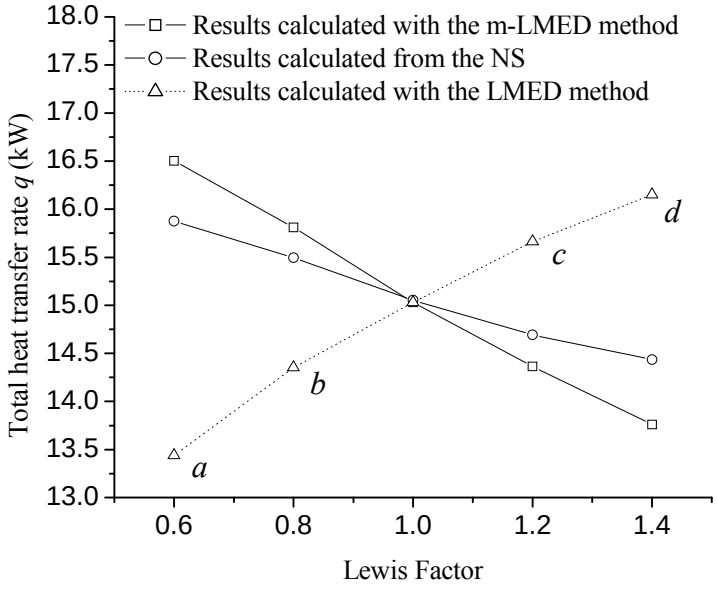

Fig.7.2 The total heat transfer rates calculated by the LMED, m-LMED methods and from the numerical solutions under different actual Lewis Factors

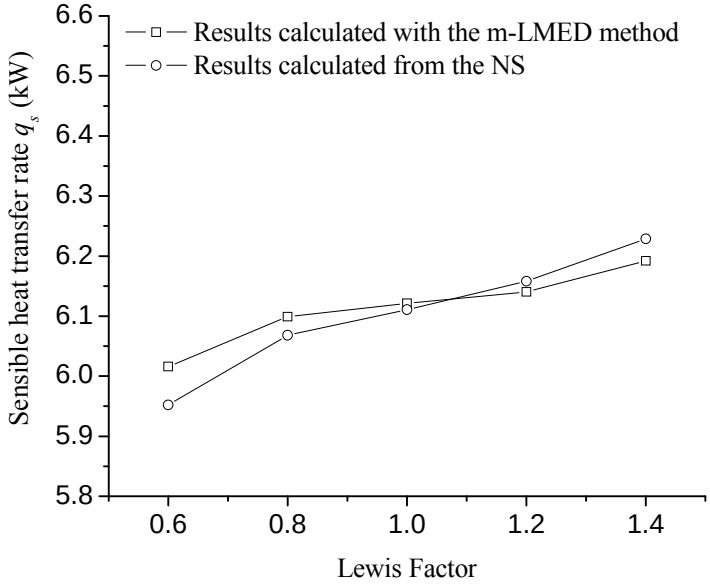

Fig.7.3 The sensible heat transfer rates calculated by the m-LMED method and from the numerical solutions under different actual Lewis Factors

The Relative Deviations for the sensible heat transfer rate, q_s, under different Lewis Factors were also calculated by substituting q with q_s in Eq. (7.31). The Relative Deviations for both q and q_s calculated by the m-LMED method and the Relative Deviations for q calculated by the LMED method under different Lewis Factors are shown in Table 7.4.

Table 7.4 Relative Deviations (RD) for the total heat transfer rate (q) and sensible heat transfer rate (q_s) calculated by the m-LMED method and LMED method, respectively

For the m-LMED method					
Lewis Factor	0.6	0.8	1.0	1.2	1.4
RD of q (%)	3.94	2.03	0.14	2.23	4.68
RD of q_s (%)	1.08	0.51	0.16	0.36	0.59
For the LMED method					
Lewis Factor	0.6	0.8	1.0	1.2	1.4
RD of q (%)	18.13	7.97	0.14	6.20	14.62

As seen in Table 7.4, the highest RD for q is about 5%; and that for q_s is about 1% when using the m-LMED method. Therefore, the m-LMED method is validated. Furthermore, it can be seen from Table 7.4 that the Relative Deviations for both q and q_s increase when the Lewis Factor deviates from 1.

7.4 Discussions

When actually applying the m-LMED method to a wet cooling coil, the Lewis Factor should be firstly determined. Pirompugd et al. [2007] provided the following equation for calculating the Lewis Factor of a wet cooling coil:

$$Le^{2/3} = 2.282 N^{0.2393} \left(\frac{S_f}{d_o}\right)^{(0.0239N+0.4332)} \left(\frac{A_a}{A_{a,t}}\right)^{(0.0321N+0.0747)} Re_{d_o}^{\left(-0.01833N-0.1094\frac{S_f}{d_o}-0.0026\frac{p_l}{d_o}-0.03012\frac{p_t}{d_o}+0.0418\right)} \quad (7.32)$$

where N is the number of tube rows of an air cooling coil; S_f and d_o, the fin spacing and outside tube diameter; $A_{a,t}$, the outside tube area; p_l and p_t; the longitudinal and transverse tube pitch.

After obtaining $Le^{2/3}$, the procedure of applying the m-LMED method as detailed in Section 7.3.2 may be then followed.

The use of the m-LMED method will require additional computational efforts than that of the LMED method, as an iterative process is involved. This is justified because a higher accuracy in evaluating the total heat transfer rate in a wet cooling coil can be attained. However, the additional computational effort is much less than

that involved in numerically solving the fundamental equations governing the heat and mass transfer in a wet cooling coil, as both the discretization of the governing differential equations and the iterative solving process are involved.

7.5 Conclusions

In this Chapter, a modified LMED method has been developed and is reported. The m-LMED method can be applied to calculating the total heat transfer rate in a wet cooling coil under both unit and non-unit Lewis Factors' operating conditions.

The m-LMED method has been validated by comparing its predictions of the total heat transfer rate to that from numerically solving the fundamental governing equations of the heat and mass transfer of a wet cooling coil, with less than 5% deviation. Therefore, the m-LMED method can replace the LMED method for evaluating the thermal performance of a wet cooling coil operated with both unit and non-unit Lewis Factors.

Chapter 8

The Analytical Solutions for Evaluating The Thermal Performances of A Wet Air Cooling Coil

8.1 Introduction

As mentioned in Literature Review presented in Chapter 2, there have been previous studies on evaluating the thermal performances of various heat exchangers including air cooling coils. Related mathematical models and solutions have been developed, which may be broadly categorized by: (1) numerical solutions to the fundamental heat and mass transfer governing equations; (2) lumped parameter models; (3) analytical solutions to the governing equations. For a numerical solution, an air cooling and dehumidifying coil is divided into a number of segments where the spatial distributions of the two key operating parameters, air temperature and humidity ratio, are neglected, and the differences of the parameters in the different segments can be calculated to reflect the distributions of the parameters. With this approach, the thermal performances of air cooling coils may be accurately evaluated, at the expenses of a longer time and a larger space for computations.

The use of a lumped parameter model can be, however, more preferred than the use of a numerical solution because of its lower computational costs. In a lumped parameter model, the enthalpy difference between air and a cooling medium is

treated as the driving force of simultaneous heat and mass transfer. Such a treatment was firstly proposed by Threlkeld [1970], based on the assumption of unit Lewis Factor, and is now recommended by ASHRAE [ASHRAE 2001] and has been popularly adopted when developing lumped parameter models. However, a number of studies have also suggested the Lewis Factor may well deviate from being one [Hong and Webb 1996, Seshimo et al. 1988, Eckels and Rabas 1987, Pirompugd et al. 2007, Wang 2008]. The unit-Lewis Factor assumption can lead to errors when using the lumped parameter model in evaluating the thermal performances of air cooling coils.

In order to be able to accurately evaluate the thermal performance of different types of heat exchangers with a lower computational cost, analytical solutions have been developed and reported [Klein and Eigenberger 2001, Kabashnikov et al. 2002, Bielski and Malinowski 2005, Ren and Yang 2006, Bandyopadhyay et al. 2008]. Although analytical solutions have been developed to investigate the thermal performances of the components in a fin-and-tube air cooling coil, for example, fins [Xia and Jacobi 2004], there are no analytical solutions to study the thermal performance of an entire fin-and-tube air cooling coil because of its complexity.

Although a lumped parameter based m-LMED model has been developed and is reported in Chapter 7, the distributions of the temperature and moisture content of bulk air in a wet air cooling coil along air flow direction cannot be evaluated by

using this m-LMED model. In this Chapter, the analytical solutions for evaluating the thermal performance of both a chilled water wet air cooling coil and a DX wet air cooling coil have been developed and are reported. The distributions of air temperature and moisture content along the air flow direction were obtained. The profiles of air temperature and moisture content derived from the analytical solutions were compared to those from numerical solutions to validate the analytical solutions. Furthermore, a comparison between the computation time required by both the analytical solutions and numerical solutions in assessing the thermal performance of a wet air cooling coil operated at the same condition was also carried out to illustrate that the analytical solutions were convenient to use, requiring much less computation time.

8.2 Development of the analytical solutions of wet air cooling coils

In this section, the analytical solutions for both a chilled water wet cooling coil and a DX wet cooling coil have been developed. The difference between the two types of cooling coil is the cooling medium, i.e., either chilled water or refrigerant, used. Nonetheless, both can be represented by Fig. 8.1 showing a typical cross flow fin-and-tube cooling coil. In evaluating its thermal performance, a cross flow cooling coil is normally treated as a counter flow cooling coil. Fig. 8.2 shows the schematics of a counter flow air cooling coil studied in this Chapter. Both the air side and

cooling medium side, and surface of the cooling coil which separates the air and cooling medium sides are shown.

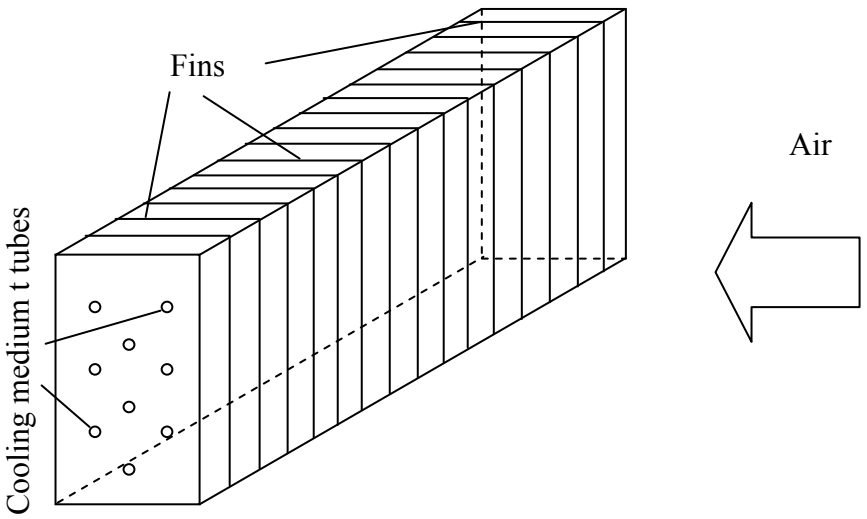

Fig. 8.1 A typical cross flow air cooling coil

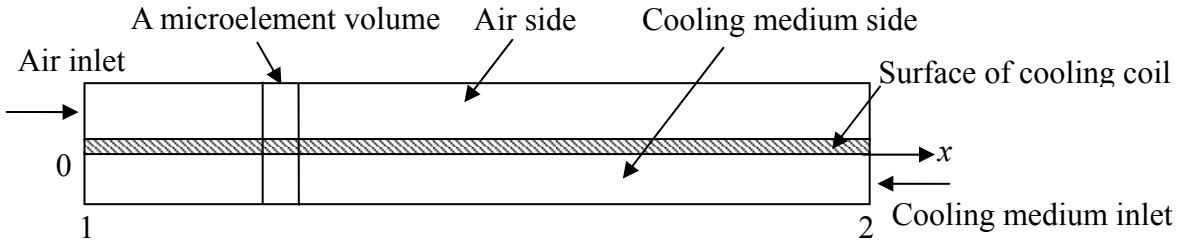

Fig. 8.2 Schematics of a counter flow air cooling coil

On the other hand, in developing the analytical solutions, the heat transfer resistances due to both the tube metal and water condensate film on the external surface of the cooling coil were small compared to those on air side and cooling medium side, thus

negligible.

The fundamental governing equations for heat and mass transfer taking place in both a chilled water wet air cooling coil and a DX wet cooling coil are

$$dq_s = \alpha_a (T_a - T_{sf}) \eta_o dA_a \tag{8.1}$$

$$dq_l = \frac{\alpha_a}{C_{pa} Le^{2/3}} h_{fg} (w_a - w_{sf}) \eta_o dA_a \tag{8.2}$$

$$dq_s = -m_a C_{pa} dT_a \tag{8.3}$$

$$dq_l = -m_a h_{fg} dw_a \tag{8.4}$$

$$dq = -\alpha_c (T_{sf} - T_c) dA_c \tag{8.5}$$

For a chilled water cooling coil

$$dq = dq_s + dq_l = -m_c C_{pc} dT_c \tag{8.6.a}$$

For a DX cooling coil

$$dq = dq_s + dq_l \tag{8.6.b}$$

8.2.1 The analytical solution for a chilled water air cooling coil

For heat transfer, combining and integrating Eqs. (8.1), (8.3), (8.5) (8.6.a) would give the relationship among T_c, and T_a and w_a,

$$T_c = T_{c,2} + \frac{m_a C_{pa}}{m_c C_{pc}}(T_a - T_{a,2}) + \frac{m_a h_{fg}}{m_c C_{pc}}(w_a - w_{a,2}) \tag{8.7}$$

Combining Eqs. (8.1) and (8.5), and because of the fixed ratio between A_a and A_c for the entire cooling coil, the temperature of coil external surface, T_{sf}, could be evaluated by:

$$T_{sf} = [1 + \frac{\alpha_c A_{c,t}(dq_s/dq)}{\alpha_a \eta_o A_{a,t}}]^{-1} \cdot [\frac{\alpha_c A_{c,t}(dq_s/dq)}{\alpha_a \eta_o A_{a,t}} T_c + T_a] \tag{8.8}$$

where $A_{a,t}$ and $A_{c,t}$ are the total surface area at the air and chilled water sides, respectively. Eliminating dq_s by combining Eqs. (8.1) and (8.3) yielded:

$$dT_a = -\frac{\alpha_a \eta_o}{m_a C_{pa}}(T_a - T_{sf})dA_a \tag{8.9}$$

Eliminating T_{sf} and T_c by combining Eqs. (8.7 - 8.9) gave:

$$dT_a = -\frac{\alpha_a \eta_o}{m_a C_{pa}} \{[1 - \frac{\alpha_a \eta_o A_{a,t} + \alpha_c A_{c,t} (dq_s/dq) \frac{m_a C_{pa}}{m_c C_{pc}}}{\alpha_a \eta_o A_{a,t} + \alpha_c A_{c,t} (dq_s/dq)}] T_a$$
$$- \frac{\alpha_c A_{c,t} (dq_s/dq) \frac{m_a h_{fg}}{m_c C_{pc}}}{\alpha_a \eta_o A_{a,t} + \alpha_c A_{c,t} (dq_s/dq)} w_a \qquad (8.10)$$
$$- \frac{\alpha_c A_{c,t} (dq_s/dq) (T_{c,2} - \frac{m_a C_{pa}}{m_c C_{pc}} T_{a,2} - \frac{m_a h_{fg}}{m_c C_{pc}} w_{a,2})}{\alpha_a \eta_o A_{a,t} + \alpha_c A_{c,t} (dq_s/dq)} \} dA_a$$

For mass transfer, w_{sf} was assumed to be linearly related to T_{sf},

$$w_{sf} = aT_{sf} + b = a[1 + \frac{\alpha_c A_{c,t} (dq_s/dq)}{\alpha_a \eta_o A_{a,t}}]^{-1} \cdot [\frac{\alpha_c A_{c,t} (dq_s/dq)}{\alpha_a \eta_o A_{a,t}} T_c + T_a] + b \qquad (8.11)$$

where the parameters, a and b, may be determined by using the properties of the saturated moist air [ASHRAE 2000].

Eliminating dq_l by combining Eqs. (8.2) and (8.4) yielded:

$$dw_a = -\frac{\alpha_a \eta_o}{m_a C_{pa} Le^{2/3}} (w_a - w_{sf}) dA_a \qquad (8.12)$$

Therefore, for mass transfer, following the same manipulation approach used for heat transfer, the relationship between dw_a and T_a as well as w_a yielded:

$$dw_a = -\frac{\alpha_a \eta_o}{m_a C_{pa} Le^{2/3}} \{ -\frac{a\alpha_a \eta_o A_{a,t} + a\alpha_c A_{c,t} (dq_s/dq) \frac{m_a C_{pa}}{m_c C_{pc}}}{\alpha_a \eta_o A_{a,t} + \alpha_c A_{c,t} (dq_s/dq)} T_a + [1 - \frac{a\alpha_c A_{c,t} (dq_s/dq) \frac{m_a h_{fg}}{m_c C_{pc}}}{\alpha_a \eta_o A_{a,t} + \alpha_c A_{c,t} (dq_s/dq)}] w_a - \frac{a\alpha_c A_{c,t} (dq_s/dq) (T_{c,2} - \frac{m_a C_{pa}}{m_c C_{pc}} T_{a,2} - \frac{m_a h_{fg}}{m_c C_{pc}} w_{a,2})}{\alpha_a \eta_o A_{a,t} + \alpha_c A_{c,t} (dq_s/dq)} - b \} dA_a \quad (8.13)$$

If assuming that dq_s/dq did not change for the entire cooling coil surface area and was equal to the ratio of the sensible heat transfer rate to the total heat transfer rate of the entire coil or sensible heat ratio (SHR), $q_{s,t}/q_t$, as adopted by Xia and Jacobi [2005], and under a fixed operating condition, q_t, $q_{s,t}$, $T_{a,2}$ and $w_{a,2}$ would be considered as fixed. Therefore, Eqs. (8.10) and (8.13) could be transformed, respectively, to:

$$dT_a = [\Gamma(1-\Pi)T_a - \Gamma\Omega w_a - \Gamma\Psi] dA_a \quad (8.14)$$

$$dw_a = [-a\Lambda\Pi T_a + \Lambda(1-a\Omega) w_a + (-a\Lambda\Psi - b\Lambda)] dA_a \quad (8.15)$$

where coefficients a, b, Γ, Λ, Π, Ω, and Ψ are constant along air flow direction; Γ, Λ, Π, Ω, and Ψ could be calculated by:

$$\Gamma = -\frac{\alpha_a \eta_o}{m_a C_{pa}} \tag{8.16a}$$

$$\Lambda = -\frac{\alpha_a \eta_o}{m_a C_{pa} Le^{2/3}} \tag{8.16b}$$

$$\Pi = \frac{\alpha_a \eta_o A_{a,t} + \alpha_c A_{c,t} (q_{s,t}/q_t) \dfrac{m_a C_{pa}}{m_c C_{pc}}}{\alpha_a \eta_o A_{a,t} + \alpha_c A_{c,t} (q_{s,t}/q_t)} \tag{8.16c}$$

$$\Omega = \frac{\alpha_c A_{c,t} (q_{s,t}/q_t) \dfrac{m_a h_{fg}}{m_c C_{pc}}}{\alpha_a \eta_o A_{a,t} + \alpha_c A_{c,t} (q_{s,t}/q_t)} \tag{8.16d}$$

$$\Psi = \frac{\alpha_c A_{c,t} (q_{s,t}/q_t) (T_{c,2} - \dfrac{m_a C_{pa}}{m_c C_{pc}} T_{a,2} - \dfrac{m_a h_{fg}}{m_c C_{pc}} w_{a,2})}{\alpha_a \eta_o A_{a,t} + \alpha_c A_{c,t} (q_{s,t}/q_t)} \tag{8.16e}$$

In Eqs. (8.16a - 8.16e), η_o is the overall fin efficiency, and might be evaluated by Eq. (8.17)

$$\eta_o = 1 - \frac{A_{f,t}}{A_{a,t}} (1 - \eta) \tag{8.17}$$

where η is the fin efficiency, For a plate fin-and-tube cooling coil, η could be determined by Hong-Webb Equation [Hong and Webb 1996]:

$$\eta = \frac{\tanh(Mr_o\phi)\cos(0.1Mr_o\phi)}{Mr_o\phi} \tag{8.18}$$

where Φ and M are evaluated by the following two equations:

$$\phi = (\frac{R_o}{r_o} - 1)[1 + 0.35\ln(\frac{R_o}{r_o})] \tag{8.19}$$

$$M = [\frac{2\alpha_a}{kt}(1 + \frac{dq_l}{dq_s}\frac{h_{fg}}{C_{pa}})]^{\frac{1}{2}} = [\frac{2\alpha_a}{kt}(1 + \frac{q_{l,t}}{q_{s,t}}\frac{h_{fg}}{C_{pa}})]^{\frac{1}{2}} \tag{8.20}$$

where r_o is the outside radius of the cooling medium tube ; k, t the heat conductivity and thickness of the fin, respectively; $q_{l,t}$, the total latent heat transfer rate; R_o, the equivalent outside tube radius of the plate fin, which was determined as follows, according to Hong and Webb [Hong and Webb 1996],

$$R_o = 1.28W_f(L_f / W_f - 0.2)^{1/2} \tag{8.21}$$

where L_f and W_f are the length and width of the fin, respectively.

Equations (8.14) and (8.15) were used to describe the thermal performance of a chilled water air cooling coil where simultaneous heat and mass transfer took place. Eqs. (8.14) and (8.15) could be transformed to:

$$d(T_a + \varepsilon_{\mathrm{I}} w_a) = [\sigma_{\mathrm{I}}(T_a + \varepsilon_{\mathrm{I}} w_a) + \zeta_{\mathrm{I}}]dA_a \tag{8.22}$$

$$d(T_a + \varepsilon_{\mathrm{II}} w_a) = [\sigma_{\mathrm{II}}(T_a + \varepsilon_{\mathrm{II}} w_a) + \zeta_{\mathrm{II}}]dA_a \tag{8.23}$$

where ε_{I}, $\varepsilon_{\mathrm{II}}$, σ_{I}, σ_{II}, ζ_{I} and ζ_{II} are the coefficients to be determined.

For ensuring the consistency between coefficients used in Eqs. (8.22) to (8.23) and Eqs. (8.14) to (8.15), it was necessary that ε_{I} and $\varepsilon_{\mathrm{II}}$ were the two conjugate roots of a quadratic equation of one variable,

$$\varepsilon^2 + \frac{\Lambda(1 - a\Omega) - \Gamma(1 - \Pi)}{a\Lambda\Pi}\varepsilon - \frac{\Gamma\Omega}{a\Lambda\Pi} = 0 \tag{8.24}$$

Then σ_{I}, σ_{II}, ζ_{I} and ζ_{II} could be evaluated by:

$$\sigma_{\mathrm{I}} = -\varepsilon_{\mathrm{I}} a\Lambda\Pi + \Gamma(1 - \Pi) \tag{8.25.a}$$

$$\sigma_{\mathrm{II}} = -\varepsilon_{\mathrm{II}} a\Lambda\Pi + \Gamma(1 - \Pi) \tag{8.25.b}$$

$$\zeta_{\mathrm{I}} = -\varepsilon_{\mathrm{I}}(a\Lambda\Psi + b\Lambda) - \Gamma\Psi \tag{8.25.c}$$

$$\zeta_{\mathrm{II}} = -\varepsilon_{\mathrm{II}}(a\Lambda\Psi + b\Lambda) - \Gamma\Psi \tag{8.25.d}$$

After the determination of ε_{I}, $\varepsilon_{\mathrm{II}}$, σ_{I}, σ_{II}, ζ_{I} and ζ_{II}, and using $T_{a,1}$, $w_{a,1}$ as boundary conditions for Eqs. (8.22) and (8.23), the solutions to these two equations were obtained:

$$T_a + \varepsilon_{\mathrm{I}} w_a + \frac{\zeta_{\mathrm{I}}}{\sigma_{\mathrm{I}}} = (T_{a,1} + \varepsilon_{\mathrm{I}} w_{a,1} + \frac{\zeta_{\mathrm{I}}}{\sigma_{\mathrm{I}}}) e^{\sigma_{\mathrm{I}} A_a} \tag{8.26.a}$$

$$T_a + \varepsilon_{\mathrm{II}} w_a + \frac{\zeta_{\mathrm{II}}}{\sigma_{\mathrm{II}}} = (T_{a,1} + \varepsilon_{\mathrm{II}} w_{a,1} + \frac{\zeta_{\mathrm{II}}}{\sigma_{\mathrm{II}}}) e^{\sigma_{\mathrm{II}} A_a} \tag{8.26.b}$$

or:

$$T_a = \frac{\varepsilon_{\mathrm{II}}(T_{a,1} + \varepsilon_{\mathrm{I}} w_{a,1} + \frac{\zeta_{\mathrm{I}}}{\sigma_{\mathrm{I}}}) e^{\sigma_{\mathrm{I}} A_a} - \varepsilon_{\mathrm{I}}(T_{a,1} + \varepsilon_{\mathrm{II}} w_{a,1} + \frac{\zeta_{\mathrm{II}}}{\sigma_{\mathrm{II}}}) e^{\sigma_{\mathrm{II}} A_a}}{\varepsilon_{\mathrm{II}} - \varepsilon_{\mathrm{I}}} - \frac{(\varepsilon_{\mathrm{II}} \frac{\zeta_{\mathrm{I}}}{\sigma_{\mathrm{I}}} - \varepsilon_{\mathrm{I}} \frac{\zeta_{\mathrm{II}}}{\sigma_{\mathrm{II}}})}{\varepsilon_{\mathrm{II}} - \varepsilon_{\mathrm{I}}} \tag{8.27}$$

$$w_a = \frac{(T_{a,1} + \varepsilon_{\mathrm{II}} w_{a,1} + \frac{\zeta_{\mathrm{II}}}{\sigma_{\mathrm{II}}}) e^{\sigma_{\mathrm{II}} A_a} - (T_{a,1} + \varepsilon_{\mathrm{I}} w_{a,1} + \frac{\zeta_{\mathrm{I}}}{\sigma_{\mathrm{I}}}) e^{\sigma_{\mathrm{I}} A_a}}{\varepsilon_{\mathrm{II}} - \varepsilon_{\mathrm{I}}} - \frac{(\frac{\zeta_{\mathrm{II}}}{\sigma_{\mathrm{II}}} - \frac{\zeta_{\mathrm{I}}}{\sigma_{\mathrm{I}}})}{\varepsilon_{\mathrm{II}} - \varepsilon_{\mathrm{I}}} \tag{8.28}$$

8.2.2 The analytical solution for a DX air cooling coil

In a DX air cooling coil, the cooling medium temperature, T_c, which was the

evaporating temperature of refrigerant, could be regarded as a constant for the entire cooling coil. Hence, T_c was equal to the inlet temperature of cooling medium, $T_{c,2}$.

A parameter Θ was defined as:

$$\Theta = \frac{\alpha_c A_{c,t}(q_{s,t}/q_t)}{\alpha_a \eta_o A_{a,t} + \alpha_c A_{c,t}(q_{s,t}/q_t)} \tag{8.29}$$

Consequently, T_a and w_a were calculated by:

$$dT_a = -\frac{\alpha_a \eta_o \Theta}{m_a C_{pa}}(T_a - T_{c,2})dA_a \tag{8.30}$$

$$dw_a = -\frac{\alpha_a \eta_o}{m_a C_{pa} Le^{2/3}}[w_a - a\Theta T_{c,2} - a(1-\Theta)T_a - b]dA_a \tag{8.31}$$

The solutions to Eqs. (8.30) and (8.31) were:

$$T_a = T_{c,2} + (T_{a,1} - T_{c,2})e^{-\frac{\alpha_a \eta_o \Theta}{m_a C_{pa}} A_a} \tag{8.32}$$

$$\begin{aligned} w_a = {} & [w_{a,1} - (aT_{c,2} + b) + \frac{a(\Theta-1)(T_{a,1} - T_{c,2})}{1 - \Theta Le^{2/3}}]e^{-\frac{\alpha_a \eta_o}{m_a C_{pa} Le^{2/3}} A_a} \\ & - \frac{[a(\Theta-1)(T_{a,1} - T_{c,2})]}{1 - \Theta Le^{2/3}} e^{-\frac{\alpha_a \eta_o \Theta}{m_a C_{pa}} A_a} + (aT_{c,2} + b) \end{aligned} \tag{8.33}$$

Equations (8.27) to (8.28) and Eqs. (8.32) to (8.33) provided the solutions of T_a, w_a in both a chilled water wet cooling coil and a DX wet cooling coil, respectively. Given that the value of $q_{s,t}/q_t$, on which a number of coefficients in these equations were dependent, was unknown at the beginning of calculation, hence, an iteration procedure was implemented in determining the final results of T_a and w_a, as follows.

- Assuming an initial value of q_s/q with which $T_{a,2}$ and $w_{a,2}$ were also determined initially, calculating the coefficients Γ, Λ, Π, Ω, and Ψ using Eq. (8.16); and ε_{I}, $\varepsilon_{\mathrm{II}}$, σ_{I}, σ_{II}, ζ_{I} and ζ_{II} using Eqs. (8.24) and (8.25); Θ using Eq. (8.29), respectively.
- Calculating $T_{a,2}$, $w_{a,2}$ using Eqs. (8.27) and (8.28) for a chilled water air cooling coil and Eqs. (8.32) and (8.33) for a DX air cooling coil, respectively, and then calculating the new value of $q_{s,t}/q_{,t}$,

$$\frac{q_{s,t}}{q_t} = \frac{m_a C_{pa}(T_{a,2} - T_{a,1})}{m_a C_{pa}(T_{a,2} - T_{a,1}) + m_a h_{fg}(w_{a,2} - w_{a,1})} \tag{8.34}$$

- Comparing originally assumed and the calculated values of $q_{s,t}/q_t$, $T_{a,2}$ and $w_{a,2,}$ the calculation ended when a convergence arrived.

8.3 Validation of the analytical solutions

In order to validate the analytical solutions developed, T_a and w_a calculated by using Eqs. (8.27) and (8.28), and Eqs. (8.32) and (8.33) were compared to the values of T_a and w_a calculated by numerically solving the fundamental heat and mass transfer governing equations, i.e., Eqs. (8.1 - 8.6). The specific operating conditions adopted for two types of cooling coils when validating the analytical solutions are shown in Table 8.1. Other general operating conditions are shown in Table 8.2. The geometrical parameters of two types of cooling coils are shown in Table 8.3. The input Lewis Factors were 0.6, 0.8, 1 and 1.2 for both the chilled water cooling coil and DX cooling coil.

To obtain the numerical solutions to the fundamental governing equations, differential equations were obtained by first order backward discretizing these governing equations along the air flow direction. The total number of microelements for discretization was 500. The iteration repeated until the relative errors of all the results were lower than 1×10^{-4}.

Table 8.1 Specific operating conditions adopted for validating the analytical solutions

Chilled water cooling coil		DX cooling coil	
Mass flow rate of chilled water, kg/s	0.35	Mass flow rate of refrigerant, kg/s	0.025
Inlet temperature of chilled water to the cooling coil, ^{o}C	8	Evaporating temperature, ^{o}C	6
		Inlet void fraction of refrigerant	0
Mass flow rate of air, kg/s	0.6	Mass flow rate of air, kg/s	0.6
Inlet air temperature, ^{o}C	24	Inlet air temperature, ^{o}C	26
Inlet air humidity ratio, kg/kg	0.016	Inlet air humidity ratio, kg/kg	0.01

Table 8.2 General operating conditions

Specific heat of chilled water, kJ/(kg K)	4193
Specific heat of air, kJ/(kg K)	1.007
Heat transfer coefficient of chilled water, W/(K m^2)	8000
Heat transfer coefficient of refrigerant in DX cooling coil, W/(K m^2)	5000
Heat transfer coefficient of air in wet condition, W/(K m^2)	70
Atmosphere pressure, kPa	101.325

Table 8.3 Geometrical parameters of the two types of cooling coils

Overall air side heat transfer area, m^2	24
Overall cooling medium side heat transfer area, m^2	1.25
Overall fin surface area, m^2	22.5
Fin length, m	0.013
Fin width, m	0.011
Fin thickness, mm	0.115
Outside diameter of the cooling medium tube, mm	9.52

Figures 8.3 and 8.4 show the variations of both T_a and w_a along air flow direction obtained by using both the analytical solution and numerical solution under different Lewis Factors, for chilled water and DX cooling coils, respectively. The variation profiles of both T_a and w_a obtained from both the analytical and the numerical solutions were basically identical. The results of $q_{s,t}$, $q_{l,t}$ and q_t obtained from both analytical solutions and numerical simulation are listed in Tables 8.4 and 8.5, for the chilled water cooling coil and DX cooling coil, respectively. The relative deviation, RD, defined in Eq. (8.35), was used to illustrate the validity of the analytical solutions. The mean RDs, listed in Tables 8.4 and 8.5, were averaged from the RDs for the four input Lewis Factors. From Tables 8.4 and 8.5, all of the mean RDs are less than 2%, verifying the validity of the analytical solutions. Such a deviation of less than 2% was most likely caused by assuming the local sensible heat ratio, dq_s/dq,

be equal to the sensible heat ratio for the entire cooling coil, $q_{s,t}/q_t$.

$$\text{RD}=\left|\frac{\text{Results of Analytical Solution} - \text{ Results of Numerical Solution}}{\text{Results of Numerical Solution}}\right|\times 100\% \quad (8.35)$$

Figure 8.5 shows the errors in the total heat transfer rate and sensible heat ratio, when $w_{a,1}$ changes from 0.01 kg/kg to 0.02 kg/kg with an increment of 0.002 kg/kg, and the Lewis Factor was at 0.6 for the DX cooling coil. It can be seen that the errors in both the total heat transfer rate and in the sensible heat ratio shown in Fig. 8.5 are not greater than 3% and 5%, respectively. This suggested that the analytical solution developed could predict these two operating parameters with a reasonably high accuracy.

In Figs. 8.3 and 8.4, the impacts of variation of Lewis Factor on the distributions of air temperature and humidity ratio are illustrated. For both the chilled water cooling coil and the DX cooling coil, the variation trends of air temperature and humidity ratio under different Lewis Factors appeared basically similar. It was further noted that the variation range of outlet air temperature from the coils was relatively small (~0.5%) under different Lewis Factors, but the outlet air humidity ratio increases with increased Lewis Factors (from 0.009 kg/kg to 0.01 kg/kg), implying that a smaller Lewis Factor would mean a greater mass transfer rate.

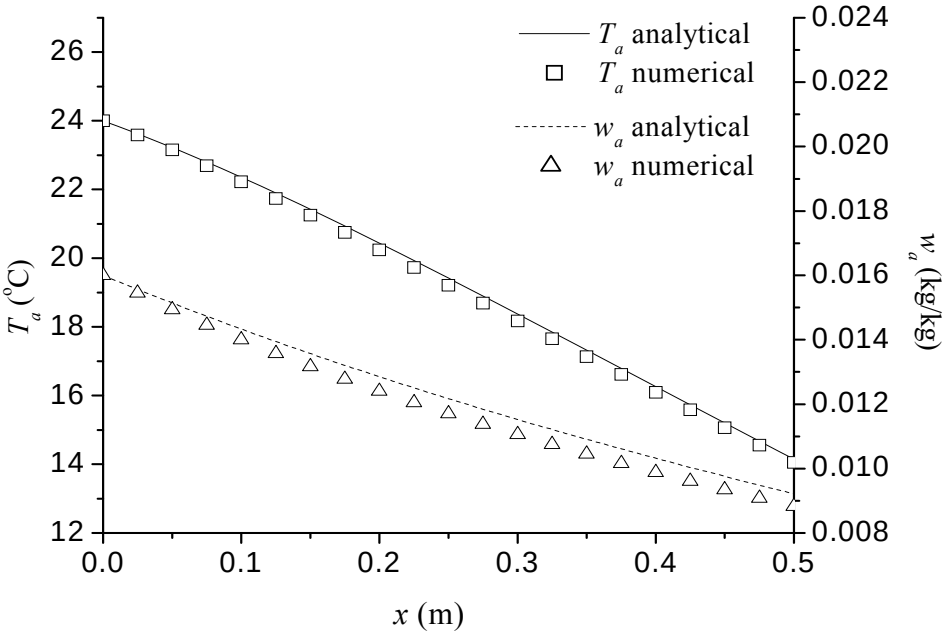

Lewis Factor = 0.6

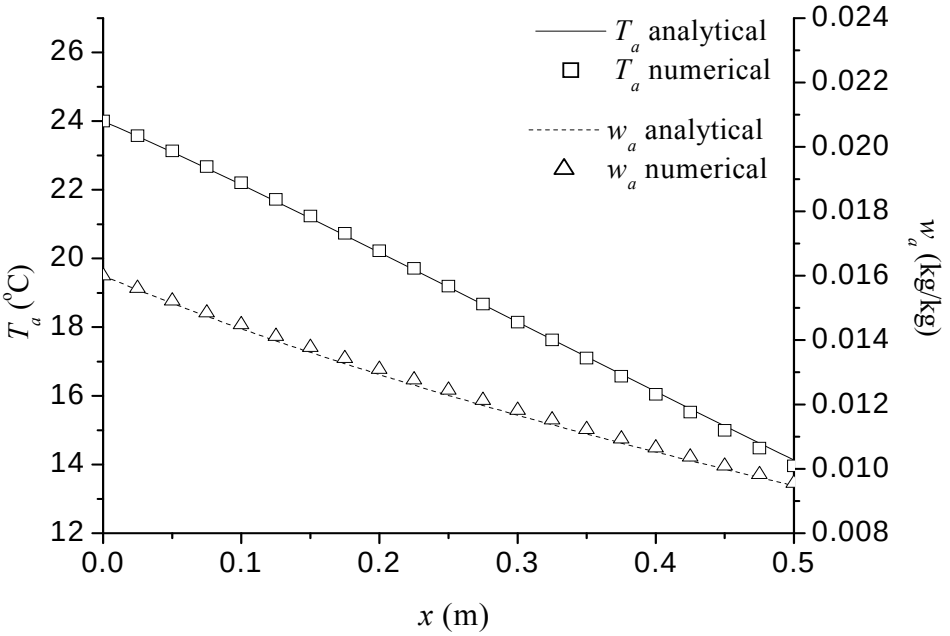

Lewis Factor = 0.8

Fig. 8.3 Variations of T_a and w_a along x axis under different Lewis Factors for the chilled water cooling coil

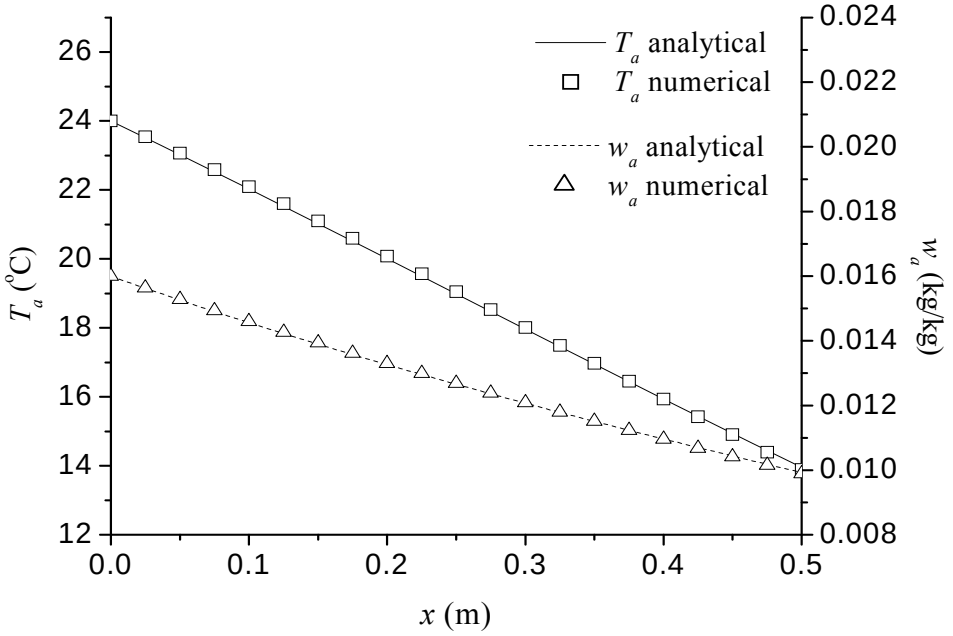

Lewis Factor = 1.0

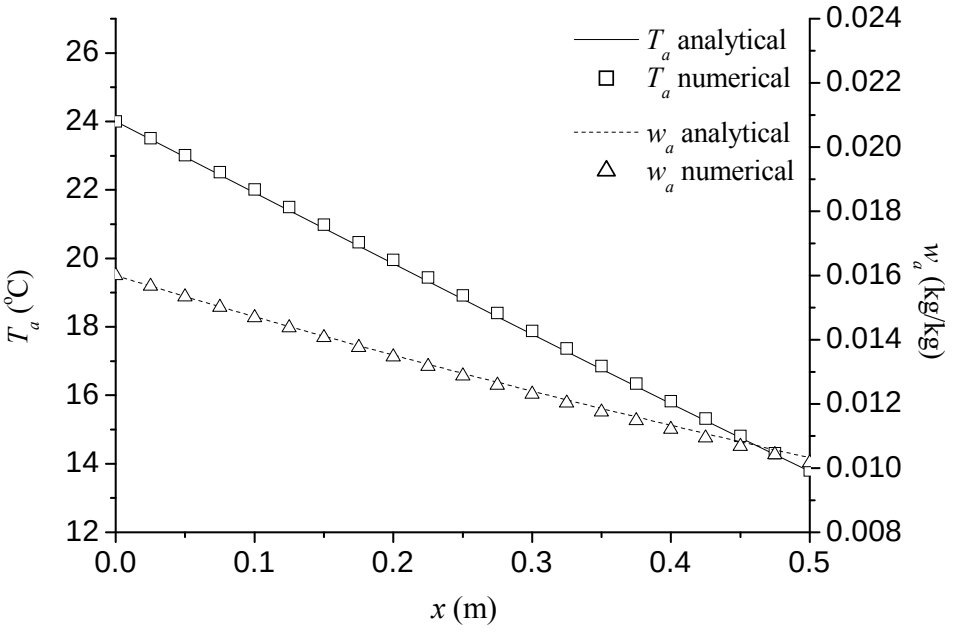

Lewis Factor= 1.2

Fig. 8.3 Variations of T_a and w_a along x axis under different Lewis Factors for the chilled water cooling coil (Continued)

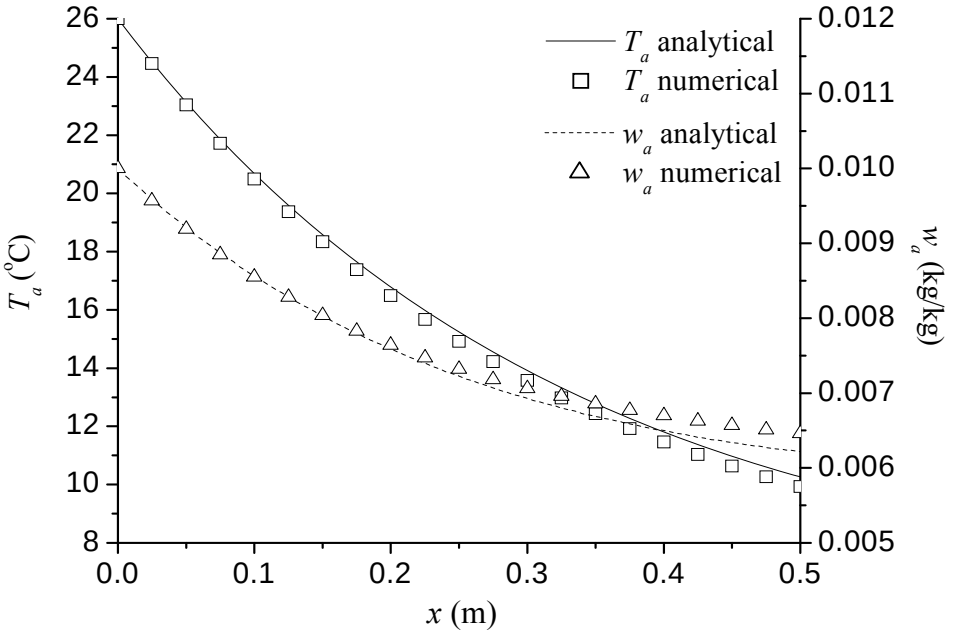

Lewis Factor= 0.6

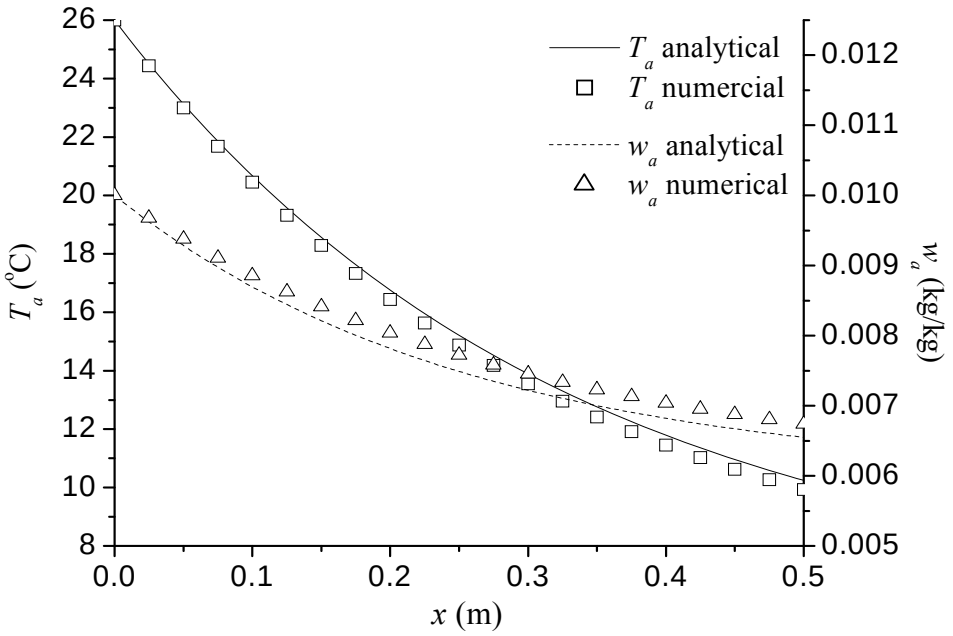

Lewis Factor= 0.8

Fig. 8.4 Variations of T_a and w_a along x axis under different Lewis Factors for the DX cooling coil

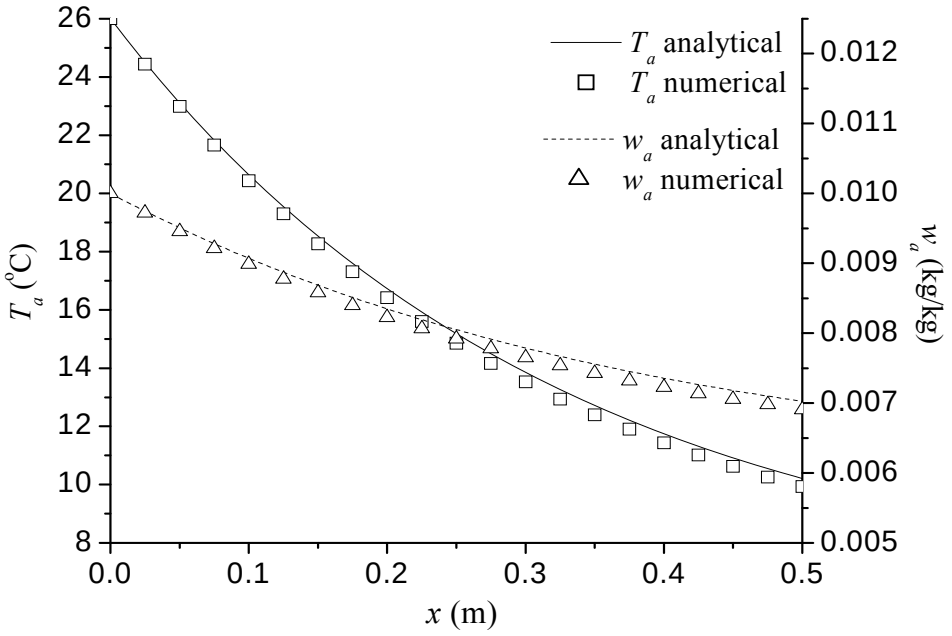

Lewis Factor= 1.0

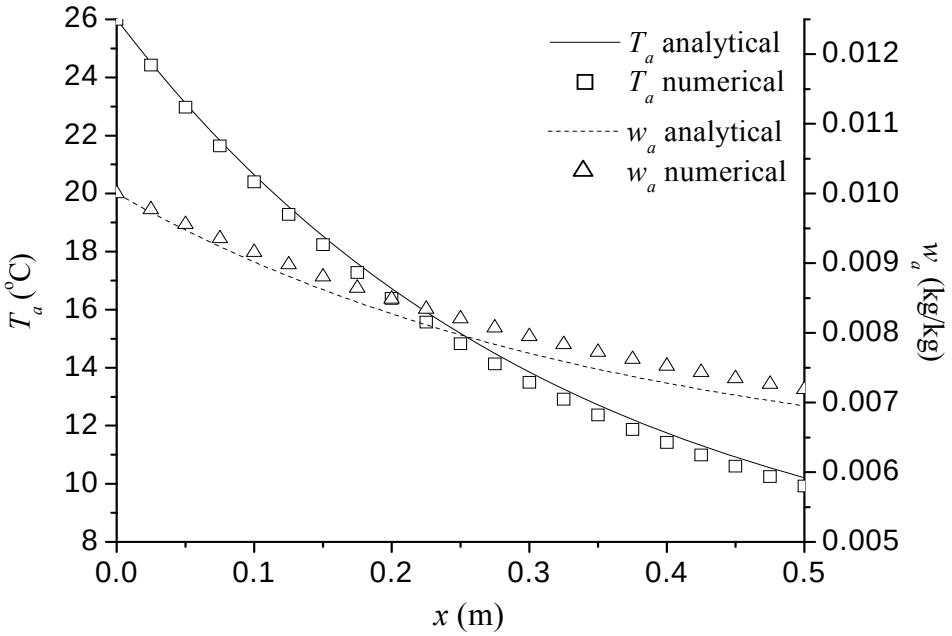

Lewis Factor= 1.2

Fig. 8.4 Variations of T_a and w_a along x axis under different Lewis Factors for the DX cooling coil (Continued)

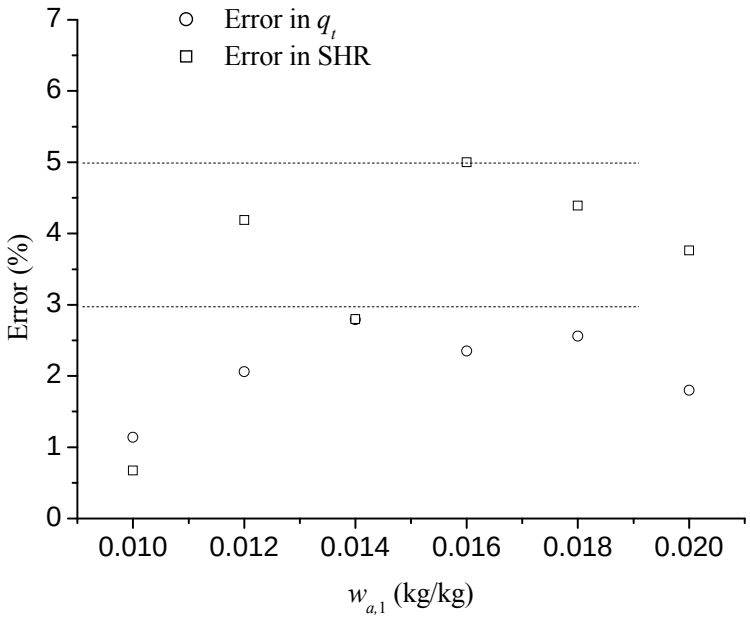

Fig. 8.5 Errors in the total heat transfer rate and SHR under different inlet air humidity ratio ($Le^{2/3}$=0.6) for the DX cooling coil

8.4 Discussions

As shown in Tables 8.4 and 8.5, a larger Lewis Factor would suggest a smaller mass or latent heat transfer and a larger sensible heat transfer. These trends were actually related to a decrease in mass transfer coefficient. Consequently, the local sensible heat transfer rate would be increased. As suggested by Eq. (8.8), the increase in the local sensible heat ratio would lead to a lower surface temperature. With a lower surface temperature, the total heat transfer rate was then reduced. This explains the

variations of results shown in both Tables 8.4 and 8.5.

Table 8.4 The sensible, latent ant total heat transfer rates obtained from analytical and numerical solutions and their mean RDs for the chilled water cooling coil

Input $Le^{2/3}$	By Analytical solutions			By Numerical solutions		
	$q_{s,t}$ (kW)	$q_{l,t}$ (kW)	q_t (kW)	$q_{s,t}$ (kW)	$q_{l,t}$ (kW)	q_t (kW)
0.6	5.791	10.219	16.010	5.952	9.925	15.877
0.8	5.993	9.580	15.573	6.068	9.429	15.497
1.0	6.096	8.913	15.008	6.111	8.941	15.052
1.2	6.189	8.324	14.513	6.158	8.534	14.692
mean RD	1.17%	1.83%	0.71%			

Table 8.5 The sensible, latent ant total heat transfer rates obtained from analytical and numerical solutions and their mean RDs for the DX cooling coil

Input $Le^{2/3}$	By Analytical solutions			By Numerical solutions		
	$q_{s,t}$ (kW)	$q_{l,t}$ (kW)	q_t (kW)	$q_{s,t}$ (kW)	$q_{l,t}$ (kW)	q_t (kW)
0.6	9.747	5.307	15.054	9.702	5.182	14.884
0.8	9.518	4.908	14.423	9.707	4.768	14.475
1.0	9.540	4.495	14.035	9.709	4.525	14.234
1.2	9.747	4.300	14.048	9.714	4.207	13.921
mean RD	0.72%	1.73%	0.95%			

The availability of the analytical solution developed provided a much quicker method in evaluating the thermal performance of a wet air cooling coil under different Lewis Factors when compared to numerically solving the governing equations. The average computation time durations required at different input Lewis Factors by the analytical solution and numerical solution to carry out the thermal performance evaluation were estimated. The average computation time durations required by using the analytical solution was about 1.043s, and 62.765s by the numerical solution for the chilled water cooling coil; and 0.922s and 25.418s for the DX cooling coil, as shown in Fig. 8.6.

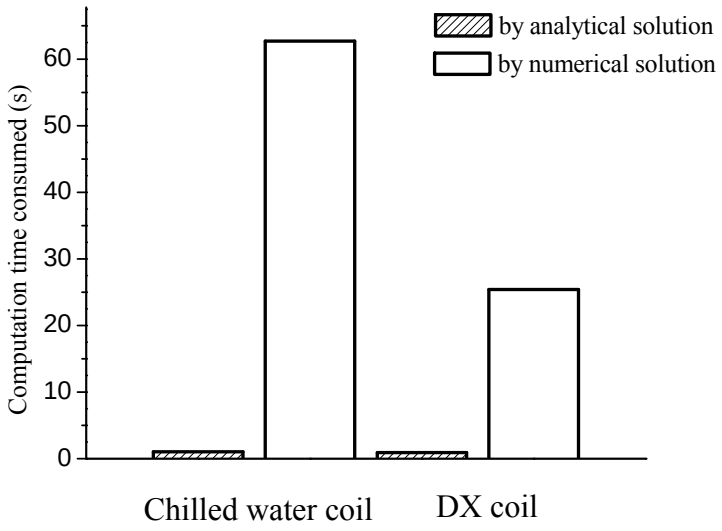

Fig. 8.6 Computation time durations consumed for achieving analytical and numerical results for the chilled water cooling coil and the DX cooling coil

8.5 Conclusions

The analytical solutions to the fundamental governing equations for the heat and mass transfer taking place in a chilled water wet cooling coil and a DX wet cooling coil for evaluating their thermal performance have been developed and are reported in this Chapter. Using the analytical solutions, the distributions of air temperature and humidity ratio along the air flow direction under different Lewis Factors were obtained. The analytical solutions were validated by comparing their predictions with those from numerical solutions to the same governing equations. It has been shown that the averaged relative deviations were less than 2% for the total heat transfer evaluation for all the input Lewis Factors for both types of cooling coils. The errors in the calculated total heat transfer rate and the calculated SHR were not greater than 3% and 5%, respectively, under all different operating conditions when Lewis Factor was 0.6.

Furthermore, the computation time duration required by using the analytical solution was much less than that by directly numerically solving the governing equations. Therefore, the analytical solutions reported in this Chapter can be used as a low-cost replacement to the numerical solutions in evaluating the thermal performance of wet air cooling coils.

Based on the results obtained using the analytical solution developed. It can be seen that with different Lewis Factors, mass transfer in a wet cooling coil can be different. A smaller Lewis Factor would imply a better mass transfer, a better dehumidifying effect in a wet cooling coil.

Chapter 9

Conclusions and Future Work

9.1 Conclusions

A programmed research work on studying the simultaneous heat and mass transfer taking place in a DX cooling coil has been successfully carried out and is reported in this thesis. The conclusions of the thesis are:

1) A complete set of Calculation Method for calculating the steady-state Equipment SHR of a DX cooling coil has been developed and is reported in Chapter 5. The Method which is based on known refrigerant evaporating temperature in a DX coil has been experimentally validated. With the Method developed, the Equipment SHR may well be predicted and analyzed with change of refrigerant evaporating temperature. This would be helpful for further studying simultaneous heat and mass transfer in a DX cooling coil and developing effective control strategies to obtain comfortable indoor thermal environment.

2) Chapter 6 reports two Types of Experiments carried out for examining the assumption of dry airside in the SPR in a DX cooling coil. The experimental data were processed using a lumped parameter Calculation Procedure specially developed to determine the surface conditions of the air side and water vapor

condensing rate in a SPR under different experimental conditions. The experimental results showed that no dry airside surface in SPR existed in the experimental DX cooling coil during all experiments. Therefore, the assumption of dry airside in a SPR was questionable. Assuming dry airside of SPR in a DX cooling coil can lead to an underestimated total amount of water vapor condensed on the entire air side of a DX cooling coil, ranging most likely between 3% and 7%. Consider one major possible reason of assuming dry airside in a SPR being computational time, and with the powerful computation facilities currently available, it is suggested that in future lumped parameter models, wet air side in a SPR should be adopted to improve modeling accuracy.

3) A modified LMED method has been developed and is reported in Chapter 7. The m-LMED method can be applied to calculating the total heat transfer rate in a wet cooling coil under both unit and non-unit Lewis Factors' operating conditions. The m-LMED method has been validated by comparing its predictions of the total heat transfer rate to that from numerically solving the fundamental governing equations of the heat and mass transfer of a wet cooling coil, with less than 5% difference. Therefore, the m-LMED method can replace the LMED method for evaluating the thermal performance of a wet cooling coil operated with both unit and non-unit Lewis Factors.

4) The analytical solutions to the fundamental governing equations for the heat and

mass transfer taking place in a chilled water wet cooling coil and a DX wet cooling coil for evaluating their thermal performance have been developed and are reported in Chapter 8. Using the analytical solutions, the distributions of air temperature and humidity ratio along the air flow direction under different Lewis Factors were obtained. The analytical solutions were validated by comparing their predictions with those from numerical solutions to the same governing equations. It has been shown that the averaged relative deviations were less than 2% for the total heat transfer evaluation for all the input Lewis Factors for both types of cooling coils. The errors in the calculated total heat transfer rate and the calculated SHR were not greater than 3% and 5%, respectively, under all different operating conditions when Lewis Factor was 0.6. Furthermore, the computation time duration required by using the analytical solution was much less than that by directly numerically solving the governing equations. Therefore, the analytical solutions reported in Chapter 8 can be used as a low-cost replacement to the numerical solutions in evaluating the thermal performance of wet air cooling coils.

The project reported in this thesis has made important contributions to studying the simultaneous heat and mass transfer taking place in DX cooling coils. The results obtained in this thesis are very useful to evaluating and analyzing the thermal performance of DX cooling coils under different operating conditions. The long-term significance of the project is that it helps facilitate a better understanding of the

thermal performance of DX cooling coils. Hence, effective control strategies for DX A/C systems to maintain indoor air temperature and RH within suitable ranges can be developed.

9.2 Proposed future work

A number of future studies following on the successful completion of the project reported in this thesis are proposed:

1) The calculation of the steady-state Equipment SHR of a DX A/C system is based on the evaporating temperature which is an important operating parameter of the DX A/C system. However, in the Calculation Method presented in Chapter 5, the evaporating temperature must be assigned as an input. It is therefore highly desirable to further develop the Calculation Method by eliminating the need of assigning the evaporating temperature as an input.

2) The m-LMED method reported in Chapter 7 can be applied to calculating the total heat transfer rate in a DX cooling coil under both unit and non-unit Lewis Factors. Further experimental validation should be therefore carried out. In future experiments, exact Lewis Factors can also be obtained and input to the m-LMED method for calculating the total heat transfer rate. The calculated total

heat transfer rate and the experimental results should be compared for validation purpose.

3) The analytical solutions to the fundamental governing heat and mass transfer equations presented in Chapter 8 can be used to determine the distributions of the temperature and moisture content along the air flow direction in a cooling coil. However, the actual distributions are in fact much more complicated because a cooling coil is 3-dimensional, not 2-dimensional. More accurate and detailed analytical solution should be derived for a 3-dimensional cooling coil.

Appendix

Photos of the Experimental DX A/C Station

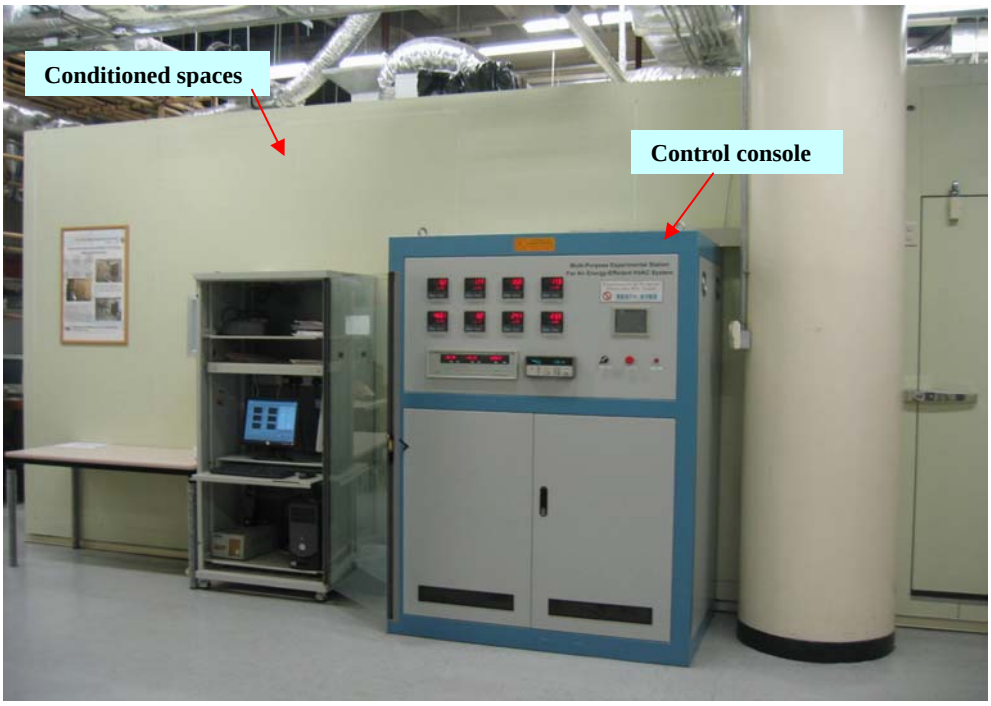

Photo 1 Overview of the experimental station (1)

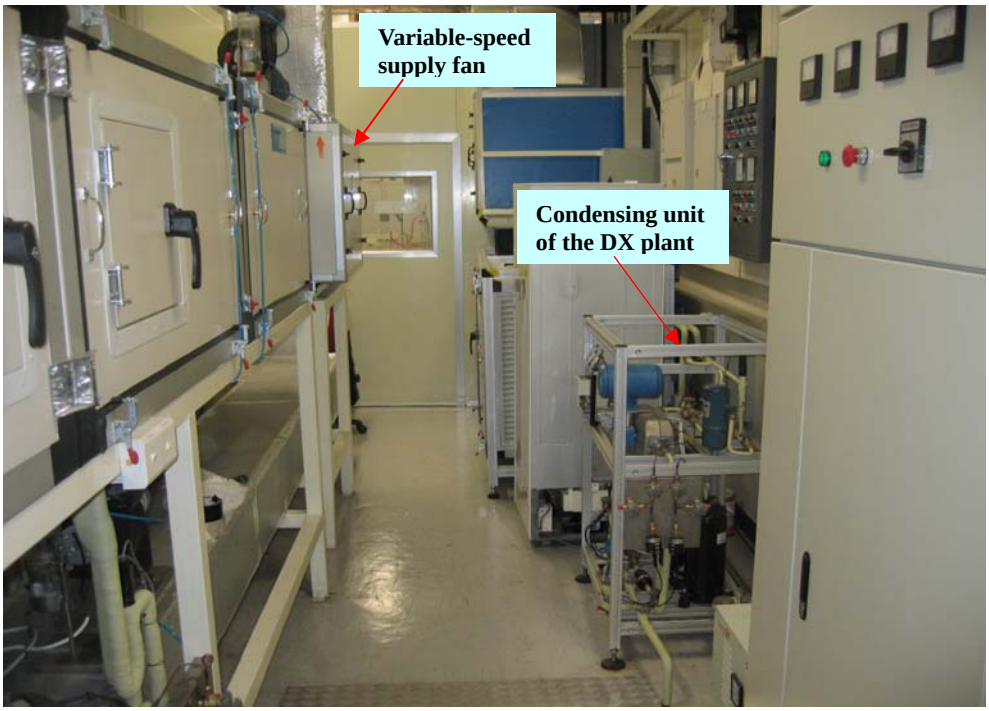

Photo 2 Overview of the experimental station (2)

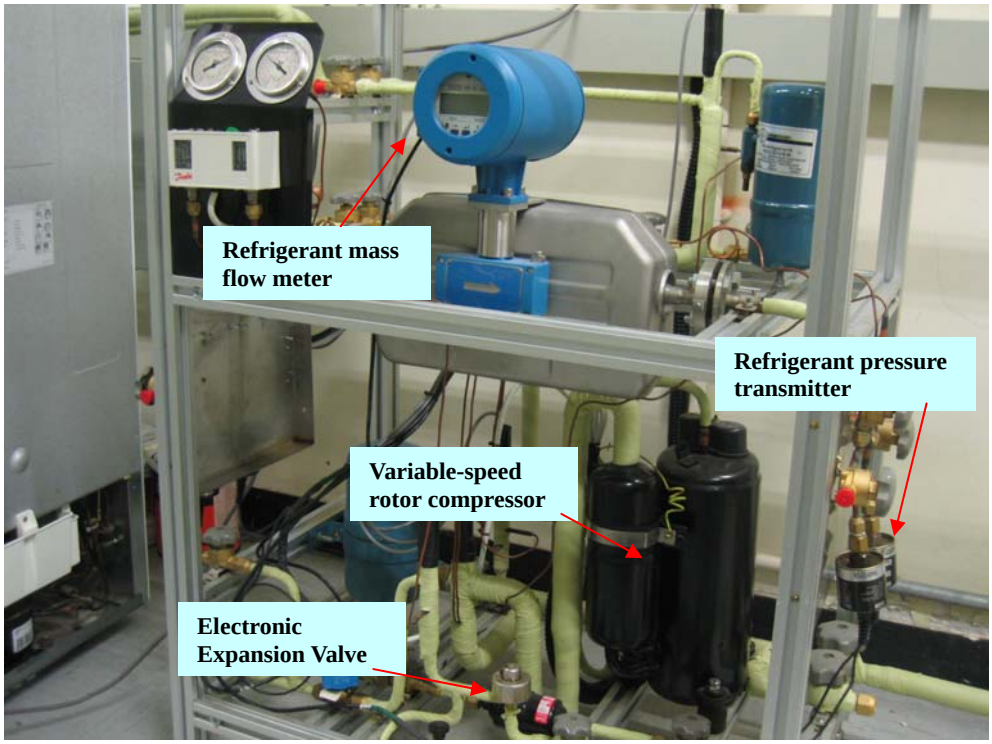

Photo 3 Condensing unit of the DX plant

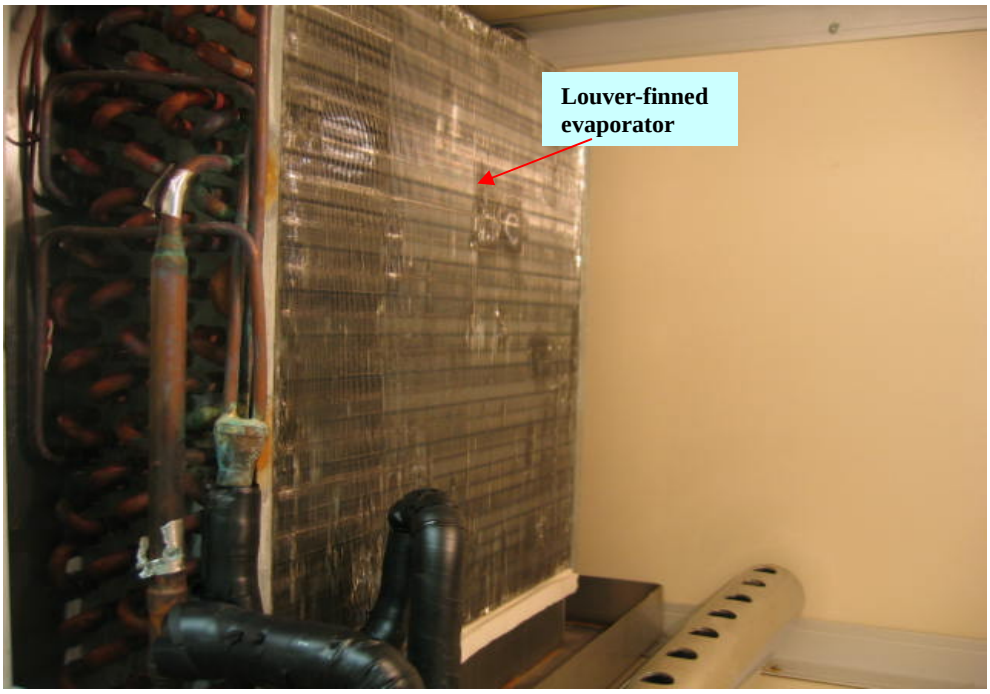

Photo 4 DX cooling coil in the VAV air-distribution sub-system

Photo 5　Load generation unit inside conditioned spaces

References

1. Alpuche et al. 2005
Alpuche, M.G., Heard, C. Best, R. and Rojas, J.
Energy analysis of air cooling systems in buildings in hot humid climates. *Applied Thermal Engineering*, 2005, Vol. 25, No. 4, pp. 507-517 (2005)

2. Andrade et al. 2002
Andrade, M.A., Bullard, C.W., Hancock, S. and Lubliner, M.
Modulating blower and compressor capacities for efficient comfort control. *ASHRAE Transactions*, 2002, Vol. 108, Part. 1, pp. 631-637 (2002)

3. ANSI/ASHRAE 2001
ASHRAE
ANSI/ASHRAE Standard 62-2001, Ventilation for Acceptable Indoor Air Quality (2001)

4. ASHRAE 1983
ASHRAE
Handbook-HVAC Systems and Equipment (1983)

5. ASHRAE 2000
ASHRAE
Handbook-HVAC Systems and Equipment (2000)

6. ASHRAE 2001
ASHRAE
Handbook of Fundamentals (2001)

7. Amrane et al. 2003
Amrane, K., Hourahan, G.C. and Potts, G.
Latent performance of unitary equipment. *ASHRAE Journal*, 2003, Vol. 45, No. 1, pp. 28-31 (2003)

8. Andersson and Lindholm 2001
Andersson, J.V. and Lindholm, T.
Desiccant cooling for Swedish office buildings. *ASHRAE Transactions*, 2001, Vol. 107, Part. 1, pp. 490-500 (2001)

9. Arens and Baughman 1996
Arens, E.A. and Baughman, A.V.
Indoor humidity and human health: part II-buildings and their systems. *ASHRAE Transactions*, 1996, Vol. 102, No. 1, pp. 212-221 (1996)

10. ASHRAE 2005
ASHRAE
ASHRAE Fundamentals 2005, Mass Transfer (2005)

11. Bailey et al. 1996
Bailey, D.W., Bauer, F.C., Slama, C.F., Barringer, C.G. and Flack, J.R.
Investigation of dynamic latent heat storage effects of building construction and furnishings. *ASHRAE Transactions*, 1996, Vol. 102, No. 2, pp. 133-141 (1996)

12. Bandyopadhyay et al. 2008
Analytical and semi-analytical solutions for short-time transient response of ground heat exchangers. *Energy and Buildings*, 2008, Vol. 40, No. 10, pp. 1816-1824 (2008)

13. Barringer and McGugan 1989
Barringer, C.G. and McGugan, C.A.
Development of a dynamic model for simulating indoor air temperature and humidity. *ASHRAE Transactions*, 1989, Vol. 95, Part. 2, pp. 449-460 (1989)

14. Bielski and Malinowski 2005
Bielski S. and Malinowski L.
An analytical method for determining transient temperature field in a parallel-flow three fluid heat exchanger. *International Communications in Heat and Mass Transfer*, 2005, Vol. 32, No. 8, pp. 1034-1044 (2005)

15. Berbari 1998
Berbari, G. J.
Fresh air treatment in hot and humid climates. *ASHRAE Journal*, 1998, Vol. 40, No. 10, pp. 64-70 (1998)

16. Boissieux et al. 2000
Boissieux, X., Heikal, M. R. and Johns, R. A.
Two-phase heat transfer coefficients of three HFC refrigerants inside a horizontal smooth tube, part I: evaporation. *International Journal of Refrigeration*, 2000, Vol. 23, No. 4, pp. 269-283 (2000)

17. Bordick and Gilbride 2002
Bordick J. and Gilbride T.L.
Focusing on buyer's needs: DOE's engineering technology programme. *Energy Engineering*, 2002, Vol. 99, No. 6, pp. 18-38 (2002)

18. Brandemuehl and Katejanekarn 2004
Brandemuehl, M.J. and Katejanekarn, T.
Dehumidification characteristics of commercial building applications. *ASHRAE Transactions*, 2004, Vol. 114, Part. 2, pp. 65-76 (2004)

19. Bump 1963
Bump, T.R.
Average temperatures in simple heat exchangers. *Journal of Heat Transfer*, 1963, Vol. 85, No. 2, pp. 182-183. (1963)

20. Byun et al. 2007
Byun, J.S., Lee, JH. and Choi, J.Y.
Numerical analysis of evaporation performance in a finned-tube heat exchanger. *International Journal of Refrigeration*, 2007, Vol. 30, No. 5, pp. 812-820 (2007)

21. Capehart 2003
Capehart, B.
Air conditioning solutions for hot, humid climates. *Energy Engineering: Journal of the Association of Energy Engineering*, 2003, Vol. 100, No. 3, pp. 5-8 (2003)

22. Chan and Halselden 1981a
Chan, C. Y., Haselden G. G.
Computer-based refrigerant thermodynamic properties, Part I: Basic equations. *International Journal of Refrigeration*, Vol. 4, No. 4, pp. 7-12 (1981)

23. Chan and Halselden 1981b
Chan, C. Y., Haselden, G. G.
Computer-based refrigerant thermodynamic properties, Part II: Program listings. *International Journal of Refrigeration*, Vol. 4, No. 4, pp. 52-60 (1981)

24. Chan and Halselden 1981c
Chan, C. Y., Haselden, G. G.
Computer-based refrigerant thermodynamic properties, Part III: Use of the program in the computation of standard refrigerant cyclses. *International Journal of Refrigeration*, Vol. 4, No. 4, pp.131-134 (1981)

25. Chen and Deng 2006
Chen, W., Deng, S. M.
Development of a dynamic model for a DX VAV air conditioning system. *Energy Conversion & Management*, Vol. 27, No. 18-19, pp. 2900-2924

(2006)

26. Chi and Didion 1982
Chi, J. and Didion, D.
A simulation model of the transient performance of a heat pump. *International Journal of Refrigeration*, 1982, Vol. 5, No. 3, pp. 176-184 (1982)

27. Cleland 1986
Cleland A. C.
Computer sub-routines for rapid evaluation of refrigerant thermodynamic properties. *International Journal of Refrigeration*, Vol. 9, No. 9, pp.346-351 (1986)

28. Coad 2000
Coad, W.J.
Energy conservation is an ethic. *ASHRAE Journal*, 2000, Vol. 42, No. 7, pp. 16-21 (2000)

29. Corberan and Melon 1998
Corberan, J.M. and Melon, M.G.
Modelling of plate finned tube evaporators and condensers working with R134a. *International Journal of Refrigeration*, 1998, Vol. 21, No. 4, pp. 273-284. (1998)

30. Dai et al. 2001
Dai, Y.J., Wang, R.Z., Zhang, H.F. and Yu, J.D.
Use of liquid desiccant cooling to improve the performance of vapor compression air conditioning. *Applied Thermal Engineering*, 2001, Vol. 21, No. 12, pp. 1185-1202 (2001)

31. Deng 2000
Deng, S.M.
A dynamic mathematical model of a direct expansion (DX) water-cooled air-conditioning plant. *Building and Environment*, 2000, Vol. 35, No. 7, pp. 603-613 (2000)

32. Dieckmann et al. 2004
Dieckmann, J., Roth, K.W. and Brodrick, J.
Liquid desiccant air conditioners. *ASHRAE Journal*, 2004, Vol. 46, No. 4, pp. 58-59 (2004)

33. Ding et al. 1992
Ding G. L., Zhang C., Li H.
Polynomial curve-fitting method for refrigerant thermodynamic saturation properties. *Journal of Shanghai Jiao Tong University*, Vol. E-4, No. 2, pp.73-77 (1992) [In Chinese]

34. Dittus and Boelter 1930
Dittus, F.W. and Boelter, L.M.K.
Heat transfer in automobile radiators of the turbulent type. *University of California Publications in Engineering*, 1930, Vol. 2, pp. 443-461 (1930)

35. Eckels and Rabas 1987
Eckels P.W. and Rabas T.J.
Dehumidification: on the correlation of wet and dry transport process in plate finned-tube heat exchangers, *ASME Journal of Heat Transfer*, Vol. 109, pp. 575-582 (1987)

36. Edward 1989
Edward, G.P.
Air conditioning principles and systems: An energy approach. Second edition. (1989)

37. El Diasty et al. 1993
El Diasty, R., Fazio, P. and Budaiwi, I.
Dynamic modeling of moisture absorption and desorption in buildings. *Building and Environment*, 1992, Vol. 28, No. 1, pp. 21-32 (1993)

38. Elmahdy and Mitalas 1977
Elmahdy, A.H. and Mitalas, G.P.
A simple model for cooling and dehumidifying coils for use in calculating energy requirements for buildings. *ASHRAE Transactions*, 1977, Vol. 83, No. 2, pp.103-117. (1977)

39. Elsarrag et al. 2005
Elsarrag, E., Ali, E.E.M. and Jain, S.
Design guidelines and performance study on a structured packed liquid desiccant air-conditioning system. *HVAC and R Research*, 2005, Vol. 11, No. 2, pp. 319-337 (2005)

40. Fanger 2001
Fanger, P.O.
Human requirements in future air-conditioned environments. *International Journal of Refrigeration*, 2001, Vol. 24, No. 2, pp. 148-153 (2001)

41. Fairey and Keresteciogl u 1985
Fairey, P.W. and Keresteciogl u, A.A.
Dynamic modeling of combined thermal and moisture transport in buildings: effects on cooling loads and space conditions. *ASHRAE Transactions*, 1985, Vol. 91, Part. 2A, pp. 461-473 (1985)

42. Fairey et al. 1986
Fairey, P., Keretecioglu, A., Vieirfa, R., Swami, M. and Chandra, S.
Latent and sensible load distributions in conventional and energy-efficient residences, final report. *Prepared by the Florida Solar Energy Center for the Gas Research Institute, FSEC Report FSEC-CR-153-86, GRI Report GRI-86/0056*, pp. 4.8-4.12 (1986)

43. Fisher and Rice 1983
Fisher, S.K. and Rice, C.K.
The Oak Ridge heat pump model: I. A steady-state computer design model for air-to-air heat pumps. ORNL/CON-80/R1, Energy Division, Oak Ridge National Lab, 1983. (1983)

44. Fountain et al. 1999
Fountain, M.E., Arens, E., Xu, T.F., Bauman, F.S. and Oguru M.
An investigation of thermal comfort at high humidities. *ASHRAE Transactions*, 1999, Vol. 105, Part. 2, pp. 94-103 (1999)

45. Gungor and Winterton 1987
Gungor, K. E., and Winterton, R.H.S.
Simplified general correlation for saturated flow boiling and comparisons of correlations with data. *The Canadian Journal of Chemical Engineering, Chemical Engineering Research & Design*, 1987, Vol. 65, pp.148-156 (1987)

46. Gray and Webb 1986
Gray D.L.and Webb R.L.
Heat transfer and friction correlations fro plate finned-tube heat exchangers having plain fins. *Proceedings of The Eighth International Heat Transfer Conference,* San Francisco: American Society of Mechanical Engineers (1986)

47. Green 1982
Green, G.H.
The positive and negative effects of building humidification. *ASHRAE Transactions*, 1982, Vol. 88, No. Part. 1, pp. 1049-1061 (1982)

48. Harriman III et al. 1999
Harriman III L.G., Czachoriski M., Witte M.J. and Kosar D.R.
Evaluating active desiccant systems for ventilating commercial buildings. *ASHRAE Journal*, Vol. 40, No. 10, pp. 28-37 (1999)

49. Harriman III et al. 2001
Harriman III, L.G., Brundrett, G.W. and Kittler, R.
Humidity control design guide for commercial and institutional buildings. *ASHRAE engineers, Inc*. (2001)

50. Harriman III and Judge 2002
Harriman III, L. G. and Judge, J.
Dehumidification equipment advances. *ASHRAE Journal*, 2002, Vol. 44, No. 8, pp. 22-29 (2002)

51. Henderson 1992
Henderson, H.I.
Simulating combined thermostat, air conditioner, and building performance in a house. *ASHRAE Transactions*, 1992, Vol. 98, No. Part. 1, pp. 370-380 (1992)

52. Henderson et al. 1992
Henderson, H.I.Jr., Rengarjan, K. and Shirey, D.B.
The impact of comfort control on air conditioner energy use in humid climates. *ASHRAE Transactions*, 1992, Vol. 98, No. Part. 2, pp. 104-112 (1992)

53. Henderson and Rengarajan 1996
Henderson, H.I.Jr. and Rengarajan, K.
A model to predict the latent capacity of air conditioners and heat pumps at part-load conditions with constant fan operation. *ASHRAE Transactions*, 1996, Vol. 102, No. 1, pp. 266-274 (1996)

54. Hesse and Kruse 1988
Hesse U.and Kruse H.
Predection of the behavior of oil refrigerant mixtures. *Proceedings of the Purdue Refrigeration Conference*, Purdue University (1988)

55. Hickey 2001
Hickey, D.
Focus on humidity control. *ASHRAE Journal*, 2001, Vol. 43, No. 10, pp. 10-11 (2001)

56. Hill and Jeter 1991
Hill, J.M. and Jeter, S.M.
A linear subgrid cooling and dehumidification coil model with emphasis on mass transfer. *ASHRAE Transactions*, 1991, Vol. 97, Part 2, pp. 118-128 (1991)

57. Holman 1994
Holman, J. P.
Experimental methods for engineers. New York: McGraw-Hill (1994).

58. Hourahan 2004
Hourahan, G.C.
How to properly size unitary equipment. *ASHRAE Journal*, 2004, Vol. 46, No. 2, pp. 15-18 (2004)

59. Hong and Webb 1996
Hong T. K. and Webb R. L.
Calculation of fin efficiency for wet and dry fins. *International Journal of HVAC&R Research*, Vol. 2, No. 1, pp. 27-41 (1996)

60. Huzzayyin et al. 2007
Huzzayyin A.S., Nada, S.A. and Elattar, H.F.
Air-side performance of wavy-finned-tube direct expansion cooling and dehumidifying air coil. *International Journal of Refrigeration*, 2007, Vol. 30, No. 2, pp. 230-244 (2007)

61. Jacobi and Goldschmildt 1990
Jacobi, A.M. and Goldschmidt, V.W.
Low Reynolds number heat and mass transfer measurements of an overall counter-flow baffled finned-tube condensing heat exchanger. *Journal of Heat transfer*, 1990, Vol. 33, No. 4, pp. 755-765 (1990)

62. Jalalzadeh-Azar et al. 1998
Jalalzadeh-Azar, A.A., Hodge, B.K. and Steele, W.G.
Thermodynamic assessment of desiccant systems with targeted and relaxed humidity control schemes. *ASHRAE Transactions*, 1998, Vol. 104, No. 2, pp. 313-319 (1998)

63. Jia et al. 1995
Jia, X., Tso, C.P., Jolly, P. and Chia, P.K.
A distributed model for prediction of the transient response of an evaporator. *International Journal of Refrigeration*, 1995, Vol. 18, No. 5, pp. 336-342 (1995)

64. Jia et al. 1999
Jia, X., Tso, C.P., Jolly, P. and Wong, Y.W.
Distributed steady and dynamic modeling of dry-expansion evaporators. *International Journal of Refrigeration*, 1999, Vol. 22, No. 2, pp. 126-136 (1999)

65. Jin et al. 2006
Jin, G.Y., Cai, W.J., Wang, Y.W. and Yao Y.
A simple dynamic model of cooling coil unit. *Energy Conversion & Management*, 2006, Vol. 47, No. 15-16, pp. 2659-2672 (2006)

66. Judge and Radermacher 1997
Judge, J. and Radermacher R.
A heat exchanger model for mixtures and pure refrigerant cycle simulations. *International Journal of Refrigeration*, 1997, Vol. 20, No. 4, pp. 244-255 (1997)

67. Kabashnikov et al. 2002
Kabashnikov, V.P., Danilevskii, L.N., Nekrasov, V.P. and Vityaz, I.P.
Analytical and numerical investigation of the characteristics of a soil heat exchanger for ventilation systems. *International Journal of Heat and Mass Transfer*, 2002, Vol. 45, No. 11, pp. 2407-2418 (2002)

68. Kabelac 1989
Kabelac, S.
The transient response relations for a serpentine cross-flow heat exchanger with water velocity disturbance. *International Journal of Heat and Mass Transfer*, 1989, Vol. 32, No. 6, pp. 1183-1189 (1989)

69. Kandlikar 1990
Kandlikar, S. G.
A general correlation for saturated two-phase flow boiling heat transfer inside horizontal and vertical tubes. *ASME Journal of Heat Transfer*, 1990, Vol. 112, No. 1, pp. 219-228 (1990).

70. Katipamula et al. 1988
Katipamula, S., O'Neal, D.L. and Somasundaram, S.
Simulation of dehumidification characteristics of residential central air conditioners. *ASHRAE Transactions*, 1988, Vol. 88, No. 2, pp. 829-849 (1988)

71. Kazeminejad 1995
Kazeminejad, H.
Analysis of one-dimensional fin assembly heat transfer with

dehumidification. *International Journal of Heat and Mass Transfer*, 1995, Vol. 38, No. 2, pp. 455-462 (1995)

72. Keresteciogluе et al. 1990
Kerestecioglue, A., Swami, M. and Kamel, A.
Theoretical and computational investigation of simultaneous heat and moisture transfer in buildings: effective penetration depth theory. *ASHRAE Transactions*, 1990, Vol. 96, Part. 1, pp. 447-454 (1990)

73. Khattar et al. 1987
Khattar, M.K., Swami, M.V. and Ramanan, N.
Another aspect of duty cycling: effects on indoor humidity. *ASHRAE Transactions*, 1987, Vol. 93, No. Pt. 1, pp. 1678-1687 (1987)

74. Kim and Bullard 2002
Kim, M.H. and Bullard, C.W.
Air-side performance of brazed aluminum heat exchangers under dehumidifying conditions. *International Journal of Refrigeration*, 2002, Vol. 25, No. 7, pp. 924-934 (2002)

75. Klein and Eigenberger 2001
Klein, H. and Eigenberger, G.
Approximate solutions for metallic regenerative heat exchangers. *International Journal of Heat and Mass Transfer*, 2001, Vol. 44, No. 18, pp. 3553-3563 (2001)

76. Kohloss 1981
Kohloss, F.H.
Opportunities to save energy in tropical climates. *ASHRAE Transactions*, 1981, Vol. 87, No. 1, pp. 1415-1425 (1981)

77. Kosar et al.1998
Kosar, D.R., Witte, M.J., Shirey, D.B. III and Hedrick, R.L.
Dehumidification issues of standard 62-1989. *ASHRAE Journal*, 1998, Vol. 40, No. 3, pp. 71-75 (1998)

78. Krakow et al. 1995
Krakow, K. I., Lin S. and Zeng, Z.S.
Temperature and humidity control during cooling and dehumidifying by compressor and evaporator fan speed variation. *ASHRAE Transactions*, 1995, Vol. 101, No. 1, pp. 292-304 (1995)

79. Kundu 2007
Kundu, B.

Performance and optimization analysis of SRC profile fins subject to simultaneous heat and mass transfer. *International Journal of Heat and Mass Transfer*, 2007, Vol. 50, No. 7-8, pp. 1545-1558 (2007)

80. Kurtz 2003
Kurtz, B.
Being size wise. *ASHRAE Journal*, 2003, Vol. 45, No. 1, pp. 17-21 (2003)

81. Kusuda 1983
Kusuda, T.
Indoor humidity calculation. *ASHRAE Transactions*, 1983, Vol. 89, Part. 2, pp. 728-738 (1983)

82. Lam 1996
Lam, J.C.
An analysis of residential sector energy use in Hong Kong. *Energy*, 1996, Vol. 21, No. 1, pp. 1-8 (1996)

83. Lam 2000
Lam, J.C.
Residential sector air conditioning loads and electricity use in Hong Kong. *Energy Conversion & Management*, 2000, Vol. 41, pp. 1757-1768 (2000)

84. Li and Deng 2007
Li, Z. and Deng S.M.
An experimental study on the inherent operational characteristics of a direct expansion (DX) air conditioning (A/C) unit. *Building and Environment*, 2006, Vol. 42, No. 1, pp. 1-10 (2007)

85. Li and Deng 2007a
Li, Z. and Deng S.M.
A DDC-based capacity controller of a direct expansion (DX) air conditioning (A/C) unit for simultaneous indoor air temperature and humidity control Part I: Control algorithms and preliminary controllability tests. *International Journal of Refrigeration*, Vol. 30, pp. 113-123 (2007)

86. Li and Deng 2007b
Li, Z. and Deng S.M.
A DDC-based capacity controller of a direct expansion (DX) air conditioning (A/C) unit for simultaneous indoor air temperature and humidity control Part II: Further development of the controller to improve control sensitivity. *International Journal of Refrigeration*, Vol. 30, pp. 124-133 (2007)

87. Liang et al. 2000
Liang, S.Y., Liu, M., Wong, T.N. and Nathan, G.K.
Comparison of one-dimensional and two-dimensional models for wet-surface fin efficiency of a plate-fin-tube heat exchanger. *Applied Thermal Engineering*, 2000, Vol. 20, No. 10, pp. 941-962 (2000)

88. Liang et al. 2001
Liang, S.Y., Wong, T.N. and Nathan, G.K.
Numerical and experimental studies of refrigerant circuitry of evaporator coils. *International Journal of Refrigeration*, 2001, Vol. 24, No. 8, pp. 823-833 (2001)

89. Lstiburek 2002
Lstiburek, J.
Residential ventilation and latent loads. *ASHRAE Journal*, 2002, Vol. 44, No. 4, pp. 18-22 (2002)

90. Lu 2003
Lu, X.S.
Estimation of indoor moisture generation rate from measurement in buildings. *Building and Environment*, 2003, Vol. 38, No. 5, pp. 665-675 (2003)

91. MacArthur 1984
MacArthur, J.W.
Transient heat pump behavior: a theoretical investigation. *International Journal of Refrigeration*, 1984, Vol. 7, No. 2, pp. 123-132 (1984)

92. Martz et al. 1996
Martz W. L., Burton C. M., Jacobi A. M.
Local composition modeling of the thermodynamic properties of refrigerant and oil mixtures. *Int. J. Refrig.*, Vol. 19, No. 1, pp. 25-33 (1996)

93. Mazzei et al. 2005
Mazzei, P., Minichiello, F., and Palma, D.
HVAC dehumidification systems for thermal comfort: a critical review. *Applied Thermal Engineering*, Vol. 26, pp. 1545-1551 (2006)

94. McGahey 1998
McGahey, K.
New commercial applications for desiccant-based cooling. *ASHRAE Journal*, 1998, Vol. 40, No. 7, pp. 41-45 (1998)

95. McQuiston 1975
McQuiston, F.C.
Fin efficiency with combined heat and mass transfer. *ASHRAE Transactions*, 1975, Vol. 81, No. 1, pp. 350-355 (1975).

96. McQuiston 1978
McQuiston, F.C.
Heat, mass and momentum transfer data for five plate-fin-tube heat transfer surfaces. *ASHRAE Transactions*, 1978, Vol. 84, Part. 1, pp. 266-293 (1978)

97. McQuiston and Parker 1994
McQuiston, F.C. and Parker, J.D.
Heating ventilating and air conditioning, Fourth edition (1994)

98. Mirth and Ramadhyani 1993
Mirth, D.R. and Ramadhyani, S.
Prediction of cooling-coil performance under condensing conditions. *International Journal of Heat and Fluid Flow*, 1993, Vol. 14, No.4, pp. 391-400 (1993)

99. Moffat 1988
Moffat, R.J.
Describing the uncertainties in experimental results. *Experimental Thermal Fluid Science*, 1988, Vol. 1, pp. 2681-2691(1988).

100. Mullen et al. 1997
Mullen, C.E., Bridges, B.D., Porter, K.J., Hahn, G.W. and Bullard, C.W.
Development and validation of a room air-conditioning simulation model. *ACRC TR*-1l6, 1997 (1997)

101. Murphy 2002
Murphy, J.
Dehumidification performance of HVAC systems. *ASHRAE Journal*, 2002, Vol. 44, No. 3, pp. 23-31 (2002)

102. Myers 1967
Myers R.J.
The effect of dehumidification on the air-side heat transfer coefficient for a finned-tube coil. MS thesis, Department of Civil Engineering, University of Minnesota, 1967 (1967)

103. Myers et al. 1970
Myers, G.E., Mitchell, J.W. and Linderman C.F.
The transient response of heat exchanger having an infinite capacitance rate

fluid. *ASME Journal of Heat Transfer*, 1970, Vol. 92, Series C, No. 2, pp. 269-275 (1970)

104. Miller 1984
Miller, J. D.
Development and validation of a moisture mass balance model for predicting residential cooling energy consumption. *ASHRAE Transactions*, 1984, Vol. 90, Part. 2B, pp. 275-293 (1984)

105. Olesen and Brager 2004
Olesen, B.W. and Brager, G.S.
A better way to predict comfort. *ASHRAE Journal*, 2004, Vol. 46, No. 8, pp. 20-28 (2004)

106. Oskarsson et al. 1990
Oskarsson, S.P., Krakow, K.I. and Lin, S.
Evaporator models for operating with dry, wet and frosted finned surfaces. Part I: Heat transfer and fluid flow theory. *ASHRAE Transactions*, 1990, Vol. 96, Part 1, pp. 373-380 (1990)

107. Peng and Howell 1981
Peng C.S. and Howell J.R.
Analysis and design of efficient absorbers for low-temperature desiccant air conditioners. *Journal of Solar Energy*, Vol. 103, pp. 67-74 (1981)

108. Pirompugd et al. 2007
Pirompugd, W. Wang, C.C. and Wongwises, S.
Finite circular fin method for heat and mass transfer characteristics for plain-fin-and-tube heat exchangers under fully and partially wet surface conditions. *International Journal of Heat and Mass Transfer*, 2007, Vol. 50, No. 3-4, pp. 552-565 (2007)

109. Qi and Deng 2008
Qi, Q. and Deng, S.M.
Multivariable control-oriented modeling of a direct expansion (DX) air conditioning (A/C) system. *International Journal of Refrigeration*, 2008, Vol. 31, No. 5, pp. 841-849 (2008)

110. Raggazi 1995
Raggazi, F.
Thermodynamic optimization of evaporators with zeotropic refrigerant mixtures. PHD Dissertation, Department of Mechanical Science and Engineering, University of Illinois at Urbana-Champaign (1995)

111. Ramachandran 1984
Ramachandran, P.V.
Simulation and optimization of cooling coils. PHD Thesis, Department of Mechanical Engineering, Indian Institute of Technology, 1984 (1984)

112. Ren and Yang 2006
Ren, C. and Yang, H.
An analytical model for the heat and mass transfer processes in indirect evaporative cooling with parallel/counter flow configurations. *International Journal of Heat and Mass Transfer*, 2006, Vol. 49, No. 3-4, pp. 617-627 (2006)

113. Rowland et al. 2005
Rowland, C.A., Wendel, Jr. and Martin, J.
Dehumidification technologies. *HPAC Heating, Piping, AirConditioning Engineering*, 2005, Vol. 77, No. 3, pp. 48 (2005)

114. Salah El-Din 1998
Salah El-Din, M.M.
Performance analysis of partially-wet fin assembly. *Applied Thermal Engineering*, 1998, Vol. 18, No. 5, pp. 337-349 (1998)

115. Saman and Alizadeh 2002
Saman W.Y. and Alizadeh S.
An experimental study of a cross-flow type plate heat exchanger for dehumidification/cooling. *Solar Energy*, Vol. 73, No. 1, pp. 59-71 (2002)

116. Seshimo et al. 1988
Seshimo Y., Ogawa K., Marumoto K. and Fujii M.
Heat and mass transfer performances on plate fin and tube heat exchangers with dehumidification, *Transactions of JSME*, Vol. 54, pp. 716-721 (1988)

117. Shah 1982
Shah, M. M.
Chart correlation for saturated boiling heat transfer: equations and further study, *ASHRAE Transactions*, Vol. 88, No. 1, pp. 185-196 (1982)

118. Shaw and Luxton 1988
Shaw, A. and Luxton, R.E.
A comprehensive method of improving part-load air-conditioning performance. *ASHRAE Transactions*, 1988, Vol. 94, Part. 1, pp. 442-457 (1988)

119. Sherman 1999
Sherman, M.

Indoor air quality for residential buildings. *ASHRAE Journal*, 1999, Vol. 41, No. 5, pp. 26-30 (1999)

120. Shirey 1993
Shirey, D.B.III
Demonstration of efficient humidity control techniques at an art museum. *ASHRAE Transactions*, 1993, Vol. 99, No. Pt. 1, pp. 694-703 (1993)

121. Shirey and Henderson 2004
Shirey, D.B. III and Henderson, H.I.Jr.
Dehumidification at part load. *ASHRAE Journal*, 2004, Vol. 46, No. 3, pp. 42-47 (2004)

122. Sterling et al. 1985
Sterling, E.M., Arundel, A. and Sterling, T.D.
Criteria for human exposure to humidity in occupied buildings. *ASHRAE Transactions*, 1985, Vol. 91, No. Part. 1B, pp. 611-622 (1985)

123. Stevens et al. 1957
Stevens, R.A., Fernandez, J., and Woolf, J.
Mean temperature difference in one- two- and three-pass crossflow heat exchangers. *Transactions ASME*, 1957, Vol. 79, pp. 287-297 (1957).

124. Straube 2002
Straube, J.F.
Moisture in buildings. *ASHRAE Journal*, 2002, Vol. 44, No. 1, pp. 15-19 (2002)

125. Subramanyam et al. 2004
Subramanyam, N., Maiya, M.P. and Murthy, S.S.
Application of desiccant wheel to control humidity in air-conditioning systems. *Applied Thermal Engineering*, 2004, Vol. 24, No. 17-18, pp. 2777-2788 (2004)

126. Tanabe et al. 1987
Tanabe, S., Kimura, K. and Hara, T.
Thermal comfort requirements during the summer season in Japan. *ASHRAE Transactions*, 1987, Vol. 93, No. Pt. 1, pp. 564-577 (1987)

127. Theerakulpisut and Priprem 1998
Theerakulpisut, S. and Priprem, S.
Modeling cooling coils. *International Communications in Heat and Mass Transfer*, 1998, Vol. 25, No. 1, pp. 127-137 (1998)

128. Toftum and Fanger 1999
Toftum, J. and Fanger, P.O.
Air humidity requirements for human comfort. *ASHRAE Transactions*, 1999, Vol. 105, Part. 2, pp. 641-647 (1999)

129. Threlkeld 1970
Threlkeld, J.L.
Thermal Environmental Engineering (1970)

130. Trowbridge et al. 1994
Trowbridge, J.T., Ball, K.S., Peterson, J.L., Hunn, B.D. and Grasso, M.M.
Evaluation of strategies for controlling humidity in residences in humid climates. *ASHRAE Transactions*, 1994, Vol. 100, No. 2, pp. 59-73 (1994)

131. Turaga et al. 1988
Turaga M., Lin S., Fazio P. F.
Correlations for heat transfer and pressure drop factors for direct expansion air cooling and dehumidifying coils. *ASHRAE Trans.*, Vol. 94, part 2, pp. 616-629 (1988)

132. Vardhan and Dhar 1998
Vardhan, A. and Dhar P.L.
A new procedure for performance prediction of air conditioning coils. *International Journal of Refrigeration*, 1998, Vol. 21, No. 1, pp. 77-83 (1998)

133. Wang et al. 1999
Wang C. C., Lee C. J., Chang C. T., et al.
Heat transfer and friction correlation for compact louvered fin-and-tube heat exchangers. *International Journal of Heat and Mass Transfer*, Vol. 42, No. 11, pp. 1945-1956 (1999)

134. Wang et al. 2000a
Wang, C.C., Lin, Y.T. and Lee, C.J.
An air side correlation for plain fin-and-tube heat exchangers in wet conditions. *International Journal of Heat and Mass Transfer*, 2000, Vol. 43, No. 10, pp. 1869-1872 (2000)

135. Wang et al. 2000b
Wang, C.C., Lin, Y.T. and Lee, C.J.
Heat and momentum transfer for compact louvered fin-and-tube heat exchangers in wet conditions. *International Journal of Heat and Mass Transfer*, 2000, Vol. 43, No. 18, pp. 3443-3452 (2000)

136. Wang et al. 2007
Wang G., Liu M.S. and Claridge D.E.
Decoupled modeling of chilled-water cooling coils. *ASHRAE Transactions*, 2007, Vol. 113, No. 1, pp. 484-493 (2007)

137. Wang 2008
Wang C.C.
On the heat and mass transfer analogy of fin-and-tube heat exchanger, *International Journal of Heat and Mass Transfer*, Vol. 51, pp. 2055-2059 (2008)

138. Wang and Hihara 2003
Wang, J. and Hihara, E.
Prediction of air coil performance under partially wet and totally wet cooling conditions using equivalent dry-bulb temperature method. *International Journal of Refrigeration*, 2003, Vol. 26, No. 3, pp. 293-201 (2003)

139. Wang and Touber 1991
Wang, H. and Touber, S.
Distributed and non-steady-state modeling of an air cooler. *International Journal of Refrigeration*, 1991, Vol. 14, No. 2, pp. 98-111 (1991)

140. Webb 1990
Webb R. L.
Air-side heat transfer correlations for flat and wavy plate fin-and tube geometries. *ASHRAE Trans.*, Vol. 96, part 2, pp. 445-449 (1990)

141. Westphalen 2004
Westphalen, D.
Energy savings for rooftop AC. *ASHRAE Journal*, 2004, Vol. 46, No. 3, pp. 38-46 (2004)

142. Westphalen et al. 2004
Westphalen, D., Roth, K.W., Dieckmann, J. and Brodrick, J.
Improving latent performance. *ASHRAE Journal*, 2004, Vol. 46, No. 8, pp. 73-75 (2004)

143. Wu and Bong 1994
Wu, G. and Bong, T.Y.
Overall efficiency of a straight fin with combined heat and mass transfer. *ASHRAE Transaction*, 1994, Vol. 100, No. 1, pp. 367-374 (1994)

144. Xia and Jacobi 2005
Xia, Y. and Jacobi, A.M.

Air-side data interpretation and performance analysis for heat exchangers with simultaneous heat and mass transfer: wet and frosted surfaces. *International Journal of Heat and Mass Transfer*, 2005, Vol. 48, No. 25-26, pp. 5089-5102 (2005)

145. Xia and Jacobi 2004
Xia, Y. and Jacobi, A.M.
An exact solution to steady heat conduction in a two-dimensional slab on a one-dimensional fin: application to frosted heat exchangers. *International Journal of Heat and Mass Transfer*, 2004, Vol. 47, No. 14-16, pp. 3317-3326 (2004)

146. Yu et al. 2005
Yu, X., Jin, W. and Smith, T.F.
A model for the dynamic response of a cooling coil. *Energy and Buildings*, 2005, Vol. 37, No. 12, pp. 1278-1289 (2005)

147. Zhang et al. 2000
Zhang C. L., Ding G. L., Li H.
An implicit curve-fitting method for thermodynamic property of refrigerant gas. *Journal of Engineering Thermodynamic*, Vol. 21, No. 5, pp. 533-536 (2000)

148. Zhang 2002
Zhang, G.Q.
China HVACR Annual Business Volume Ⅱ. *Chinese Construction Industry Press*, pp. 44-45 (2002)